
Article:

Duncan, LC, Watling, DP orcid.org/0000-0002-6193-9121, Connors, RD orcid.org/0000-0002-1696-0175 et al. (2 more authors) (2023) Formulation and solution method of bounded path size stochastic user equilibrium models – consistently addressing route overlap and unrealistic routes. Transportmetrica A: Transport Science. ISSN 2324-9935

https://doi.org/10.1080/23249935.2023.2178240

Formulation and solution method of bounded path size stochastic user equilibrium models – consistently addressing route overlap and unrealistic routes

Lawrence Christopher DUNCAN [a,b] *, David Paul WATLING [b], Richard Dominic CONNORS [b,c], Thomas Kjær RASMUSSEN [a], Otto Anker NIELSEN [a]

[a] Department of Technology, Management and Economics, Technical University of Denmark
Bygningstorvet 116B, 2800 Kgs. Lyngby, Denmark.
[b] Institute for Transport Studies, University of Leeds
36-40 University Road, Leeds, LS2 9JT, United Kingdom.
[c] University of Luxembourg, Faculté des Sciences, des Technologies et de Médecine,
Maison du Nombre, 6 Avenue de la Fonte, L-4364, Esch-sur-Alzette, Luxembourg.

* corresponding author:
Department of Technology, Management and Economics, Technical University of Denmark
Bygningstorvet 116B, 2800 Kgs. Lyngby, Denmark.
E-mail: lawdun@dtu.dk

Highlights

- Stochastic User Equilibrium (SUE) conditions for Bounded Path Size (BPS) models
- Proof of existence for BPS SUE solutions and BPS SUE solution algorithm
- Numerical experiments conducted on Sioux Falls and Winnipeg networks
- Computation/flow results compared between BPS SUE models and with PS SUE models
- Computational feasibility & insensitivity to unrealistic routes in the choice sets shown
- Uniqueness conditions for BPS SUE solutions demonstrated numerically

Abstract

Bounded Path Size (BPS) route choice models (Duncan et al, 2021) offer a theoretically consistent and practical approach to dealing with both route overlap and unrealistic routes. It captures correlations between overlapping routes by including correction terms within the probability relations, and has a consistent criterion for assigning zero choice probabilities to unrealistic routes while eliminating their path size contributions. This paper establishes Stochastic User Equilibrium (SUE) conditions for BPS models, where the choice sets of realistic routes are equilibrated along with the route flows. Solution existence and uniqueness are addressed. A generic solution algorithm is proposed, where realistic route choice sets are equilibrated from a pre-generated approximated universal set of routes. Numerical experiments on the Sioux Falls and Winnipeg networks show that BPS SUE models can be solved in feasible computation times compared to non-bounded versions, while providing potential for significantly improved robustness to the adopted master route choice set.

Key Words: bounded path size, stochastic user equilibrium, solution algorithm, fixed-point, convergence, equilibrated choice sets

1 Introduction

The Stochastic User Equilibrium (SUE) traffic assignment model proposed by Daganzo & Sheffi (1977) is a well-known approach for investigating the behaviours of travellers on congested road networks (e.g. in cordon-based congestion pricing (Liu et al, 2013), investigating traffic assignment paradoxes (Yao et al, 2018), and with elastic demand (Kitthamkesorn et al, 2014; Meng et al, 2014)). SUE relaxes the perfect information assumption of the Deterministic User Equilibrium model by supposing that route choice is based on costs that include stochastic terms. This accounts for the differing perceptions travellers have of the attractiveness of routes. Two specific challenges for SUE modelling are: 1) generating realistic route choice sets, and 2) capturing correlations between overlapping routes, and numerous approaches have been developed for independently addressing each of these issues.

For 1), the typical approach has been to employ some kind of heuristic method that attempts to explicitly generate a working route choice set containing just the used routes considered realistic (see e.g. Bekhor et al (2006), Prato & Bekhor (2006), Prato (2009), Bovy & Fiorenzi (2009), Rieser-Schussler et al (2012), Tahlyan & Pinjari (2020)). This is because in real-life problems it is both behaviourally unrealistic and computationally infeasible to operate with the full set of available routes, since the set contains millions of routes even in medium-sized networks (Watling et al, 2015; Rasmussen et al, 2015), the majority of which are very circuitous and will not be used.

For 2), different stochastic route cost terms have been proposed in the literature that give rise to three general types of correlation-based route choice models that have been applied to SUE: GEV (Generalised Extreme Value) structure models (e.g. Cross-Nested Logit, Generalised Nested Logit, Paired Combinatorial Logit), simulation models (e.g. Multinomial Probit, Multinomial Gammit), and correction term models (e.g. C-Logit, Path Size Logit (PSL), Path Size Weibit, Path Size Hybrid). For a detailed review of correlation-based route choice models, with literature references, see Duncan et al (2020, 2021), and for a detailed review of SUE applications of correlation-based models, with literature references, see Duncan et al (2022).

The typical approach for addressing both 1) and 2) has been sequential: to first generate a working route set, and then to apply a correlation-based SUE model to that set, see for example Bekhor & Prashker (2001), Bekhor et al (2008), Chen et al (2012a,b, 2014), Hoogendoorn-Lanser et al (2005), Zhou et al (2012), Yan & Guo (2021), Zill et al (2019). However, this is problematic for two key reasons.

Firstly, although unrealistic routes unintentionally generated in the working route set may themselves only receive small choice probabilities, the correlation-capturing components in many correlation-based SUE models (i.e. GEV structure and correction-terms models) do not distinguish between realistic and unrealistic routes when considering the route overlap. These models therefore have the potential to be negatively and significantly impacted by unintentionally generated unrealistic routes, since the probabilities of the realistic routes will be adjusted to capture correlations with *all* overlapping routes, regardless of their realism (Bovy et al, 2008; Bliemer & Bovy, 2008; Ramming, 2002; Ben-Akiva & Bierlaire, 1999; Bekhor et al, 2008; Duncan et al, 2020,2021,2022).

Secondly, the approach leads to theoretical inconsistencies, since the route generation criteria is not consistent with the calculation of the flows among generated routes (Watling et al, 2018). For example, routes are often generated based on free-flow travel costs, whereas the route choice probabilities are based on equilibrated congested costs.

Recent years have seen the emergence of SUE modelling approaches that go some way towards addressing both of these issues, but with some limitations. We wish to explain these approaches below and outline these limitations as these were important motivating factors for the proposed approach in this paper.

Specifically addressing the first issue, Duncan et al (2022) explored the application of the Adaptive PSL (APSL) route choice model (Duncan et al, 2020) to SUE. Extended from the PSL model (Ben-Akiva & Bierlaire, 1999), APSL captures route correlations by including correction terms within the probability relations to adjust for route overlap. Where APSL differs from PSL, however, is the (consistent) weighting of path size contributions, to reduce the negative impact that any unintentionally generated unrealistic routes may have on the path size correction terms of realistic routes, and thus the choice probabilities of those routes. This thereby relaxes the importance of generating working route choice sets without any unrealistic alternatives. However, while improving upon the choice set robustness to unrealistic routes compared to PSL SUE (as well as other GEV structure and correction term models as demonstrated in Duncan et al (2022)), APSL SUE does not solve the issue entirely since the path size contributions of routes defined as unrealistic are only reduced instead of eliminated.

Specifically addressing the second issue, Watling et al (2015) and Rasmussen et al (2015,2017) developed a PSL Restricted SUE (RSUE) approach whereby the choice set of used routes is determined by some explicit constraint(s) that is(/are) dependent on the equilibrium solution. This consequently ensures that the routes are also generated based on the equilibrated congested route travel costs, ensuing consistency. However, the key issue with PSL RSUE approaches is that the models are not well-behaved: a) flow outputs are not continuous, in turn meaning that the approach is not robust (i.e. potentially sensitive to small changes to network/model specifications); and b) examples have been found where solutions do not exist or solutions do exist but are non-unique.

So, the main contribution of the present paper is to address the contrasting deficiencies of the APSL SUE and PSL RSUE models, by developing a new correlation-based SUE model that eliminates (rather than reduces) the negative impacts of unrealistic routes, in a consistent, robust, and well-behaved way. To do this, we explore the application of the Bounded Path Size (BPS) route choice model (Duncan et al, 2021) to SUE. Extended from the Bounded Choice Model (BCM) (Watling et al, 2018), the BPS model implicitly determines which routes are used/realistic and unused/unrealistic by imposing a bound upon route travel cost, so that routes receive zero choice probabilities if they have a cost greater than some threshold away from the minimum costing route. Moreover, crucially, this is done so in a way that is consistent with the choice probabilities of used routes, and in a way that ensures a continuous probability function. Where the BPS model differs from the BCM, is the inclusion of path size correction factors within the probability relations to capture route correlations. Importantly, the path size contributions are weighted (akin to APSL) so that correlations are only considered between the routes defined as realistic/used, which is also done so in a particular way to ensure the probability function is continuous.

The next steps, however, are integrating the BPS route choice model within an SUE model, developing an efficient solution method for applying it, and exploring how well-behaved the model is. As will be apparent in the paper, there are certain complications/uncertainties involved in doing this that do not make it a trivial task. In particular, the adaptive variant of the BPS model (i.e. the Bounded Adaptive Path Size (BAPS) model, akin to APSL), is naturally expressed as a fixed-point problem. The BAPS model therefore comes at a price of needing to solve a fixed-point problem even to compute route choice probabilities at given travel cost/utility levels. Thus, there are questions of whether it will be computationally feasible to implement such a method within an SUE framework, since it apparently needs to embed a fixed-point problem (for calculating choice probabilities) within another fixed-point problem (for equilibrating flows).

The solution techniques developed in Duncan et al (2022) for solving APSL SUE – which is a similar bi-level fixed-point problem – provide promise for efficiently solving BAPS SUE, but it is uncertain how well these techniques will transfer given the used route choice sets also need to be equilibrated. For example, at each iteration of the solution algorithm there may be a different selection of routes, which compromises the information gained from the previous iteration. Also, the algorithm developed for solving Bounded SUE in Watling et al (2018) requires some tweaking for solving BAPS SUE in order to satisfy the equilibrium conditions and flow domain, as well as measure convergence.

Moreover, the BAPS model is technically not continuous, though continuity can be approximated to arbitrary precision. We therefore explore whether this can impact on solving the model and the behaviour of the outputs. And, since BAPS probability solutions are only unique under certain conditions, we also explore whether this can impact on solving BAPS SUE, and under what conditions BAPS SUE solutions are unique.

The structure of the paper is as follows. In Section 2 we introduce congested network notation. In Section 3 we establish SUE conditions for BPS models and address solution existence/uniqueness. In Section 4 we detail a generic solution algorithm for solving BPS SUE models given approximated/actual pre-generated universal choice sets. In Section 5 we conduct numerical experiments to assess computational performance, compare flow results, and investigate BPS SUE solution uniqueness. Section 6 concludes the paper.

2 Congested Network Notation

A road network consists of link set A and $m = 1, \dots, M$ OD movements. R_m is the choice set of all simple routes (no cycles) for OD movement m of size $N_m = |R_m|$, where $N = \sum_{m=1}^{M} N_m$ is the total number of routes. $A_{m,i} \subseteq A$ is the set of links belonging to route $i \in R_m$, and $\delta_{a,m,i} = \begin{cases} 1 & if\ a \in A_{m,i} \\ 0 & otherwise \end{cases}$.

The travel demand for OD movement m is $q_m > 0$, and $\boldsymbol{Q}_m$ is the $N_m \times N_m$ diagonal matrix of the travel demand for OD movement m (i.e. with q_m on each diagonal element). The flow on route $i \in R_m$ is $f_{m,i}$, and $\boldsymbol{f}_m$ is the N_m-length vector of route flows for OD movement m. $\boldsymbol{f}$ is the N-length vector of all OD movement route flow vectors such that $\boldsymbol{f} = (\boldsymbol{f}_1, \dots \boldsymbol{f}_M)$, where $f_{m,i}$ refers to element number $i + \sum_{k=1}^{m-1} N_k$ in $\boldsymbol{f}$. Ω denotes the set of all demand-feasible non-negative universal route flow vector solutions:

$$\Omega = \left\{ \boldsymbol{f} \in \mathbb{R}_+^N : \sum_{i \in R_m} f_{m,i} = q_m, m = 1, \dots, M \right\}.$$

Furthermore, x_a denotes the flow on link $a \in A$, and $\boldsymbol{x} = (x_1, x_2, \dots, x_{|A|})$ is the vector of all link flows. X denotes the set of all demand-feasible non-negative link flow vectors:

$$X = \left\{ \boldsymbol{x} \in \mathbb{R}_+^{|A|} : \sum_{m=1}^{M} \sum_{i \in R_m} \delta_{a,m,i} f_{m,i} = x_a, \forall a \in A, \boldsymbol{f} \in F \right\}.$$

For link $a \in A$ experiencing a flow of x_a, denote the generalised travel cost for that link as $t_a(x_a)$, where $\boldsymbol{t}(\boldsymbol{x})$ is the vector of all generalised link travel cost functions. In vector/matrix notation, let $\boldsymbol{x}$ and $\boldsymbol{f}$ be column vectors, and define $\boldsymbol{\Delta}$ as the $|A| \times N$-dimensional link-route incidence matrix. Then the relationship between link and route flows may be written as $\boldsymbol{x} = \boldsymbol{\Delta f}$. Supposing that the travel cost for a route can be attained through summing up the total cost of its links, then the generalised travel cost for route $i \in R_m$, $c_{m,i}$, can be computed as follows: $c_{m,i}\big(\boldsymbol{t}(\boldsymbol{\Delta f})\big) = \sum_{a \in A_{m,i}} t_a(\boldsymbol{\Delta f})$, where $\boldsymbol{c}_m\big(\boldsymbol{t}(\boldsymbol{\Delta f})\big)$ is the vector of generalised travel cost functions for OD movement m.

Let the route choice probability for route $i \in R_m$ be $P_{m,i}$, where $\boldsymbol{P}_m = \big(P_{m,1}, P_{m,2}, \dots, P_{m,N_m}\big)$ is the vector of route choice probabilities for OD movement m, and D_m is the domain of possible route choice probability vectors for OD movement m, $m = 1, \dots, M$.

3 Bounded Path Size Stochastic User Equilibrium Models

As demonstrated in Duncan et al (2020), the Path Size Logit (PSL) model (see Appendix A) is problematic in that results are sensitive to unrealistic routes in the adopted choice sets. Addressing this, PSL variants such as Generalised PSL (GPSL), alternative GPSL (GPSL′), and Adaptive PSL (APSL) (see also Appendix A) weight the contributions of routes to path size terms so that the negative impact that unrealistic routes have upon the correction factors of realistic routes – and thus the choice probabilities of those routes – is reduced. This technique, however, does not solve this problem entirely and only worsens in effectiveness as the choice sets are expanded and more unrealistic routes are included.

Duncan et al (2021) thus investigate developing a path size route choice model that eliminates the path size contributions of unrealistic routes entirely, and once more, that removes all the negative effects of unrealistic routes, thereby fully solving the issue.

To tackle this, the integration of PSL concepts with the Bounded Choice Model (BCM) (see Appendix A) was explored. The BCM provides a consistent criterion for determining restricted choice sets of feasible routes and route choice probability, though route correlation is not considered. In Duncan et al (2021), the natural form for a Bounded Path Size (BPS) choice model is derived from inserting path size choice model utilities into the BCM formula in (24). As they show, however, appropriately defining the path size contribution factors within the path size terms is problematic, as demonstrated with a series examples. A series of desired properties are consequently established for a mathematically well-defined BPS model formulation that utilises a consistent criterion for assigning zero choice probabilities to unrealistic routes while eliminating their path size contributions.

Solving these challenges, an alternative form for a BPS model is proposed and two models are consequently formulated that adopt this form: the Bounded Bounded Path Size (BBPS) model and Bounded Adaptive Path Size (BAPS) model, which satisfy desired properties, as discussed/demonstrated. In this section, we provide SUE definitions for the BBPS & BAPS models, then address the existence and uniqueness of solutions.

Just like the BCM, the BPS models propose that routes are defined as unrealistic if they have generalised travel costs greater than the cost bound, i.e. routes $i \in R_m$ such that $c_{m,i}(\boldsymbol{t}) \geq \varphi \min\left(c_{m,l}(\boldsymbol{t}): l \in R_m\right)$, where $\varphi > 1$ is the bound parameter. For a given setting of the link/route costs (and bound parameter), $\bar{R}_m(\boldsymbol{c}_m(\boldsymbol{t}); \varphi) \subseteq R_m$ is defined as the restricted choice set (for OD movement m) of all routes $i \in R_m$ where $c_{m,i}(\boldsymbol{t}) < \varphi \min\left(c_{m,l}(\boldsymbol{t}): l \in R_m\right)$. $\bar{R}_m$ is the active choice set of the realistic/used routes that will receive non-zero probabilities, with size $|\bar{R}_m| = \bar{N}_m$. Unrealistic routes $i \notin \bar{R}_m(\boldsymbol{c}_m(\boldsymbol{t}); \varphi)$ with costs above the bound receive zero choice probabilities.

Where the BPS models differ from the BCM is with the inclusion of path size correction factors within the probability relation, to adjust the probabilities to capture route correlations. Moreover, the key behavioural feature/assumption of the BPS models is that route correlations are considered between only the routes defined as realistic. Thus, only the realistic routes $i \in \bar{R}_m(\boldsymbol{c}_m(\boldsymbol{t}); \varphi)$ have path size terms and contribute to / impact the path size terms of other realistic routes. Unrealistic routes $i \notin \bar{R}_m(\boldsymbol{c}_m(\boldsymbol{t}); \varphi)$ do not have path size terms and do not contribute to / impact the path size terms of realistic routes.

As stated, BPS models assume that drivers only consider correlation between routes defined as realistic, i.e. those that they will choose between / are used. This is nothing new, however. The typical approach of applying a correlation-based SUE model to a generated choice set also makes this assumption, since the choice set is assumed to contain no unrealistic routes. One can imagine an extremely circuitous route that will certainly not be in set of routes that drivers consider sensible to take. It appears to make sense that such a route should not impact route choices in any way, which includes how drivers perceive the distinctiveness of a realistic route. One could perhaps argue that it is less clear whether a route only marginally adjudged to be unrealistic/unused (i.e. a cost just over the bound) should impact the perceived distinctiveness of an overlapping realistic route, but to include path size contributions of (some) unused routes would clearly present consistency issues and uncertainties in how this should/would be done.

From the above, one might argue that the alternative form for a BPS model compromises consistency, since the bound is imposed upon travel cost rather than the full deterministic utility including path size correction. However, while the main reason that the natural BPS model form (that does impose the bound upon the full deterministic utility) was not pursued, is that it is deeply flawed practically (e.g. not well-defined), it is our belief that there is also a strong theoretical and behavioural basis for the alternative approach. For example, it appears logical that routes are judged as unrealistic (assigned zero choice probability / have zero path size contributions) if they have an excessively large travel cost, but not necessarily unrealistic if they are very indistinct (have small path size terms). Routes are still penalised according to their indistinctiveness and the choice probabilities / path size contributions decreases as the path size time decreases, but routes are not bounded according to indistinctiveness. See Duncan et al (2021) for further discussion.

In SUE application, the travel costs are flow-dependent, and therefore the routes defined as (un)realistic depend upon the flows set. The restricted choice sets of realistic routes for the BPS models in SUE are thus equilibrated along with the route flows. The theoretical difference between the BBPS model and BAPS model is in how the path size contribution factors are formulated, as we discuss below.

3.1 Bounded Bounded Path Size SUE

The BBPS model proposes that the path size contribution factors consider ratios of the odds that routes are within the bound. Given $\bar{R}_m(\boldsymbol{c}_m(\boldsymbol{t}); \varphi)$ for OD movement m, the BBPS model choice probability relation for route $i \in R_m$ is:

$$P_{m,i}\left(\boldsymbol{c}_m(\boldsymbol{t}), \bar{\boldsymbol{\gamma}}_m^{BBPS}(\boldsymbol{t})\right) = \begin{cases} \dfrac{\left(h_{m,i}\left(-\theta \boldsymbol{c}_m(\boldsymbol{t})\right) - 1\right) \cdot \left(\bar{\gamma}_{m,i}^{BBPS}(\boldsymbol{t})\right)^{\beta}}{\sum_{j \in \bar{R}_m(\boldsymbol{c}_m(\boldsymbol{t}); \varphi)} \left(h_{m,j}\left(-\theta \boldsymbol{c}_m(\boldsymbol{t})\right) - 1\right) \cdot \left(\bar{\gamma}_{m,j}^{BBPS}(\boldsymbol{t})\right)^{\beta}} & if\ i \in \bar{R}_m(\boldsymbol{c}_m(\boldsymbol{t}); \varphi) \\ 0 & if\ i \notin \bar{R}_m(\boldsymbol{c}_m(\boldsymbol{t}); \varphi) \end{cases}, \quad (1)$$

where $h_{m,i}\big(-\theta\boldsymbol{c}_m(\boldsymbol{t})\big) = \exp\Big(-\theta\big(c_{m,i}(\boldsymbol{t}) - \varphi\min\big(c_{m,l}(\boldsymbol{t})\colon l \in R_m\big)\big)\Big)$, and the path size term for route $i \in \bar{R}_m(\boldsymbol{c}_m(\boldsymbol{t});\varphi)$ is:

$$\bar{\gamma}_{m,i}^{BBPS}(\boldsymbol{t}) = \sum\nolimits_{a\in A_{m,i}} \frac{t_a}{c_{m,i}(\boldsymbol{t})} \frac{\big(h_{m,i}\big(-\lambda\boldsymbol{c}_m(\boldsymbol{t})\big)-1\big)}{\sum_{k\in\bar{R}_m(\boldsymbol{c}_m(\boldsymbol{t});\varphi)}\big(h_{m,k}\big(-\lambda\boldsymbol{c}_m(\boldsymbol{t})\big)-1\big)\delta_{a,m,k}}. \tag{2}$$

$\theta > 0$ is the Logit scaling parameter, $\beta \geq 0$ is the path size scaling parameter, $\varphi > 1$ is the universal bound parameter, and $\lambda > 0$ is the path size contribution scaling parameter.

The BBPS path size contribution weighting $W_{m,k} = h_{m,k}\big(-\lambda\boldsymbol{c}_m(\boldsymbol{t})\big) - 1$ (see Appendix A) is stipulated as such so to satisfy the desired properties for a BPS model established in Duncan et al (2020). This includes ensuring the choice probability function is continuous, which is vital for SUE application. As can be seen, when $\lambda = \theta$, $W_{m,k}$ matches the travel cost component in the BBPS model probability relation exactly, and thus choice probabilities and path size contributions tend towards zero concurrently and meet at zero. This ensures the smooth removal of a route from the active choice set as it's travel cost is decreased below the bound.

An additional path size contribution scaling parameter, λ, is included, in the spirit of the GPSL and GPSL' models (see Appendix A), to allow for the de-coupling of the scale of the model from the path size effect. Larger values of λ accentuate the differences in cost within the contribution factors, so that the more expensive routes have more diminished (though still positive) contributions. In the same way that the GPSL$'_{(\lambda=\theta)}$ model is developed, however, one can equate the travel cost scales setting by $\lambda = \theta$ – thus formulating the BBPS$_{(\lambda=\theta)}$ model – to improve internal consistency and reduce the number of model parameters to estimate. In Duncan et al (2020) and Duncan et al (2021), through theoretical and empirical analysis, we question the credibility of large λ values for BBPS/GPSL models.

The attraction of the BBPS route choice model is that it has a closed-form, continuous, and well-defined choice probability function (see Duncan et al (2021)), and it is relatively quick to compute the choice probabilities (as opposed to the BAPS model). The BBPS model is however not fully internally consistent since the path size contribution factors do not consider route distinctiveness, though consistency is improved by setting $\lambda = \theta$.

The BBPS model approaches the GPSL$'$ model as $\varphi \to \infty$, and thus the BBPS$_{(\lambda=\theta)}$ model is also equivalent to the GPSL$'_{(\lambda=\theta)}$ model in the limit as $\varphi \to \infty$. This provides the BBPS model with a theoretical connection to the family of PSL models. The BBPS model is also equivalent to the BCM for $\beta = 0$, which is equivalent to the MNL model in the limit as $\varphi \to \infty$.

BBPS SUE can be formulated as follows:

BBPS SUE: A universal route flow vector $\boldsymbol{f}^* \in \Omega$ is a BBPS SUE solution iff the route flow vector for OD movement m, $\boldsymbol{f}_m^*$, is a solution to the fixed-point problem

$$\boldsymbol{f}_m = \boldsymbol{Q}_m \boldsymbol{P}_m\Big(\boldsymbol{c}_m\big(\boldsymbol{t}(\boldsymbol{\Delta f})\big), \bar{\boldsymbol{\gamma}}_m^{BBPS}\big(\boldsymbol{t}(\boldsymbol{\Delta f})\big)\Big), \qquad m = 1, \dots, M, \tag{3}$$

where $P_{m,i}$ is as in (1) for route $i \in R_m$ and $\bar{\gamma}_{m,i}^{BBPS}$ is as in (2) for route $i \in \bar{R}_m(\boldsymbol{c}_m(\boldsymbol{t});\varphi)$, given the universal route flow vector $\boldsymbol{f}$.

3.2 Bounded Adaptive Path Size SUE

Like the APSL model, the BAPS model proposes that the path size contribution factors consider choice probability ratios, and as such BAPS SUE can also be defined in two different ways.

3.2.1 Definition 1: BAPS SUE

By adopting choice probability ratio path size contribution factors, the BAPS model has a consistent criterion for assigning zero choice probabilities to unrealistic routes, eliminating the path size contributions of unrealistic routes, and determining route choice probabilities and path size contributions (internally consistent). The BAPS model is, however, not closed-form and the probability relation is an implicit function, naturally expressed as a fixed-point problem.

As discussed in more detail in Duncan et al (2021), the standard formulation for the BAPS model is problematic, since the probability domain is not defined on a closed set, forcing difficulties proving the existence and uniqueness of solutions. To circumvent this, a modified version is formulated for which solutions are proven to exist and uniqueness conditions are established. The modified BAPS model formulation does not have a continuous probability distribution, but the standard formulation can be approximated to arbitrary precision, thus also approximating continuity. In practice the modified version is used and hence we formulate SUE conditions for this formulation.

The modified BAPS formulation is defined as follows, see Duncan et al (2021) for more details on the derivation and theoretical properties of the model. Given $\bar{R}_m(\boldsymbol{c}_m(\boldsymbol{t});\varphi)$, of size $|\bar{R}_m| = \bar{N}_m$, the BAPS model route choice probabilities for OD movement m, $\boldsymbol{P}_m^*(\boldsymbol{t})$, are a solution to the fixed-point problem $\boldsymbol{P}_m = \boldsymbol{Z}_m\left(\boldsymbol{z}_m\big(\boldsymbol{c}_m(\boldsymbol{t}), \bar{\boldsymbol{\gamma}}_m^{BAPS}(\boldsymbol{t}, \boldsymbol{P}_m)\big)\right)$, given the link cost vector $\boldsymbol{t}$, where:

$$Z_{m,i}\left(z_{m,i}\big(\boldsymbol{c}_m(\boldsymbol{t}), \bar{\boldsymbol{\gamma}}_m^{BAPS}(\boldsymbol{t}, \boldsymbol{P}_m)\big)\right) = \begin{cases} \tau_m + (1 - \bar{N}_m \tau_m) \cdot z_{m,i}\big(\boldsymbol{c}_m(\boldsymbol{t}), \bar{\boldsymbol{\gamma}}_m^{BAPS}(\boldsymbol{t}, \boldsymbol{P}_m)\big) & if\ i \in \bar{R}_m(\boldsymbol{c}_m(\boldsymbol{t}); \varphi) \\ 0 & if\ i \notin \bar{R}_m(\boldsymbol{c}_m(\boldsymbol{t}); \varphi) \end{cases}, \tag{4}$$

$$z_{m,i}\big(\boldsymbol{c}_m(\boldsymbol{t}), \bar{\boldsymbol{\gamma}}_m^{BAPS}(\boldsymbol{t}, \boldsymbol{P}_m)\big) = \begin{cases} \dfrac{\big(h_{m,i}(-\theta \boldsymbol{c}_m(\boldsymbol{t})) - 1\big) \cdot \left(\bar{\gamma}_{m,i}^{BAPS}(\boldsymbol{t}, \boldsymbol{P}_m)\right)^{\beta}}{\sum_{j \in \bar{R}_m(\boldsymbol{c}_m(\boldsymbol{t}); \varphi)} \big(h_{m,j}(-\theta \boldsymbol{c}_m(\boldsymbol{t})) - 1\big) \cdot \left(\bar{\gamma}_{m,j}^{BAPS}(\boldsymbol{t}, \boldsymbol{P}_m)\right)^{\beta}} & if\ i \in \bar{R}_m(\boldsymbol{c}_m(\boldsymbol{t}); \varphi) \\ 0 & if\ i \notin \bar{R}_m(\boldsymbol{c}_m(\boldsymbol{t}); \varphi) \end{cases}, \tag{5}$$

where $h_{m,i}\big(-\theta \boldsymbol{c}_m(\boldsymbol{t})\big) = \exp\left(-\theta\big(c_{m,i}(\boldsymbol{t}) - \varphi \min\big(c_{m,l}(\boldsymbol{t}) : l \in R_m\big)\big)\right)$, and the path size term for route $i \in \bar{R}_m(\boldsymbol{c}_m(\boldsymbol{t}); \varphi)$ is:

$$\bar{\gamma}_{m,i}^{BAPS}(\boldsymbol{t}, \boldsymbol{P}_m) = \sum_{a \in A_{m,i}} \frac{t_a}{c_{m,i}(\boldsymbol{t})} \frac{P_{m,i}}{\sum_{k \in \bar{R}_m(\boldsymbol{c}_m(\boldsymbol{t}); \varphi)} P_{m,k} \delta_{a,m,k}}, \qquad \forall \boldsymbol{P}_m \in D^{(\bar{R}_m(\boldsymbol{c}_m(\boldsymbol{t}); \varphi), \tau_m)}, \tag{6}$$

$$D_m^{(\bar{R}_m(\boldsymbol{c}_m(\boldsymbol{t}); \varphi), \tau_m)} = \Big\{ \boldsymbol{P}_m \in \mathbb{R}_+^{N_m} : \tau_m \leq P_{m,i} \leq (1 - (\bar{N}_m - 1)\tau_m), \forall i \in \bar{R}_m(\boldsymbol{c}_m(\boldsymbol{t}); \varphi), and, 0 \leq P_{m,i} \leq (1 - \bar{N}_m \tau_m), \forall i \notin \bar{R}_m(\boldsymbol{c}_m(\boldsymbol{t}); \varphi), \sum_{j=1}^{N_m} P_{m,j} = 1 \Big\}.$$

The model parameters are $0 < \tau_m \leq \frac{1}{\bar{N}_m}$, $m = 1, \dots, M$, $\theta > 0$, $\beta \geq 0$, $\varphi > 1$, where τ_m is the perturbation parameter for OD movement m, which does not require estimating, but is introduced so that probability solutions to the BAPS model can be proven to exist and be unique. $\bar{\gamma}_{m,i}^{BAPS}$ in (6) is the BAPS used route path size term function, $z_{m,i}$ in (5) is the BAPS choice probability function, and $Z_{m,i}$ in (4) is the choice probability adjustment function that adjusts $z_{m,i}$ in a specific way that allows fixed-point probability solution existence/uniqueness proofs to be applied. Most notably, so that the probability domain is closed and bounded, with the lowest value for the used routes being τ_m flow. We direct the reader to Section 5.2.1 in Duncan et al (2021) for a detailed discussion on the motivation for and definition of $Z_{m,i}$.

As (6) shows, for a choice probability solution $\boldsymbol{P}_m^*$, the contribution of used route $k \in \bar{R}_m(\boldsymbol{c}_m(\boldsymbol{t}); \varphi)$ to the BAPS model path size term of used route $i \in \bar{R}_m(\boldsymbol{c}_m(\boldsymbol{t}); \varphi)$ is weighted according to the ratio of choice probabilities between the routes $\left(\frac{P_{m,k}^*}{P_{m,i}^*}\right)$, and hence as a used route approaches zero choice probability its path size contributions approach zero, until it is considered unrealistic, where it then receives a zero choice probability and its path size contributions are eliminated completely. This ensures that *in practice* the choice probability function is continuous, (when setting arbitrarily small τ_m values, see Duncan et al (2021) for details).

The modified BAPS model formulation approaches the APSL model in the limit as $\varphi \to \infty$, and is equivalent to the BCM for $\beta = 0$, which is equivalent to the MNL model in the limit as $\varphi \to \infty$.

Note that by considering the path size *correction* factors (i.e. $\left(\bar{\gamma}_{m,i}^{BAPS}\right)^{\beta}$ in (5)) within the path size *contribution* factors (i.e. $\left(\frac{P_{m,k}}{P_{m,i}}\right)$ in (6)), the BAPS model provides internal consistency. This does mean however that the route choice probabilities are consequently expressed as a fixed-point problem involving themselves, and thereby the model has endogenous explanatory variables, i.e. the θ, β, & φ parameters are correlated with the error terms. This is similar to the fixed-point correlation-based route choice model proposed by Grange et al (2012). Similar to as done by Grange et al (2012), this is resolved in application of the BAPS model by solving the BAPS choice probabilities with a fixed-point algorithm (see Section 5.1), as well as in estimation by re-solving the probabilities for each parameter setting tested during Maximum Likelihood Estimation (see Duncan et al (2021)).

BAPS SUE can be formulated as follows:

BAPS SUE: A universal route flow vector $\boldsymbol{f}^* \in \Omega$ is a BAPS SUE solution iff the route flow vector for OD movement m, $\boldsymbol{f}_m^*$, is a solution to the fixed-point problem

$$\boldsymbol{f}_m = \boldsymbol{Q}_m \boldsymbol{P}_m^*\big(\boldsymbol{t}(\boldsymbol{\Delta f})\big), \qquad m = 1, \dots, M, \tag{7}$$

where $\boldsymbol{P}_m^*$ is a route choice probability solution for OD movement m in $\boldsymbol{Y}_m$ to the fixed-point problem:

$$\boldsymbol{Y}_m = \boldsymbol{Z}_m\left(\boldsymbol{z}_m\left(\boldsymbol{c}_m\big(\boldsymbol{t}(\boldsymbol{\Delta f})\big), \bar{\boldsymbol{\gamma}}_m^{BAPS}\big(\boldsymbol{t}(\boldsymbol{\Delta f}), \boldsymbol{Y}_m\big)\right)\right), \tag{8}$$

given the universal route flow vector $\boldsymbol{f}$, where $Z_{m,i}$ and $z_{m,i}$ are as in (4) and (5), respectively, for route $i \in R_m$, and $\bar{\gamma}_{m,i}^{BAPS}$ is as in (6) for route $i \in \bar{R}_m(\boldsymbol{c}_m(\boldsymbol{t});\varphi)$.

3.2.2 Definition 2: BAPS′ SUE

Like APSL SUE Definition 2 (APSL′ SUE), BAPS SUE Definition 2 (BAPS′ SUE) is derived indirectly by utilising a different underlying route choice model, that is equivalent to the BAPS model at SUE, but only at SUE. By the definition of SUE, the route flow proportions and route choice probabilities equate at equilibrium. Therefore, the BAPS′ choice model supposes that the path size contribution factors consider route flow proportion ratios, instead of choice probability ratios.

The BAPS′ model is defined as follows. Given $\bar{R}_m(\boldsymbol{c}_m(\boldsymbol{t});\varphi)$, the BAPS′ model choice probability relation for route $i \in R_m$ is:

$$P_{m,i}\left(z_{m,i}\left(\boldsymbol{c}_m(\boldsymbol{t}),\bar{\boldsymbol{\gamma}}_m^{BAPS'}(\boldsymbol{t},\boldsymbol{f}_m)\right)\right) =$$

$$Z_{m,i}\left(z_{m,i}\left(\boldsymbol{c}_m(\boldsymbol{t}),\bar{\boldsymbol{\gamma}}_m^{BAPS'}(\boldsymbol{t},\boldsymbol{f}_m)\right)\right) = \begin{cases}\tau_m + (1-\bar{N}_m\tau_m)\cdot z_{m,i}\left(\boldsymbol{c}_m(\boldsymbol{t}),\bar{\boldsymbol{\gamma}}_m^{BAPS'}(\boldsymbol{t},\boldsymbol{f}_m)\right) & if\ i \in \bar{R}_m(\boldsymbol{c}_m(\boldsymbol{t});\varphi) \\ 0 & if\ i \notin \bar{R}_m(\boldsymbol{c}_m(\boldsymbol{t});\varphi)\end{cases}, \tag{9}$$

$$z_{m,i}\left(\boldsymbol{c}_m(\boldsymbol{t}),\bar{\boldsymbol{\gamma}}_m^{BAPS'}(\boldsymbol{t},\boldsymbol{f}_m)\right) = \begin{cases}\dfrac{\left(h_{m,i}(-\theta\boldsymbol{c}_m(\boldsymbol{t}))-1\right)\cdot\left(\bar{\gamma}_{m,i}^{BAPS'}(\boldsymbol{t},\boldsymbol{f}_m)\right)^{\beta}}{\sum_{j\in\bar{R}_m(\boldsymbol{c}_m(\boldsymbol{t});\varphi)}\left(h_{m,j}(-\theta\boldsymbol{c}_m(\boldsymbol{t}))-1\right)\cdot\left(\bar{\gamma}_{m,j}^{BAPS'}(\boldsymbol{t},\boldsymbol{f}_m)\right)^{\beta}} & if\ i \in \bar{R}_m(\boldsymbol{c}_m(\boldsymbol{t});\varphi) \\ 0 & if\ i \notin \bar{R}_m(\boldsymbol{c}_m(\boldsymbol{t});\varphi)\end{cases}, \tag{10}$$

where $h_{m,i}(-\theta\boldsymbol{c}_m(\boldsymbol{t})) = \exp\left(-\theta\left(c_{m,i}(\boldsymbol{t}) - \varphi\min\left(c_{m,l}(\boldsymbol{t}): l \in R_m\right)\right)\right)$, and the path size term for route $i \in \bar{R}_m(\boldsymbol{c}_m(\boldsymbol{t});\varphi)$ is:

$$\bar{\gamma}_{m,i}^{BAPS'}(\boldsymbol{t},\boldsymbol{f}_m) = \sum_{a\in A_{m,i}}\frac{t_a}{c_{m,i}(\boldsymbol{t})}\frac{f_{m,i}}{\sum_{k\in\bar{R}_m(\boldsymbol{c}_m(\boldsymbol{t});\varphi)}f_{m,k}\delta_{a,m,k}}, \qquad \forall\boldsymbol{f}_m \in \Omega_m^{(\bar{R}_m(\boldsymbol{c}_m(\boldsymbol{t});\varphi),\tau_m)}, \tag{11}$$

$$\Omega_m^{(\bar{R}_m(\boldsymbol{c}_m(\boldsymbol{t});\varphi),\tau_m)} = \left\{\boldsymbol{f}_m \in \mathbb{R}_+^{N_m}: \tau_m \le \frac{f_{m,i}}{q_m} \le (1-(\bar{N}_m-1)\tau_m), \forall i \in \bar{R}_m(\boldsymbol{c}_m(\boldsymbol{t});\varphi), and, 0 \le \frac{f_{m,i}}{q_m} \le (1-\bar{N}_m\tau_m), \forall i \notin \bar{R}_m(\boldsymbol{c}_m(\boldsymbol{t});\varphi), \sum_{i\in R_m} f_{m,i} = q_m\right\}.$$

$0 < \tau_m \le \frac{1}{\bar{N}_m}$, $m = 1,\dots,M$, $\theta > 0$, $\beta \ge 0$, $\varphi > 1$. As shown in (11), the contribution of route $k \in \bar{R}_m(\boldsymbol{c}_m(\boldsymbol{t});\varphi)$ to the path size term of route $i \in \bar{R}_m(\boldsymbol{c}_m(\boldsymbol{t});\varphi)$ is weighted according to the ratio of flow between the routes $\left(\frac{f_{m,k}}{f_{m,i}}\right)$, and hence less feasible route alternatives with very low use/flow have a diminished contribution to the path size terms of more feasible routes with relatively high use/flow.

The BAPS′ choice model is closed-form where choice probability solutions for a given flow vector are guaranteed to exist and be unique, assuming every route with a travel cost below the bound has a non-zero flow. Stipulating that the flows for OD movement m $\boldsymbol{f}_m$ belong to the set $\Omega_m^{(\bar{R}_m(\boldsymbol{c}_m(\boldsymbol{t});\varphi),\tau_m)}$ ensures that: a) routes with costs below the bound have a non-zero flow; b) routes with costs above the bound can have a zero flow; c) the route flows are demand-feasible; d) the path size contribution factors consider ratios of route flow proportion (where the demands q_m cancel out), and, e) the BAPS′ model flow domain matches the BAPS model probability domain $D_m^{(\bar{R}_m(\boldsymbol{c}_m(\boldsymbol{t});\varphi),\tau_m)}$.

BAPS′ SUE can be formulated as follows:

BAPS′ SUE: Let $\Omega' \subseteq \bigcup_{m=1}^{M}\Omega_m^{(\bar{R}_m(\boldsymbol{c}_m(\boldsymbol{t});\varphi),\tau_m)}$ be the subset of demand-feasible universal route flow vectors $\boldsymbol{f}$ that satisfy the following conditions:

$$\tau_m \le \frac{f_{m,i}}{q_m} \le (1-(\bar{N}_m-1)\tau_m) \Leftrightarrow c_{m,i}(\boldsymbol{t}(\boldsymbol{\Delta f})) < \varphi\min\left(c_{m,l}(\boldsymbol{t}(\boldsymbol{\Delta f})): l \in R_m\right), \qquad \forall i \in R_m, m = 1,\dots,M, \tag{12}$$

$$f_{m,i} = 0 \Leftrightarrow c_{m,i}(\boldsymbol{t}(\boldsymbol{\Delta f})) \ge \varphi\min\left(c_{m,l}(\boldsymbol{t}(\boldsymbol{\Delta f})): l \in R_m\right), \qquad \forall i \in R_m, m = 1,\dots,M. \tag{13}$$

A universal route flow vector $\boldsymbol{f}^* \in \Omega'$ is a BAPS′ SUE solution iff the route flow vector for OD movement m, $\boldsymbol{f}_m^*$, is a solution to the fixed-point problem

$$\boldsymbol{f}_m = \boldsymbol{Q}_m \boldsymbol{P}_m \left(\boldsymbol{z}_m \left(\boldsymbol{c}_m(\boldsymbol{t}(\boldsymbol{\Delta f})), \boldsymbol{\gamma}_m^{BAPS'}(\boldsymbol{t}(\boldsymbol{\Delta f}), \boldsymbol{f}_m) \right) \right), \qquad m = 1, \dots, M, \tag{14}$$

where $P_{m,i}$ and $z_{m,i}$ are as in (9) and (10), respectively, for route $i \in R_m$, and $\bar{\gamma}_{m,i}^{BAPS'}$ is as in (11) for route $i \in \bar{R}_m(\boldsymbol{c}_m(\boldsymbol{t}(\boldsymbol{\Delta f})); \varphi)$.

The feasible set of flows Ω' for all OD movements prohibits route flow vectors that lead to routes having non-zero flows and cost that violates the cost bound. This ensures that $\Omega_m^{(\bar{R}_m(\boldsymbol{c}_m(\boldsymbol{t}); \varphi), \tau_m)}$ is satisfied for each OD movement $m = 1, \dots, M$, where a route with a cost below the bound must have a non-zero flow ($\geq q_m \tau_m$).

Clearly, the path size contribution factors of the BAPS′ and BAPS choice models equate only exactly at SUE. Of course, solution algorithms converge towards the SUE solution until a suitable level of convergence is achieved. Thus, the difference between route flow proportions and route choice probabilities – and thereby the difference between the BAPS and BAPS′ path size correction terms / choice probabilities – is dependent upon the of the stringency of the convergence criteria. It is therefore important that the convergence criteria are set stringent enough for a suitably converged solution. Otherwise, the BAPS′ route flow proportion ratios / BAPS choice probability ratios may not be suitably the same at the converged solution. However, the route flows will be as converged as they would be for any other model given the stipulated convergence criteria, so the predicted congestion will not be any more affected than any other SUE model would by the stringency of the convergence criteria, for example with different initial SUE conditions. In Section 5.3 we explore how the stringency of the SUE convergence criteria impacts the differences between BAPS′ route flow proportion ratios and BAPS choice probability ratios at BAPS′ SUE / BAPS SUE. We also offer a suggestion for how one can make sure the BAPS′ SUE path size contribution factors are suitably similar to the BAPS SUE factors at convergence.

Note also that the BAPS′ choice model is only internally consistent for flow distributions at SUE, since for all other flow distributions, the relative attractiveness of routes as defined in the path size contribution factors does not match the relative attractiveness in the probability relation.

The BAPS′ choice model in (9)-(11) above is defined including the BAPS model adjustment functions $Z_{m,i}$ and perturbation parameters τ_m, so that the definitions of BAPS SUE and BAPS′ SUE are equivalent. However, since the BAPS′ model is closed-form, these modifications are not required for probability solution existence/uniqueness, and the BAPS′ model can be simplified, see Appendix A.

3.3 Existence & Uniqueness of Solutions

Here, we prove the existence of BBPS SUE solutions, see below for a detailed discussion of the existence of BAPS SUE solutions, and uniqueness.

First, we define an important function: the BBPS SUE fixed-point function. Let $H_{m,i}(\boldsymbol{f}) = q_m P_{m,i}\left(\boldsymbol{c}_m(\boldsymbol{t}(\boldsymbol{\Delta f})), \bar{\boldsymbol{\gamma}}_m^{BBPS}(\boldsymbol{t}(\boldsymbol{\Delta f}))\right)$, where $P_{m,i}$ is as in (11) for route $i \in R_m$ and $\bar{\gamma}_{m,i}^{BBPS}$ is as in (2) for route $i \in \bar{R}_m(\boldsymbol{c}_m(\boldsymbol{t}(\boldsymbol{\Delta f})); \varphi)$. It is clear from (3) that a route flow solution $\boldsymbol{f}^*$ is a BBPS SUE solution iff $H_{m,i}(\boldsymbol{f}^*) = f_{m,i}^*$, $\forall i \in R_m$, $m = 1, \dots, M$.

Given $H_{m,i}(\boldsymbol{f})$, we prove that BBPS SUE model solutions are guaranteed to exist.

Proposition 1: If the link cost function $\boldsymbol{t}(\boldsymbol{\Delta f})$ is a continuous function for all $\boldsymbol{f} \in \Omega$, then at least one BBPS SUE fixed-point route flow solution, $\boldsymbol{f}^* \in \Omega$, is guaranteed to exist.

Proof. From the assumptions that $\boldsymbol{t}(\boldsymbol{\Delta f})$ is a continuous function for all $\boldsymbol{f} \in \Omega$, (and thus $H_{m,i}$ is a continuous function), and given that Ω is a nonempty, convex, and compact set, and $\boldsymbol{H}$ maps Ω into itself, then by Brouwer's Fixed-Point Theorem at least one solution $\boldsymbol{f}^*$ exists such that $H_{m,i}(\boldsymbol{f}^*) = 0$, $\forall i \in R_m$, $m = 1, \dots, M$, and hence BBPS SUE solutions are guaranteed to exist.

■

Regarding the existence of BAPS/BAPS′ SUE solutions, the only reason existence cannot be proven is that the BAPS′ probability function is not technically continuous, since probabilities cannot have values between 0 and τ_m (the perturbation parameter). But, continuity can be approximated to arbitrary precision by setting the perturbation parameter suitably small. Therefore, in any rare case a solution does not exist – i.e. a probability is due to be between 0 and τ_m but cannot – τ_m can simply be set smaller so that the solution does exist. Although, if τ_m is set negligibly small then the algorithm will converge to a solution negligibly different to the desired solution (at $\tau_m \to 0$). Thus, while in theory solutions are not guaranteed to exist, in practice this will never be an issue. This is an entirely different prospect to e.g. the PSL Restricted SUE model (see Section 1) where the underlying choice model is guaranteed to not be continuous and continuity cannot be approximated. Indeed, for such models it easy to find examples where a solution does not exist. For BAPS SUE, proving solution existence is merely a formality for solutions to exist.

If one is set on a BAPS SUE-type model for which existence can be proven, one could set the probabilities of all unused routes to some negligibly small number τ_m rather than 0, and then one can establish a BAPS model with a continuous probability function for proving BAPS SUE solution existence.

Note also that although the BAPS$''$ model (see Appendix A) does have a continuous probability function, Ω'' is not a convex set, and thus standard proofs for solution existence also do not apply. Again, this can be resolved by setting the unused route probabilities to τ_m rather 0.

Regarding the uniqueness of BBPS SUE solutions, the standard approach for establishing sufficient conditions for the uniqueness of SUE solutions requires $H_{m,i}(\boldsymbol{f})$ to be a monotonic function. Assuming the link cost functions $\boldsymbol{t}(\boldsymbol{\Delta f})$ are monotonic, then the route cost functions $\boldsymbol{c}_m\big(\boldsymbol{t}(\boldsymbol{\Delta f})\big)$ are also monotonic. However, the used route path size term functions $\bar{\boldsymbol{\gamma}}_m^{BBPS}\big(\boldsymbol{t}(\boldsymbol{\Delta f})\big)$, are not guaranteed to always be monotonic, and hence the approach is not applicable. This is not to say however that BBPS SUE solutions cannot be unique, since the mentioned approach only establishes sufficient conditions, which are quite strict. It remains to identify a less strict proof that can be applied. Nevertheless, after searching for cases with multiple solutions in numerous experiments in the current study as well as in Duncan et al (2022) for other path size SUE models, we could not find any cases where multiple solutions existed. Again, this is an entirely different prospect to e.g. the PSL Restricted SUE model where examples could easily be found where multiple solutions exist, due to the underlying route choice model not being well-behaved.

For BAPS SUE, since BAPS model probability solutions are not guaranteed to be unique, it is less clear whether BAPS SUE solutions can at all be unique. In Section 5.4 we thus investigate the uniqueness of BAPS SUE solutions numerically, where it is shown that when BAPS probability solutions are unique, BAPS SUE solutions appear to also be unique.

4 Solution Algorithm

In this section, we propose a generic algorithm for solving BPS SUE models. The algorithm is an adaptation of the generic algorithm proposed by Watling et al (2018) for the BSUE model, which is in turn an adaptation of the generic algorithm proposed by Rasmussen et al (2015) for the Restricted SUE (RSUE) model. Since it is typically not feasible to generate and operate with the universal set of routes, these algorithms propose that routes are generated from the network as the algorithm progresses. At each iteration, given the route costs from the current route flows, a column generation approach is used to find, for each OD movement, all the routes in the network that have a travel cost below the current cost bound. As Watling et al (2018) discuss, however, with the current techniques available for generating all such routes, there are questions over the suitability of the approach for large-scale networks. For example, the computational burden of the Constrained Enumeration approach (e.g. Prato & Bekhor, 2006; Hoogendoorn-Lanser et al, 2006), which they adopt, increases exponentially as the bound parameter, size of network, and network depth increase. For use of the column generation approach, more computationally efficient methods for consistent route generation may need to be adopted.

The approach we adopt in this paper for the proposed BPS SUE algorithm and its application, is to pre-generate approximated universal choice sets and make an assumption that these routes contain at least all those considered realistic. This means that with this approach the solution quality may depend on the chosen choice set generation method, as is typically the case. However, usually, for non-bounded route choice models, it is crucial for the accuracy of results that the pre-generated choice sets contain only the routes considered realistic, as the presence of unrealistic routes can significantly and negatively affect realistic route choice probabilities. But, for the bounded models, the presence of unrealistic routes in the pre-generated choice sets have no effect upon the probabilities of realistic routes (as defined by the model). Hence, choice sets can be generated as large as the computational resources allow, in order to minimise the possibility of excluding what may later turn out to be a plausible route from the choice sets. Therefore, the importance of the choice set generation method is less important. From the approximated universal choice sets, the BPS SUE algorithm equilibrates the restricted choice sets of the realistic route alternatives and assigns flows to these routes in a way that is consistent. The computational benefit of having pre-generated choice sets is that at each iteration of the BPS SUE algorithm, the travel costs for all routes can be computed and the column generation phase becomes trivial. The proposed BPS SUE algorithm given here can however be easily adapted so that routes are generated as the algorithm progresses, just like the BSUE algorithm in Watling et al (2018).

As discussed in Section 3 in Duncan et al (2021), a 'natural' form for the BPS model was initially explored, where path size utilities are inserted into the BCM formula in (24). This bounds routes according to their utility (i.e. combination of cost and path size correction), rather than just cost. However, as demonstrated, appropriately defining the path size contribution factors within the path size terms is difficult. Instead, to circumvent this issue, an alternative BPS model form was derived, which proposes that routes are bounded according to their travel cost (like the BCM), while the probability relations for routes with costs below the bound include path size correction factors to adjust for route correlations. This means that the BCM and BPS model both have the same definition for unrealistic routes: those with travel costs above the bound. This has the benefit that the algorithm and gap measures proposed for solving BSUE are applicable for solving BPS SUE with only a few minor adjustments.

The key amendments of the BPS SUE algorithm from the BSUE algorithm in Watling et al (2018) are as follows. The main amendment is the addition of a *Flow Allocation for New Routes* phase, which ensures that the allocation of flow to new routes generated from the *Column Generation Phase* is done so in a way that satisfies the demand feasible set of flows and equilibrium constraints. This is particularly important for solving the BAPS SUE model where new routes cannot be assigned zero flows. Moreover, the convergence measures must also be adapted, in order to account for the path size correction. The *Used Above Bound Convergence Phase* is also separated from the other convergence phases to be measured at the appropriate stage of the algorithm.

The BPS SUE algorithm can be summarised as follows: **Step 0:** Initialise by performing all-or-nothing assignments to obtain the initial sets of used routes (where there is a single route in each used route choice set); **Step 1:** Search for routes with a cost below the current bound and add them to the used route choice sets; **Step 2:** Allocate flow to new routes in a way that satisfies flow feasibility; **Step 3:** Compute the relevant BPS model choice probabilities for the current used routes given the current flow vector and thus link costs (knowing all of these routes will receive a non-zero probability); **Step 4:** Compute auxiliary route flow vector given the probabilities; **Step 5:** Compute the next route flow vector by averaging the previous and auxiliary flow vectors according to chosen averaging scheme; **Step 6:** Given the new flow vector, compute the link/route costs; **Step 7:** Compute the *used above bound* relative gap measure which when satisfied ensures no routes with costs *above* the cost bound are *used*; **Step 8:** Remove routes that have costs above the bound (and thus should not be used / have flow), redistribute the flows, and update costs; **Step 9:** Compute the *unused below bound* and *used below bound* relative gap measures, which when satisfied ensure that no routes with costs *below* the cost bound are *unused* and that flow is allocated across the used routes in a way that fulfils the underlying choice model, respectively. Stop if all relative gap measures are satisfied, else return to Step 1.

Step 0: Initialisation. Perform deterministic all-or-nothing assignments for all OD movements $m = 1, \dots, M$ and obtain the used route choice sets $\bar{R}_m^{(0)}$ for OD movements $m = 1, \dots, M$, and the universal route flow vector $\boldsymbol{f}^{(0)}$, where all unused routes have zero flow. Given $\boldsymbol{f}^{(0)}$, compute the link travel cost vector $\boldsymbol{t}^{(1)} = \boldsymbol{t}(\boldsymbol{\Delta f}^{(0)})$ for iteration $n = 1$, and hence also the route cost vectors $\boldsymbol{c}_m^{(1)} = \boldsymbol{c}_m(\boldsymbol{t}^{(1)}) = \boldsymbol{c}_m\left(\boldsymbol{t}(\boldsymbol{\Delta f}^{(0)})\right)$, $m = 1, \dots, M$, for iteration $n = 1$. Set $n = 1$.

Step 1: Column Generation Phase. Let $\bar{N}_m^{(n-1)}$ be the number of routes in the choice set for OD movement m at iteration $n - 1$. For each OD movement $m = 1, \dots, M$, given route cost vector $\boldsymbol{c}_m^{(n)}$ for iteration n, add all routes with costs below the current bound to the used route choice sets $\bar{R}_m^{(n)}$ for iteration n.

Step 2: Flow Allocation for New Routes. Allocate a flow to each of the new routes generated in Step 1 (and adjust existing route flows if required) in a way that satisfies the feasible set for route flows Ω, and thus obtain $\boldsymbol{f}^{(n)}$ for iteration n. If required, update $\boldsymbol{t}^{(n)} = \boldsymbol{t}(\boldsymbol{\Delta f}^{(n)})$ and $\boldsymbol{c}_m^{(n)} = \boldsymbol{c}_m(\boldsymbol{t}^{(n)})$, $m = 1, \dots, M$, for iteration n.

Step 3: Compute Route Choice Probabilities. Given the choice sets $\bar{R}_m^{(n)}$ for OD movements $m = 1, \dots, M$ and the link cost vector $\boldsymbol{t}^{(n)}$ for iteration n, and the route flow vector $\boldsymbol{f}^{(n)}$ for iteration n (or otherwise), compute the route choice probability vectors $\boldsymbol{P}_m^{(n)}$, $m = 1, \dots, M$, for iteration n.

Step 4: Compute Auxiliary Route Flow Vector. Given the route choice probability vectors $\boldsymbol{P}_m^{(n)}$, $m = 1, \dots, M$, for iteration n, compute the auxiliary route flow vector $\tilde{\boldsymbol{f}}^{(n)}$ for iteration n: $\tilde{f}_{m,i}^{(n)} = q_m P_{m,i}^{(n)}, \forall i \in \bar{R}_m^{(n)}, m = 1, \dots, M$.

Step 5: Flow-Averaging Phase. Given the route flow vector $\boldsymbol{f}^{(n)}$ and the auxiliary route flow vector $\tilde{\boldsymbol{f}}^{(n)}$ for iteration n, perform flow-averaging to find the route flow vector $\boldsymbol{f}^{(n+1)}$ for iteration $n + 1$.

Step 6: Compute Link/Route Costs. Given $\boldsymbol{f}^{(n+1)}$, compute the link travel cost vector $\boldsymbol{t}^{(n+1)} = \boldsymbol{t}(\boldsymbol{\Delta f}^{(n+1)})$ and hence also the route cost vectors $\boldsymbol{c}_m^{(n+1)} = \boldsymbol{c}_m(\boldsymbol{t}^{(n+1)})$, $m = 1, \dots, M$, for iteration $n = n + 1$.

Step 7: Used Above Bound Convergence Evaluation. Compute the *used above bound* relative gap measure, and if this is equal to zero, continue to Step 9. Otherwise, continue to Step 8.

Step 8: Bound Condition Phase. Given the used route choice sets $\bar{R}_m^{(n)}$ for all OD movements $m = 1, \dots, M$, check whether the condition $c_{m,i}^{(n+1)} < \varphi \min\left(c_{m,j}^{(n+1)}: j \in \bar{R}_m^{(n)}\right)$ is violated for any $i \in \bar{R}_m^{(n)}$ for $m = 1, \dots, M$. Thus, update the restricted choice sets of used routes for iteration $n + 1$, $\bar{R}_m^{(n+1)}$, by removing violating routes, and update $\boldsymbol{f}^{(n+1)}$ by redistributing the flow on routes removed among the remaining routes in the respective choice sets, ensuring the OD travel demands are still satisfied. Update $\boldsymbol{t}^{(n+1)} = \boldsymbol{t}(\boldsymbol{\Delta f}^{(n+1)})$ and $\boldsymbol{c}_m^{(n+1)} = \boldsymbol{c}_m(\boldsymbol{t}^{(n+1)})$, $m = 1, \dots, M$, for iteration $n + 1$.

Step 9: Below Bound Convergence Evaluation. Compute the *below bound* relative gap measures, and if all gap measures (including the *used above bound* measure) satisfy their pre-specified convergence value, output the route flow vector $\boldsymbol{f}^{(n)}$. Otherwise, set $n = n + 1$ and return to Step 1.

Algorithm 1. Generic solution algorithm for Bounded Path Size SUE models, given pre-generated approximated or actual universal choice sets.

4.1 Step 2: Flow Allocation for New Routes

For BPS SUE models in general – such as BBPS SUE – this step is straightforward: allocate all new routes zero flow. However, for the BAPS′ model, allocating new used routes zero flows violates the set of feasible flows Ω' since these routes have costs within the bound (and therefore cannot have zero flows). Therefore, to ensure that the feasibility in the conservation of OD demand is guaranteed, we propose that these new routes are each allocated τ_m flow (where τ_m is the BAPS/BAPS′ perturbation parameter, see Section 3.2), and the flows of routes already existing in the choice set are adjusted according to the following formula:

$$f_{m,i}^{(n)} = \begin{cases} f_{m,i}^{(n)} - \dfrac{\left(\bar{N}_m^{(n)} - \bar{N}_m^{(n-1)}\right)}{\bar{N}_m^{(n-1)}} \cdot \tau_m & if\ i \in \bar{R}_m^{(n)} \cap \bar{R}_m^{(n-1)} \\ \tau_m & if\ i \in \bar{R}_m^{(n)} \backslash \bar{R}_m^{(n-1)} \end{cases}, \qquad \forall i \in \bar{R}_m^{(n)},$$

where $\bar{R}_m^{(n)}$ is the OD movement m used route choice set at this stage of iteration n (after the *column generation phase*) of size $\left|\bar{R}_m^{(n)}\right| = \bar{N}_m^{(n)}$, and $\bar{R}_m^{(n-1)}$ is the OD movement m used route choice set at the end of iteration $n - 1$ (after the *bound condition phase*) of size $\left|\bar{R}_m^{(n-1)}\right| = \bar{N}_m^{(n-1)}$, $m = 1, \dots, M$. This is also required for solving BAPS SUE with follow-on initial conditions (see Section 4.2); however, otherwise (with non-follow-on conditions), new routes can be allocated zero flow. If the flows are adjusted, then the link/route costs should in theory be updated. However, in practice, the τ_m values are so small that the effects are insignificant and updating the costs is not necessary.

Note that it is not possible for previously used routes $i \in \bar{R}_m^{(n)} \cap \bar{R}_m^{(n-1)}$ to end up with zero or negative flows. This is because $f_{m,i}^{(n)}$ (before adjustment) will always be greater than or equal to τ_m (due to equation (9)), and $\frac{\left(\bar{N}_m^{(n)} - \bar{N}_m^{(n-1)}\right)}{\bar{N}_m^{(n-1)}} \cdot \tau_m$ will always be less than τ_m (since $\bar{N}_m^{(n)} \geq \bar{N}_m^{(n-1)}$ as the column generation can only add routes and $\bar{N}_m^{(n-1)} > 0$). Therefore, $f_{m,i}^{(n)} - \frac{\left(\bar{N}_m^{(n)} - \bar{N}_m^{(n-1)}\right)}{\bar{N}_m^{(n-1)}} \cdot \tau_m$ will always be greater than zero.

4.2 Step 3: Compute Route Choice Probabilities

For BBPS and BAPS′ SUE, this step is straightforward and involves a simple computation of the closed-form probability expressions.

<u>BBPS SUE</u>: Given the used route choice set $\bar{R}_m^{(n)}$ for OD movement m, the link cost vector $\boldsymbol{t}^{(n)}$, and the route flow vector $\boldsymbol{f}^{(n)}$ at this stage of iteration n, the choice probability for route $i \in R_m$ for iteration n is:

$$P_{m,i}^{(n)} = P_{m,i}\left(\boldsymbol{c}_m\left(\boldsymbol{t}^{(n)}\right), \bar{\boldsymbol{\gamma}}_m^{BBPS}\left(\boldsymbol{t}^{(n)}\right); \bar{R}_m^{(n)}\right), \qquad \forall i \in R_m,$$

where $P_{m,i}$ is as in (1) for route $i \in R_m$, and $\bar{\gamma}_{m,i}^{BBPS}$ is as in (2) for route $i \in \bar{R}_m^{(n)}$, $m = 1, \dots, M$.

<u>BAPS′ SUE</u>: Given the used route choice set $\bar{R}_m^{(n)}$ for OD movement m, the link cost vector $\boldsymbol{t}^{(n)}$, and the route flow vector $\boldsymbol{f}^{(n)}$ at this stage of iteration n, the choice probability for route $i \in R_m$ for iteration n is:

$$P_{m,i}^{(n)} = P_{m,i}\left(z_{m,i}\left(\boldsymbol{c}_m\left(\boldsymbol{t}^{(n)}\right), \bar{\boldsymbol{\gamma}}_m^{BAPS'}\left(\boldsymbol{t}^{(n)}, \boldsymbol{f}^{(n)}\right)\right); \bar{R}_m^{(n)}\right),$$

where $P_{m,i}$ and $z_{m,i}$ are as in (9) and (10), respectively, for route $i \in R_m$, and $\bar{\gamma}_{m,i}^{BAPS'}$ is as in (11) for route $i \in \bar{R}_m^{(n)}$, $m = 1, \dots, M$.

For <u>BAPS SUE</u>, computing the BAPS model choice probabilities requires a fixed-point algorithm to compute the solution. In general, there are many fixed-point algorithms available for solving the BAPS fixed-point system. In this study, we use the Fixed-Point Iteration Method (FPIM) (Isaacson & Keller, 1966). Other algorithms were considered, however the performance and convergence of the FPIM in our initial tests (not reported here) were sufficiently promising that we did not consider this worthwhile. Given the used route choice set $\bar{R}_m^{(n)}$ for OD movement m, the link cost vector

$\boldsymbol{t}^{(n)}$, and (potentially for the initial conditions) the route flow vector $\boldsymbol{f}^{(n)}$ at this stage of iteration n, the FPIM for solving the BAPS model choice probabilities for OD movement m at iteration n of the BPS SUE algorithm is as follows:

$$P_{m,i}^{[s]} = Z_{m,i}\left(z_{m,i}\left(\boldsymbol{c}_m\left(\boldsymbol{t}^{(n)}\right), \overline{\boldsymbol{\gamma}}_m^{BAPS}\left(\boldsymbol{t}^{(n)}, \boldsymbol{P}_m^{[s-1]}\right)\right); \bar{R}_m^{(n)}\right), \qquad s = 1,2,3, \ldots$$

such that

$$\lim_{s\to\infty} P_{m,i}^{[s]} = \lim_{s\to\infty} Z_{m,i}\left(z_{m,i}\left(\boldsymbol{c}_m\left(\boldsymbol{t}^{(n)}\right), \overline{\boldsymbol{\gamma}}_m^{BAPS}\left(\boldsymbol{t}^{(n)}, \boldsymbol{P}_m^{[s-1]}\right)\right); \bar{R}_m^{(n)}\right) = P_{m,i}^{*}, \qquad \forall i \in R_m, \qquad \boldsymbol{P}_m^{(0)} \in D_m^{\left(\bar{R}_m^{(n)}, \tau_m\right)},$$

where $Z_{m,i}$ and $z_{m,i}$ are as in (4) and (5), respectively, for route $i \in R_m$, and $\bar{\gamma}_{m,i}^{BAPS}$ is as in (6) for route $i \in R_m$. The FPIM is said to have converged sufficiently to an OD movement m BAPS choice probability solution $\boldsymbol{P}_m^{*} = \boldsymbol{P}_m^{[s]}$ if: $\sum_{i\in R_m}\left|P_{m,i}^{[s-1]} - P_{m,i}^{[s]}\right| < 10^{-\xi}$, where ξ is a predetermined BAPS probability convergence parameter.

In the numerical experiments in Section 5 of this paper, we explore adopting two different initial conditions for the FPIM: *fixed* initial conditions where $P_{m,i}^{[0]} = \begin{cases} \frac{1}{\bar{N}_m} & if\ i \in \bar{R}_m^{(n)} \\ 0 & if\ i \notin \bar{R}_m^{(n)} \end{cases}$, $m = 1, \ldots, M$, and *follow-on* initial conditions where $P_{m,i}^{[0]} = \begin{cases} \frac{f_{m,i}^{(n)}}{q_m} & if\ i \in \bar{R}_m^{(n)} \\ 0 & if\ i \notin \bar{R}_m^{(n)} \end{cases}$, $m = 1, \ldots, M$. The follow-on initial FPIM conditions utilise information from the previous BPS SUE algorithm iteration route flows $\boldsymbol{f}^{(n)}$ to determine the FPIM initial conditions. The idea is to harness the useful relation between route flow proportions and route choice probabilities in SUE, where these equate at equilibrium. In Duncan et al (2021), it was shown that utilising follow-on initial FPIM conditions for computing APSL probabilities solving APSL SUE, the numbers of fixed-point iterations required for APSL choice probability convergence (and thus computation times for each of the iterations) decreased as the flow-averaging algorithm progressed and the route flow proportions became closer to the APSL SUE route choice probabilities. For BAPS SUE, the set of used routes varies as the BPS SUE algorithm progresses, and therefore it is less clear how follow-on initial FPIM conditions will perform. We anticipate, however, that once the used route choice sets have equilibrated, the number of fixed-point iterations required for BAPS model choice probability convergence will decrease as the algorithm progresses (like as for APSL SUE). We test this hypothesis in Section 5.2.

4.3 Step 5: Flow-Averaging Phase

In Step 3, the route choice probabilities are computed given the current route flows, and these are used in Step 4 to obtain an auxiliary route flow vector. In Step 5, the flow-averaging phase consists of weighting the current iteration route flow vector $\boldsymbol{f}^{(n)}$ with the auxiliary route flow vector $\tilde{\boldsymbol{f}}^{(n)}$, according to some step-size η_n, to find the next route flow vector:

$$f_{m,i}^{(n+1)} = (1-\eta_n)\cdot f_{m,i}^{(n)} + \eta_n \cdot \tilde{f}_{m,i}^{(n)}, \qquad \forall i \in R_m, \qquad m = 1, \ldots, M,$$

where $0 \leq \eta_n \leq 1$. There are numerous flow-averaging step-size schemes available, all based on the famous pre-defined Method of Successive Averages (MSA). Liu et al (2009) test different alternative pre-defined averaging schemes, and introduce the Method of Successive Weighted Averages (MSWA), which we adopt for the experiments in this paper. While being pre-defined, the MSWA allows giving higher weight to auxiliary flow patterns from later iterations, and the step-size η_n at iteration n is defined as:

$$\eta_n = \frac{n^d}{\sum_{k=1}^{n} k^d}$$

where $d > 0$ is a real number. Increasing the value of d moves more flow towards the auxiliary solution. The MSA is a special case of the MSWA, namely when $d = 0$.

4.4 Steps 7&9: Convergence Evaluation Phases

In this subsection, we propose three gap measures to monitor convergence of the BPS SUE algorithm to a solution satisfying the BPS SUE conditions. These gap measures are similar to those detailed for the BSUE model in Watling et al (2018). Two parts monitor convergence of the equilibrated choice sets and one part monitors the convergence of the allocation of flow to fulfil the underlying choice model.

Step 7: Used Above Bound Convergence Evaluation: Given the route cost vectors $\boldsymbol{c}_m^{(n+1)}$, $m = 1, \ldots, M$, and the route flow vector $\boldsymbol{f}^{(n+1)}$ (for iteration $n+1$) at this stage of iteration n, the *used above bound* relative gap measure is as follows:

$$Rel.\,gap_{used\ above\ bound}^{(n)} = \frac{\sum_{m=1}^{M} \sum_{i\in \bar{R}_m^{(n)}} f_{m,i}^{(n+1)} \cdot \left(c_{m,i}^{(n+1)} - \varphi \min\left(\boldsymbol{c}_m^{(n+1)}\right)\right)_+}{\sum_{m=1}^{M} \sum_{i\in \bar{R}_m^{(n)}} f_{m,i}^{(n+1)} \cdot c_{m,i}^{(n+1)}}. \quad (15)$$

This gap measure in (15) ensures that (at convergence) no routes with a cost *above* the cost bound are *used*. Moreover, it measures the total violation relative to the total costs across all routes. When across all OD movements, no used routes have costs above the bound, then the gap is zero, and the convergence criteria are satisfied.

Step 9: Below Bound Convergence Evaluation: Given the current used route choice sets $\bar{R}_m^{(n)}$ and thus also the unused route choice sets $R_m \backslash \bar{R}_m^{(n)}$, $m = 1, \dots, M$, at this stage of iteration n, and the route cost vectors $\boldsymbol{c}_m^{(n+1)}$, $m = 1, \dots, M$, (for iteration $n+1$) at this stage of iteration n, the *unused below bound* relative gap measure for iteration n is as follows:

$$Rel.\,gap_{unused\ below\ bound}^{(n)} = \frac{\sum_{m=1}^{M} q_m \cdot \left(\varphi \min\left(\boldsymbol{c}_m^{(n+1)}\right) - c_{m,i}^{(n+1)} : i \in R_m \backslash \bar{R}_m^{(n)}\right)_+}{(\varphi - 1) \cdot \sum_{m=1}^{M} q_m \cdot \min\left(\boldsymbol{c}_m^{(n+1)}\right)}, \quad (16)$$

This gap measure in (16) ensures that no routes with a cost *below* the cost bound are *unused*. Moreover, for each OD movement, it measures the average relative non-violation of the bound for the unused routes not violating the bound the most. When across all OD movements, no unused routes have a cost below the bound, then the gap is zero, and the convergence criteria are satisfied.

Given the current used route choice sets $\bar{R}_m^{(n)}$, $m = 1, \dots, M$, at this stage of iteration n, and the route flow vector $\boldsymbol{f}^{(n+1)}$ (for iteration $n+1$) at this stage of iteration n, the *used below bound* relative gap measure for iteration n is as follows:

$$Rel.\,gap_{used\ below\ bound}^{(n)} = \frac{\sum_{m=1}^{M} \sum_{i\in \bar{R}_m^{(n)}} f_{m,i}^{(n+1)} \cdot \left(\tilde{c}_{m,i}\left(\boldsymbol{f}^{(n+1)}\right) - \min\left(\tilde{c}_{m,j}\left(\boldsymbol{f}^{(n+1)}\right) : j \in \bar{R}_m^{(n)}\right)\right)}{\sum_{m=1}^{M} \sum_{i\in \bar{R}_m^{(n)}} f_{m,i}^{(n+1)} \cdot \tilde{c}_{m,i}\left(\boldsymbol{f}^{(n+1)}\right)}. \quad (17)$$

This gap measure in (17) ensures that flow is allocated across used routes in a way that fulfils the underlying choice model. For this we extend ideas from Rasmussen et al (2015) and Watling et al (2018), where transformed cost measures $\tilde{c}_{m,i}\left(\boldsymbol{f}^{(n+1)}\right)$ were defined for the MNL choice model and the BCM, respectively, and convergence was proven for when (17) is equal to zero using this. For BPS models, we define $\tilde{c}_{m,i}\left(\boldsymbol{f}^{(n+1)}\right)$ to be used in (17) instead to be:

$$\tilde{c}_{m,i}\left(\boldsymbol{f}^{(n+1)}\right) = \frac{f_{m,i}^{(n+1)}}{\left(h_{m,i}\left(-\theta \boldsymbol{c}_m\left(\boldsymbol{t}\left(\boldsymbol{\Delta f}^{(n+1)}\right)\right)\right) - 1\right) \cdot \left(\bar{\gamma}_{m,i}\left(\boldsymbol{t}\left(\boldsymbol{\Delta f}^{(n+1)}\right), \boldsymbol{W}_m\left(\boldsymbol{f}^{(n+1)}\right)\right)\right)^{\beta}}, \quad (18)$$

where $h_{m,i}$ is the same as in (1), $\bar{\gamma}_{m,i}$ is the used route path size term for route $i \in \bar{R}_m^{(n)}$, and $W_{m,i}\left(\boldsymbol{f}^{(n+1)}\right) = \left(h_{m,i}\left(-\theta \boldsymbol{c}_m\left(\boldsymbol{t}\left(\boldsymbol{\Delta f}^{(n+1)}\right)\right)\right) - 1\right)$ for the BBPS model, and $W_{m,i}\left(f_{m,i}^{(n+1)}\right) = f_{m,i}^{(n+1)}$ for the BAPS & BAPS′ models. At equilibrium, $\tilde{c}_{m,i}\left(\boldsymbol{f}^{(n+1)}\right)$ will be the same across all utilised routes for OD movement m, and the gap is zero. However, the convergence criteria is said to be satisfied if $Rel.\,gap_{used\ below\ bound}^{(n)} < 10^{-\zeta}$, where ζ is a predetermined convergence parameter. Although for the BAPS model $W_{m,i}\left(\boldsymbol{f}^{(n)}\right) = P_{m,i}^{*}\left(\boldsymbol{t}\left(\boldsymbol{\Delta f}^{(n)}\right)\right)$ for the underlying choice model, this requires solving choice probability fixed-point problems just for computing the gap measures, and instead we recommend that this is circumvented by utilising the route flow proportions, which will be equal to the choice probabilities at convergence.

4.5 Step 8: Bound Condition Phase

There are numerous ways in which the flows of violating routes can be redistributed among the remaining routes in the choice set. The aim is to redistribute them in a way that has the least impact on the flows of the remaining routes. One such way, as proposed in Watling et al (2018), is to reassign the violating flows according to the BCM choice probabilities of the routes. This ensures that a) all of the violating flows are redistributed (since the probabilities sum up to 1), b) flow is only assigned to paths with costs below the bound, and c) the most/least costly routes receive the most/least flow. Thus, given that $\bar{R}_m^{(n+1)} \subseteq \bar{R}_m^{(n)}$ is the (current) restricted choice set of the remaining routes, i.e. $\bar{R}_m^{(n)}$ excluding the violating routes, the remaining route flows are updated according to the following redistribution of the violating flows:

$$f_{m,i}^{(n+1)} = f_{m,i}^{(n+1)} + \left(\sum_{s \in \bar{R}_m^{(n)} \setminus \bar{R}_m^{(n+1)}} f_{m,s}^{(n+1)} \right) \cdot \frac{\left(\exp\left(-\theta \left(c_{m,i}^{(n+1)} - \varphi \min\left(c_{m,l}^{(n+1)} : l \in R_m \right) \right) \right) - 1 \right)_+}{\sum_{j \in R_m} \left(\exp\left(-\theta \left(c_{m,j}^{(n+1)} - \varphi \min\left(c_{m,l}^{(n+1)} : l \in R_m \right) \right) \right) - 1 \right)_+}, \forall i \in \bar{R}_m^{(n+1)},$$

where $\bar{R}_m^{(n)} \setminus \bar{R}_m^{(n+1)}$ is the set of violating routes, so that $\sum_{s \in \bar{R}_m^{(n)} \setminus \bar{R}_m^{(n+1)}} f_{m,s}^{(n+1)}$ is the sum of violating flows. One could also redistribute the violating flows evenly to the remaining routes.

Note that once one has performed the redistribution and re-computed the link/route costs, one should check again whether any of the remaining routes now violate the bound conditions and consequently redistribute again, until no route violates the bound. Note also, however, that given the violating routes will have large costs, their flows should be among the smallest, at least in latter iterations.

As proposed also in Watling et al (2018), to improve on computation times, the Bound Condition Phase could be conducted every n iterations. Also, to avoid significantly affecting the remaining route flows from the redistribution (which may hinder convergence), one could redistribute just the most costly violating route / a few of the most costly violating routes.

5 Numerical Experiments

In this section, some numerical experiments are conducted to compare the computational performance and flow results of bounded SUE models (namely BSUE, BBPS, BAPS, & BAPS′ SUE) as well as with other SUE models (namely MNL, PSL, GPSL, GPSL′, APSL, & APSL′ SUE, as defined in Duncan et al (2022) with flow-dependent path size terms). We examine results in the case where there are pre-generated approximated universal choice sets. Bounded SUE models are solved with the BPS SUE algorithm in Algorithm 1, and non-bounded SUE models are solved with a Flow-Averaging Algorithm (FAA) (see Duncan et al, 2022). The BPS SUE algorithm can be seen as an extension of the FAA, where *column generation*, *flow allocation for new routes*, and *bound condition* phases are added for the equilibration of choice sets. We also investigate the uniqueness of BAPS SUE solutions.

5.1 Experiment Setup

The computer used has a 2.10GHz Intel Xeon CPU and 512GB RAM, and the code was implemented in Python. In our experiments, we consider three networks: a small example network (Fig. 1), and two well-known networks Sioux Falls and Winnipeg. The small example network consists of 3 nodes, 4 links, and 1 OD movement (with demand 200), the Sioux Falls network consists of 24 nodes, 64 links, and 528 OD movements (with positive demands), and the Winnipeg network consists of 1052 nodes, 2836 links, and 4345 OD movements.

In general, the generalised travel cost, $t_a(x_a)$, for link $a \in A$ may consist of several flow-dependent and flow-independent attributes, for example congested travel time, length, number of left turns, etc. However, for the numerical experiments in this section and for all networks, the travel cost of link $a \in A$ is specified as the flow-dependent travel time $T_a(x_a)$ only, where the volume-delay link cost functions for all networks are based on the Bureau of Public Road (BPR) formula with link-specific parameters:

$$t_a(x_a) = T_a(x_a) = T_{0,a} \left(1 + D \left(\frac{x_a}{K_a} \right)^B \right),$$

where $T_{0,a}$ and K_a are the free-flow travel time and capacity of link $a \in A$, respectively, and $D, B \geq 0$. For the small example network, $D = 0.15$, $B = 4$, $K_a = 100$ for all links, and $T_{0,a}$ for each link is shown in Fig. 1. For the Sioux Falls and Winnipeg networks, the link-cost function values as well as the network and demand data are obtained from https://github.com/bstabler/TransportationNetworks.

For the small example network, the pre-generated choice set is the actual universal set of all 4 routes, where the routes are Route 1: 1 → 3, Route 2: 1 → 4, Route 3: 2 → 3, Route 4: 2 → 4. For Sioux Falls and Winnipeg, we utilise choice sets generated in Duncan et al (2022). For the Sioux Falls network, the choice sets were obtained by generating all routes with a free-flow travel time less than 2.5 times as much as the free-flow travel time on the quickest route for each OD movement. For Winnipeg, a simulation approach was adopted (Sheffi & Powell, 1982), where the link costs were drawn randomly from a truncated normal distribution with mean value being free-flow travel time and standard deviation being 0.6 times the mean. The link costs were simulated 150 times for each OD movement and for each simulation shortest path was conducted to generate a route, where a maximum of 100 unique routes were generated for each choice set. The average and maximum free-flow travel time relative deviations from the quickest route in each choice set were 1.15 and 3.3, respectively. For Sioux Falls, 42,976 routes were generated in total, and the maximum, average, and median choice set sizes for an OD movement were 898, 116, and 6, respectively. For Winnipeg, 305,005 routes were generated in total, and the maximum, average, and median choice set sizes for an OD movement were 100, 70, and 88, respectively.

Note that these choice sets are relatively large, compared to e.g. those generated for Sioux Falls and Winnipeg by Bekhor et al (2008) and used also by Chen et al (2012a,b,2013,2014), Xu et al (2012), & Zhou et al (2012). This was by design as it is our belief the aim of Bekhor et al (2008) was to generate a set of realistic alternatives without any possibility of generating unrealistic routes. However, as discussed in the previous section, it is our aim to generate as large choice sets as we deem the computational resources will allow, in order to minimise the possibility of excluding what will later turn out to be a plausible route from the eventual equilibrated realistic route choice set. Therefore, after experimenting with different settings and generation methods, the above approaches were chosen.

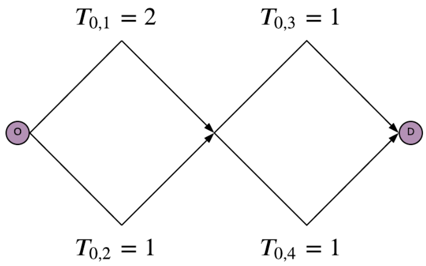

Fig. 1. Small example network.

Convergence for the bounded SUE models is measured with the *used below bound*, *used above bound*, and *unused below bound* relative gap measures in Section 4.4, where convergence is said to be reached when $Rel.\,gap^{(n)}_{used\ above\ bound} = 0$, $Rel.\,gap^{(n)}_{unused\ below\ bound} = 0$, and $Rel.\,gap^{(n)}_{used\ below\ bound} < 10^{-4}$ ($\zeta = 4$).

For non-bounded SUE models, SUE convergence is measured using the *used below bound* relative gap measure (where all routes are used), which is as follows for iteration n:

$$Rel.\,gap^{(n)}_{used\ below\ bound} = \frac{\sum_{m=1}^{M}\sum_{i\in R_m} f_{m,i}^{(n+1)} \cdot \left(\tilde{c}_{m,i}\left(\boldsymbol{f}^{(n+1)}\right) - \min\left(\tilde{c}_{m,j}\left(\boldsymbol{f}^{(n+1)}\right): j \in R_m\right)\right)}{\sum_{m=1}^{M}\sum_{i\in R_m} f_{m,i}^{(n+1)} \cdot \tilde{c}_{m,i}\left(\boldsymbol{f}^{(n+1)}\right)}. \tag{19}$$

where,

$$\tilde{c}_{m,i}\left(\boldsymbol{f}^{(n+1)}\right) = \frac{f_{m,i}^{(n+1)}}{\exp\left(-\theta c_{m,i}\left(\boldsymbol{t}\left(\boldsymbol{\Delta f}^{(n+1)}\right)\right)\right) \cdot \left(\gamma_{m,i}\left(\boldsymbol{f}^{(n+1)}\right)\right)^{\beta}}. \tag{20}$$

$\gamma_{m,i}\left(\boldsymbol{f}^{(n+1)}\right)$ is the flow-dependent path size term for route $i \in R_m$, different for each Path Size Logit SUE model, and equal to 1 for MNL SUE. For APSL SUE, the APSL$'$ SUE path size terms are used (to avoid solving fixed-point problems), since these are equal at convergence. Convergence is said to be reached also when $Rel.\,gap^{(n)}_{used\ below\ bound} < 10^{-4}$.

Unless stated otherwise, specifications are also as follows. The initial conditions for non-bounded SUE models are set as the even split route flows, i.e. $f_{m,i} = \frac{q_m}{N_m}$, $\forall i \in R_m$, $m = 1, \dots, M$. The MSWA parameter is set as $d = 15$. For computing BAPS and APSL probabilities with the FPIM, the probability convergence parameter is set as $\xi = 6$. The utilised model parameters for the Sioux Falls network are $\theta = \lambda^{BBPS} = 0.3$, $\beta = 0.8$, $\lambda^{GPS} = 10$, and $\varphi = 2$. $\theta = 0.5$, $\beta = 0.8$, $\lambda^{GPS} = 10$, and $\varphi = 2$ for the Winnipeg network.

5.2 Computational Performance

In this section, we conduct some numerical experiments to assess and compare the computational performances of the different models. We begin in Section 5.2.1 by comparing the convergence patterns of the different models for a given setting of the parameters/demand. In Section 5.2.2 we then explore different techniques for solving the BAPS($'$) SUE model to improve computation times. In Section 5.2.3, we investigate how computational results vary according to different settings of the parameters/demand.

5.2.1 Comparing Convergence Patterns

We begin the numerical experiments by analysing here the computational performance of the BPS SUE algorithm for solving the bounded SUE models, and comparing computational performance with that for solving non-bounded Path Size Logit SUE models with the FAA.

First, Table 1 displays for all SUE models, during a single run of the solution algorithm, the average computation times to compute the choice probabilities / perform an iteration on the Sioux Falls and Winnipeg networks.

As shown and as expected for the non-bounded SUE models, the MNL probabilities are the quickest to compute, followed by the PSL, GPSL, GPSL′, and APSL′ probabilities, which have similar computation times. APSL probabilities take significantly longer due to solving the fixed-point probabilities. Furthermore, for the non-bounded SUE models, computing the probabilities takes up a significant proportion of the computation time for each iteration. Computing the convergence measure takes up most of the rest of the computation time.

For the bounded SUE models, there are additional steps in the BPS SUE algorithm compared to the FAA for equilibrating the used route choice sets. Thus, computing the probabilities takes up a smaller proportion of the computation time for each iteration. As shown by the probability computation times, the bounded model probabilities are slightly more complex to compute compared to their associated non-bounded model, i.e. the limit models (BCM & MNL, BBPS & GPSL′, BAPS & APSL, BAPS′ & APSL′). Like APSL, the fixed-point BAPS model probabilities are computationally expensive to compute. For BAPS′, as discussed below, a greater proportion of the total iterations during a BPS SUE algorithm run are performed with the choice sets equilibrated where the computational burden is less than for pre-equilibrated. Therefore, the average computation time to perform an iteration across the iterations is less for BAPS′ than for BBPS, despite similar probability computation times.

	MNL	PSL	GPSL	GPSL′	APSL	APSL′	BCM	BBPS	BAPS	BAPS′
Sioux Falls	0.003/ 0.010	0.034/ 0.049	0.034/ 0.049	0.034/ 0.049	1.465/ 1.478	0.034/ 0.049	0.004/ 0.069	0.017/ 0.087	0.844/ 0.909	0.017/ 0.066
Winnipeg	0.02/ 0.05	0.14/ 0.22	0.14/ 0.22	0.14/ 0.22	4.33/ 4.40	0.14/ 0.22	0.05/ 0.16	0.19/ 0.72	5.85/ 6.38	0.19/ 0.55

Table 1. Average computation time [mins] to compute the probabilities / perform an iteration on the Sioux Falls and Winnipeg networks.

Fig. 2A-B display for the Sioux Falls and Winnipeg networks, respectively, the convergence patterns for the bounded SUE models for a single run of the BPS SUE algorithm. Fig. 3A-B display results in terms of computation time, and Fig. 4A-B display how the average used route choice set size varies as the algorithm progresses. Fig. 5A-B display for Winnipeg the convergence patterns for the non-bounded SUE models for a single run of the FAA in terms of iterations and computation time, respectively.

As shown in Fig. 2/Fig. 3, the convergence patterns for the BSUE, BBPS SUE, & BAPS SUE models are different but not drastically different, and converge in similar numbers of SUE iterations. BBPS SUE takes longer to solve than BSUE, however, due to the longer choice probability computation times from computing path size terms. BAPS SUE takes significantly longer than BSUE / BBPS SUE, due to the computationally expensive fixed-point probabilities. For the BAPS′ SUE model, as is evident from the BAPS′ SUE convergence patterns being squashed to the left of the figures, while the number of iterations required to equilibrate the used route choice sets is similar to BSUE / BBPS SUE / BAPS SUE (can also be seen in Fig. 4), once the choice sets are equilibrated, convergence of the flows is slow compared to BSUE / BBPS SUE / BAPS SUE.

Comparing the corresponding convergence patterns in Fig. 2 and Fig. 3, under close inspection one can observe that the region where the *unused below bound* and *used above bound* relative gap measures are non-zero appear more concentrated to the left of the figures in Fig. 2 than in Fig. 3 (more evident in Fig. 2A/Fig. 3A for Sioux Falls). This indicates that the earlier iterations are more time consuming than later iterations, which is as expected since the steps for equilibrating the choice sets in earlier iterations are more active e.g. redistributing the flows of violating routes in the *Bound Violation Check* phase.

As shown in Fig. 4, the average used route choice set sizes for the bounded SUE models generally expand as the BPS SUE algorithm progresses, up until choice set equilibration. Again, the average choice set size patterns are different for each model, but not drastically different.

As shown in Fig. 5 for Winnipeg, in analogous results to the bounded versions of the non-bounded SUE models, the number of iterations required for MNL, PSL, GPSL, GPSL′, & APSL SUE convergence are similar, while APSL′ SUE convergence is comparatively slow. PSL/GPSL/GPSL′ SUE take longer than MNL SUE due to the path size term computation. APSL′ SUE takes longer than PSL/GPSL/GPSL′ SUE due to slower convergence, and APSL SUE takes significantly longer due to the fixed-point probabilities. The APSL′ SUE convergence patterns are also concentrated to the left of the figures, indicating that the slow convergence arises in achieving higher levels of convergence (i.e. convergence gets increasingly slow as the convergence measure is made more strict). Unlike for the bounded SUE models, the convergence patterns with respect to the iterations (Fig. 5A) appear in the figures similar to the convergence patterns with respect to computation time (Fig. 5B), i.e. the patterns are not skewed left or right of each other. This is because the computational burden is roughly uniform across the iterations, with the same number of active routes in each iteration.

Interestingly, the bounded SUE models in this case converge in similar numbers of iterations to the non-bounded versions. APSL′ SUE is significantly slower than BAPS′ SUE, however, and APSL SUE actually takes longer than BAPS SUE. Otherwise, the bounded SUE models take longer than the non-bounded versions.

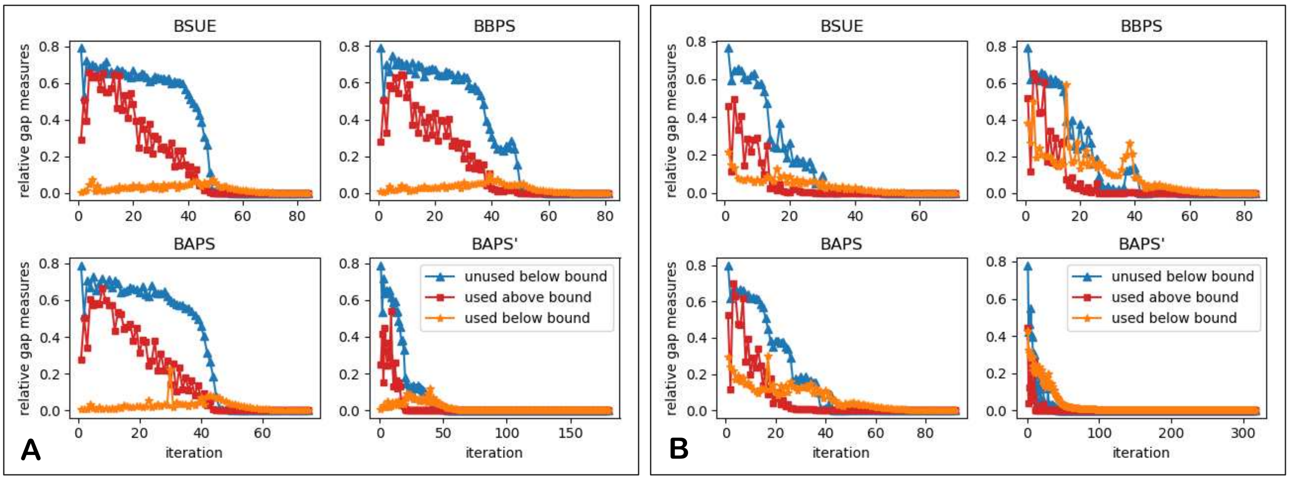

Fig. 2. Relative gap measures for the bounded SUE models at each iteration of the BPS SUE Algorithm. **A:** Sioux Falls. **B:** Winnipeg.

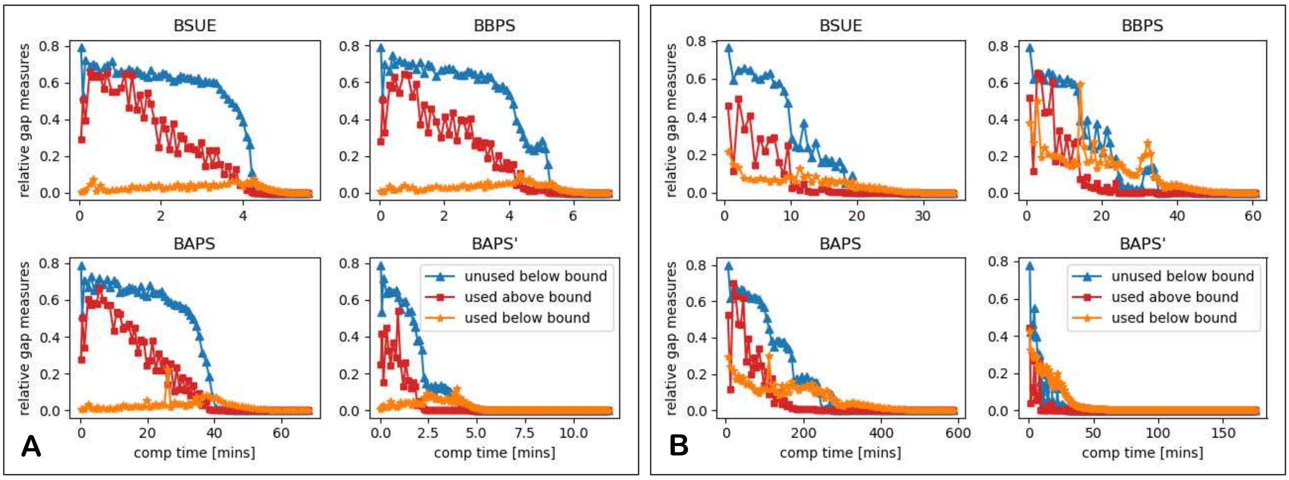

Fig. 3. Relative gap measures for the bounded SUE models in computation time [mins] of the BPS SUE Algorithm. **A:** Sioux Falls. **B:** Winnipeg.

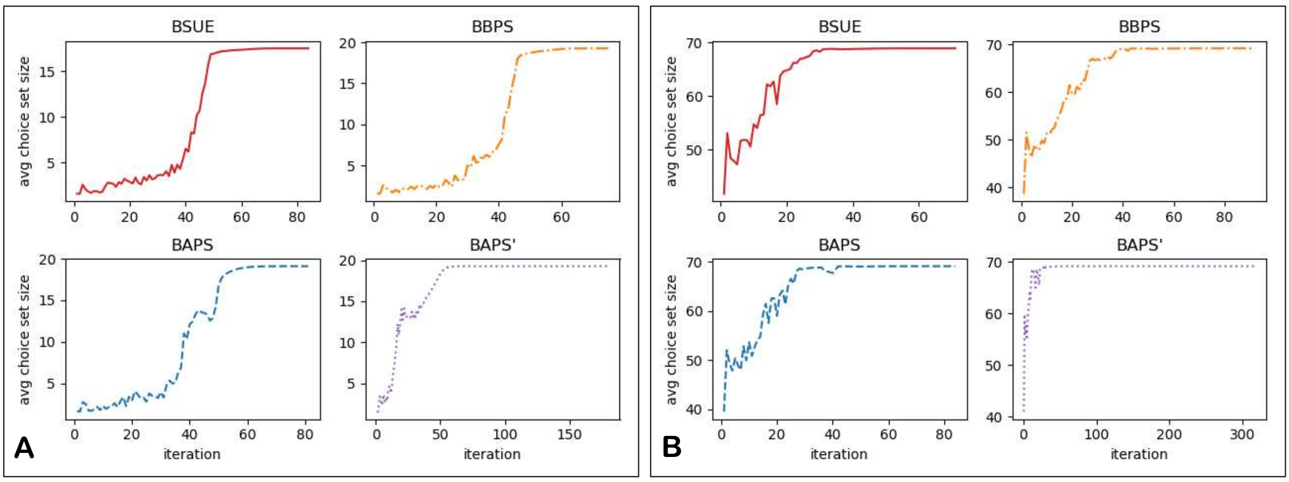

Fig. 4. Average used route choice set sizes for the bounded SUE models at each iteration of BPS SUE algorithm. **A:** Sioux Falls. **B:** Winnipeg.

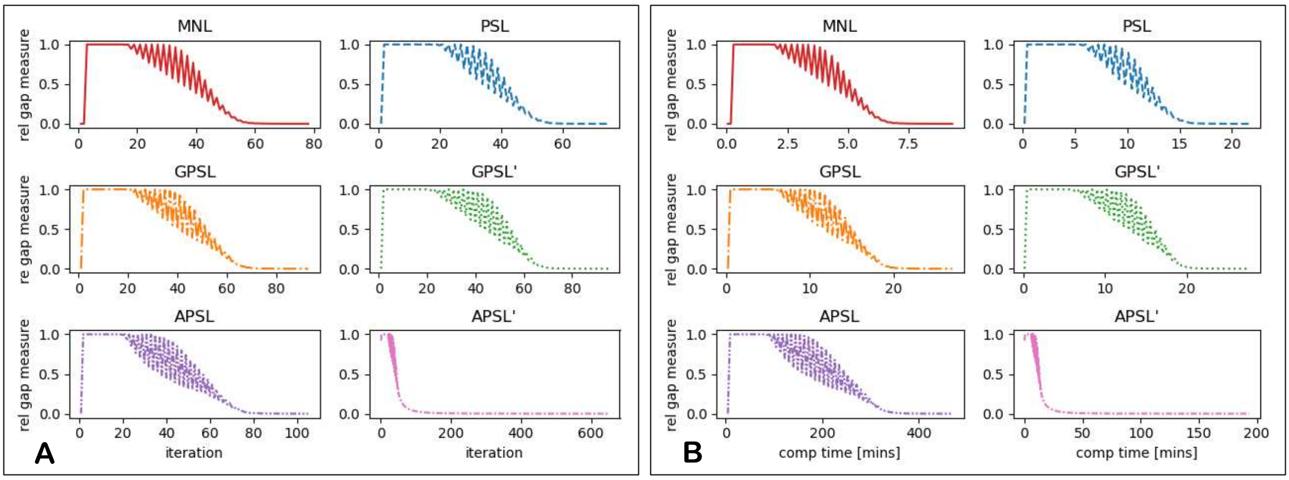

Fig. 5. Winnipeg: Relative gap measures for the non-bounded SUE models at each iteration (**A**) / in computation time [mins] (**B**) of the FAA.

5.2.2 Techniques for Solving BAPS SUE

Duncan et al (2021) demonstrated that while the number of iterations required for APSL SUE convergence tended to be similar to that required for MNL, PSL, & GPSL SUE under identical configurations of the FAA, the requirement of solving APSL choice probability fixed-point problems at each iteration resulted in significantly greater total computation times. On-the-other-hand, while the computational burden involved in computing the APSL′ choice probabilities during each iteration solving APSL′ SUE was no more than that for PSL & GPSL, APSL′ SUE convergence was comparatively very slow, and thus total computational times were also much longer. As they showed however, tuning the APSL SUE algorithm showed how one can trade-off the accuracy of APSL probabilities (and thus computation times of each iteration) with rate of SUE convergence. Several tuning techniques were explored, and it was shown how total computation times can be greatly improved. We shall now explore the success of these techniques for solving BAPS SUE, where it is less clear.

For BAPS SUE, the scale of the computational burden involved at each BPS SUE algorithm iteration in solving the BAPS model choice probability fixed-point problems depends on numerous factors; some of which can be controlled by the modeller, for example the choice of fixed-point algorithm, and the fixed-point algorithm initial conditions and probability convergence parameter ξ. The current study focuses on the FPIM as the fixed-point algorithm.

Fig. 6A-B display for the Sioux Falls and Winnipeg networks, respectively, the cumulative computation times of the iterations during a single run of the BPS SUE algorithm solving BAPS SUE, with fixed and follow-on FPIM initial conditions (see Section 4.2). Fig. 7A-B shows the average number of fixed-point iterations per OD movement required for BAPS choice probability convergence at each iteration of the BPS SUE algorithm. As shown for Sioux Falls, once the choice sets have equilibrated, utilising follow-on initial conditions improves the computation times of each iteration due to the reduction in the number of FPIM iterations required for probability convergence. Before the choice sets have equilibrated, however, more FPIM iterations are required for follow-on initial conditions, due to the greater oscillations in flow among the different active choice sets of routes between iterations. For Winnipeg, utilising follow-on conditions is more effective though, since the choice sets are equilibrated sooner.

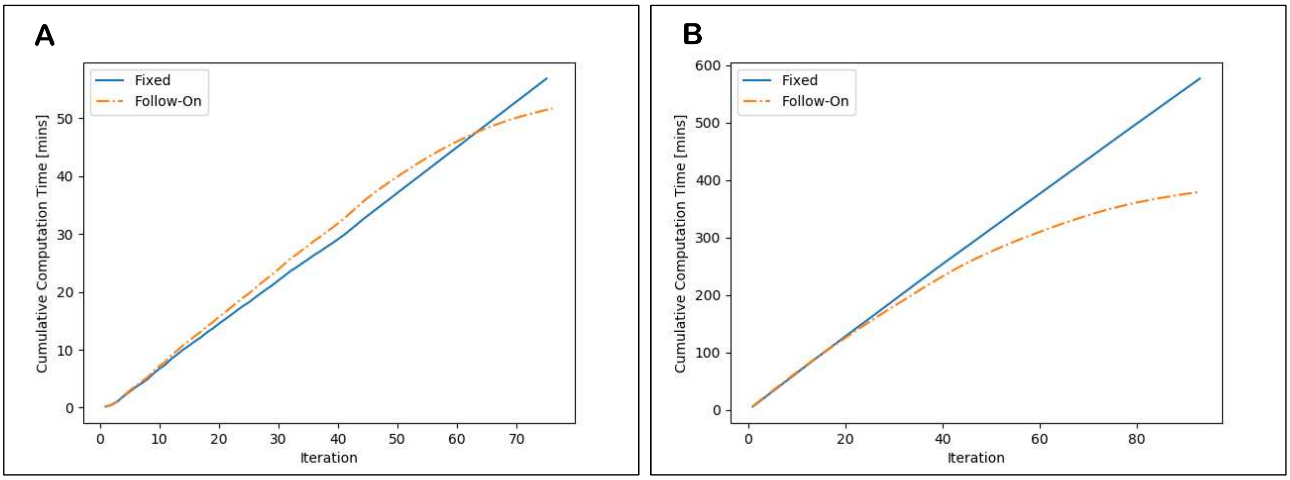

Fig. 6. Cumulative computation times of the iterations during a single run of the BPS SUE algorithm solving BAPS SUE with fixed and follow initial FPIM conditions. **A:** Sioux Falls. **B:** Winnipeg.

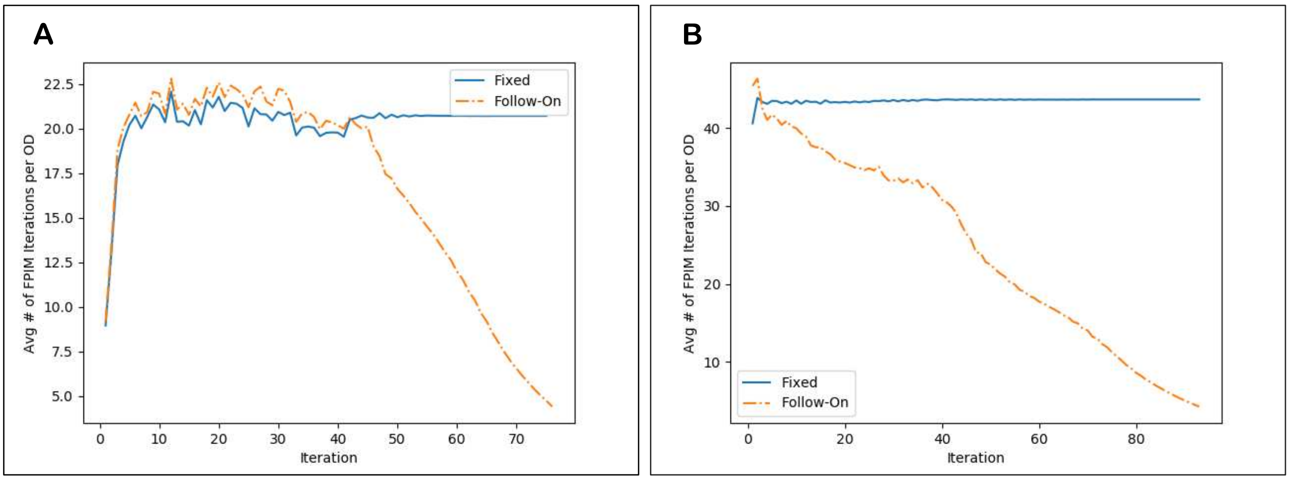

Fig. 7. Average number of BAPS probability fixed-point iterations at each iteration of the BPS SUE algorithm solving BAPS SUE with fixed and follow-on initial conditions. **A:** Sioux Falls. **B:** Winnipeg.

Fig. 8A-B display for the Sioux Falls and Winnipeg networks, respectively, how the total computation time for solving BAPS SUE varies as the FPIM probability convergence parameter ξ is increased, with fixed and follow-on initial FPIM conditions. Fig. 9A-B display how the average number of BAPS fixed-point iterations and total number of BPS SUE algorithm iterations vary as ξ is increased.

With fixed FPIM initial conditions, BAPS SUE could not be solved for $\xi < 6$ due to the inaccuracies of the APSL probabilities. For $\xi \geq 6$, as shown, as ξ increases, while the number of iterations required for SUE convergence remains constant, greater numbers of FPIM iterations are required for APSL probability convergence and thus total computation times increase.

With follow-on FPIM initial conditions, like as for APSL SUE, BAPS SUE could be solved for all ξ. For $\xi = -1$, only single FPIM iterations are required for BAPS probability convergence, and with follow-on initial FPIM conditions, solving BAPS SUE this way simulates solving BAPS′ SUE. Increasing ξ increases the number of FPIM iterations required for BAPS probability convergence and the accuracy of the BAPS probabilities, but the BAPS SUE solution obtained is the same. As shown, convergence of BAPS′ SUE (BAPS SUE with small ξ & follow-on conditions) is slow. Increasing ξ (generally) improves SUE convergence, with exceptions at small ξ, up until a minimum number of BPS SUE algorithm iterations is reached for solving with accurate BAPS probabilities. With these algorithm and model specifications, the convergence of BAPS′ SUE is not so slow that total computation times are high. However, best total computation times come from intermediate values of ξ whereby suitable SUE convergence meets suitable iteration computation times, approximately $\xi = 1$ and $\xi = 0$ for Sioux Falls and Winnipeg, respectively.

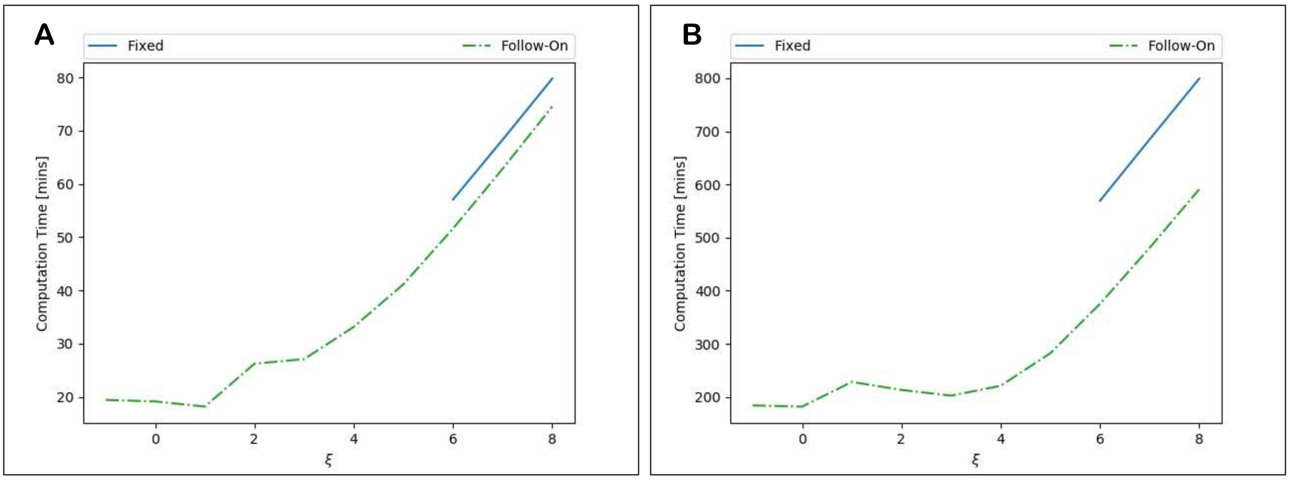

Fig. 8. Computation time for solving BAPS SUE as the BAPS model probability convergence parameter ξ is increased, with fixed and follow-on initial FPIM conditions. **A:** Sioux Falls. **B:** Winnipeg.

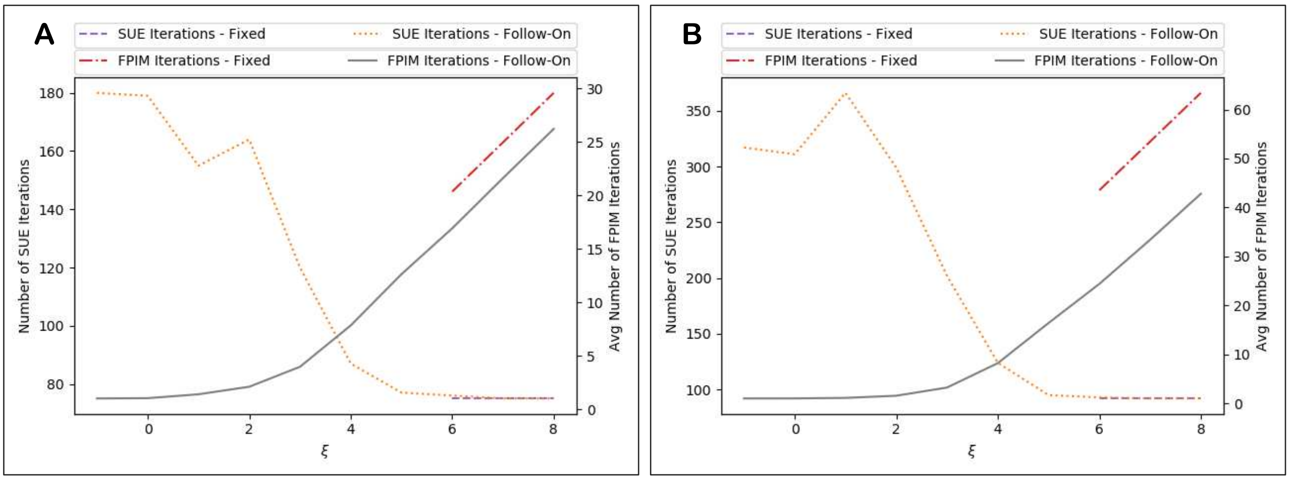

Fig. 9. Average number of BAPS model fixed-point iterations and total number of BPS SUE algorithm iterations solving BAPS SUE as ξ is increased. **A:** Sioux Falls. **B:** Winnipeg.

Alternatively, utilising follow-on conditions, one can stipulate a set number of FPIM iterations to perform at each BPS SUE algorithm iteration. Supposing that k FPIM iterations are conducted, Fig. 10A-B display the total computation times and number of BPS SUE algorithm iterations solving BAPS SUE, for the Sioux Falls and Winnipeg networks, respectively. As shown, conducting just two FPIM iterations (instead of one) can significantly reduce the number of BPS SUE algorithm iterations required for convergence, and thus total computation times. The optimal values for k appear to be 2 and 3 FPIM iterations, respectively, where suitable SUE convergence meets suitable iteration computation times.

One can also utilise a combination of both techniques for reducing BAPS SUE total computation times and stipulate a maximum number of FPIM iterations to perform and a maximum level of BAPS probability convergence, i.e. the FPIM is stopped if either a maximum of h iterations are conducted or the probabilities have converged sufficiently according to the set parameter ξ. This can potentially save computation times in latter BPS SUE algorithm iterations where the stipulated amount of FPIM iterations unnecessarily overly-converges the BAPS probabilities. Fig. 11A and Fig. 12A display for Sioux Falls how computation times and the number of BPS SUE algorithm iterations / average number of FPIM iterations vary, respectively, for different settings of ξ, where a maximum of 2 FPIM iterations are conducted. Fig. 11B and Fig. 12B display results for Winnipeg where a maximum of 3 FPIM iterations are conducted. As shown, best total computation times come from larger ξ values and the time saved in latter iterations is not significant compared to a greater number of iterations being required for SUE convergence. This is different from the results for APSL SUE in Duncan et al (2022), and is likely due to the iterations being more complex in the BPS SUE algorithm than the FAA. Optimal values of ξ with this technique are approximately $\xi = 7$ and $\xi = 8$ for Sioux Falls and Winnipeg, respectively.

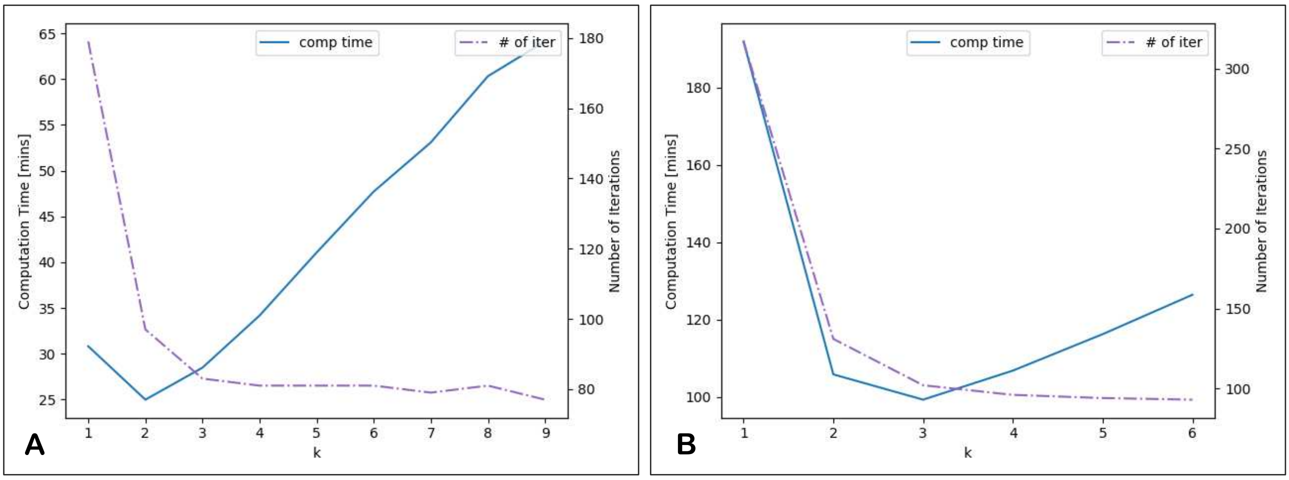

Fig. 10. Total computation times and number of BPS SUE algorithm iterations for solving BAPS SUE utilising follow-on conditions, with h FPIM iterations conducted. **A:** Sioux Falls. **B:** Winnipeg.

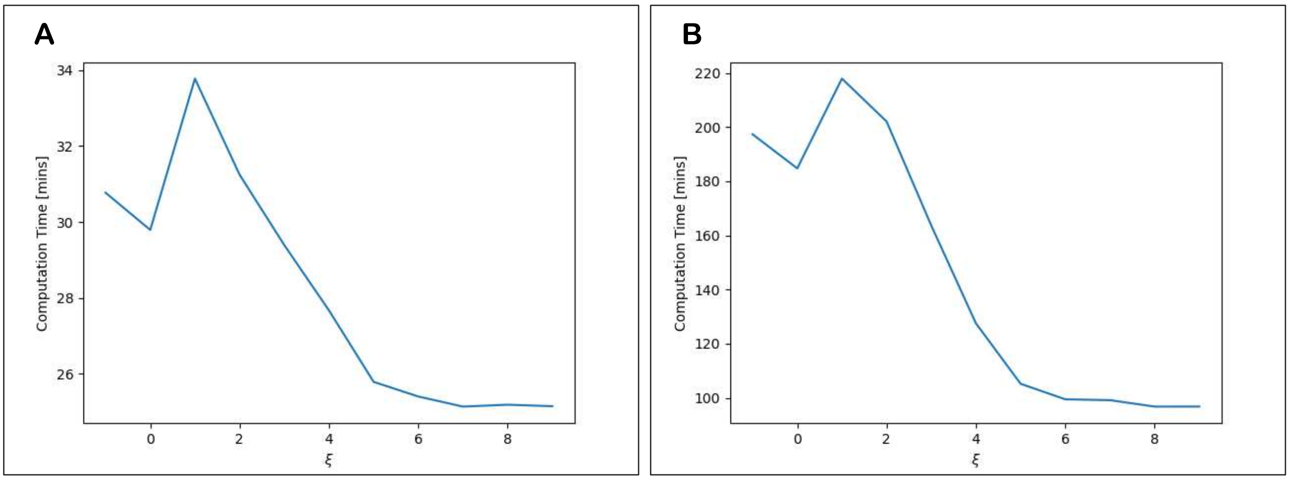

Fig. 11. Total computation times for solving BAPS SUE utilising follow-on conditions as ξ is varied, with a max number of FPIM iterations conducted h. **A:** Sioux Falls ($h = 2$). **B:** Winnipeg ($h = 3$).

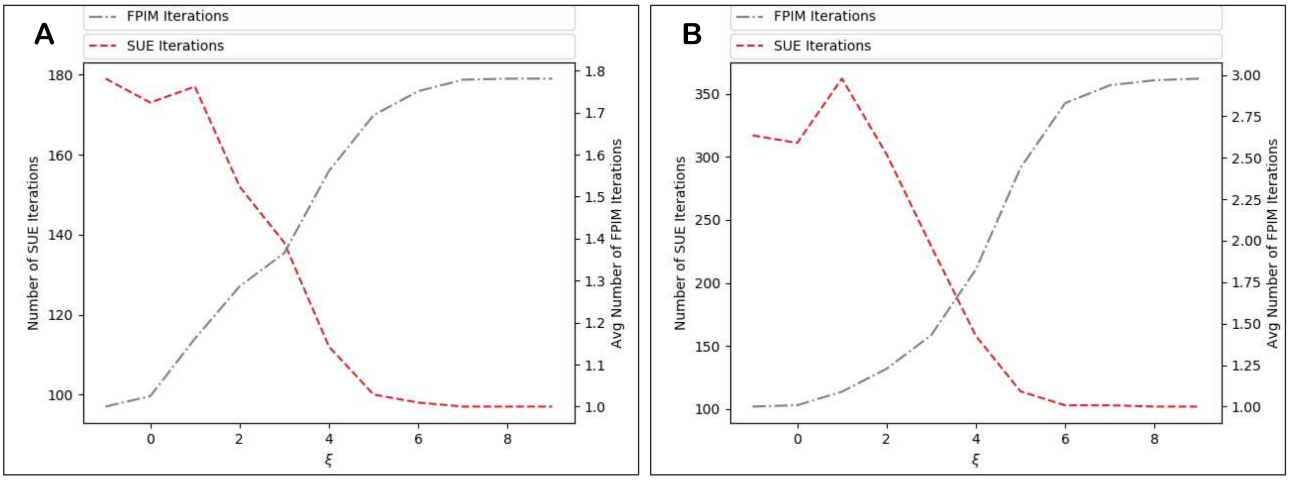

Fig. 12. Number of BPS SUE algorithm iterations, and average number of FPIM iterations for solving BAPS SUE utilising follow-on conditions as ξ is varied, with a max number of FPIM iterations conducted h. **A:** Sioux Falls ($h = 2$). **B:** Winnipeg ($h = 3$).

Considering the above results, for the remainder of the paper, unless stated otherwise, we solve BAPS SUE by stipulating a maximum number of FPIM iterations to perform at each BPS SUE algorithm iteration and a maximum level of BAPS model probability convergence. For Sioux Falls, a maximum of 2 FPIM iterations are conducted with $\xi = 7$. For Winnipeg, 3 FPIM iterations are used with $\xi = 8$. We label for reference this method BAPS SUE*. This 'optimal' method for solving BAPS SUE is of course particular to the network, model, and algorithm specifications, e.g. model parameters, adopted step-size scheme, sizes of the approximated universal choice sets. However, by fixing the optimised values for that particular specification, and then varying the specifications, we will show that the method is robust in its effectiveness compared to solving BAPS SUE in a standard way (i.e. where the BAPS fixed-point probabilities are accurately solved with non-follow-on initial conditions).

Fig. 13A-B display for the Sioux Falls and Winnipeg networks, respectively, the convergence patterns for BAPS SUE* for a single run of the BPS SUE algorithm. Fig. 14A-B display results in terms of computation time, and Fig. 15A-B display how the average used route choice set size varies as the algorithm progresses. As shown, for BAPS SUE*, the number of iterations required to obtain levels of convergence is now less than for BAPS′ SUE, though more than required for BAPS SUE (see Fig. 2). Hence, since the computation times for each iteration of BAPS SUE* are significantly less than for BAPS SUE, total computation times are improved.

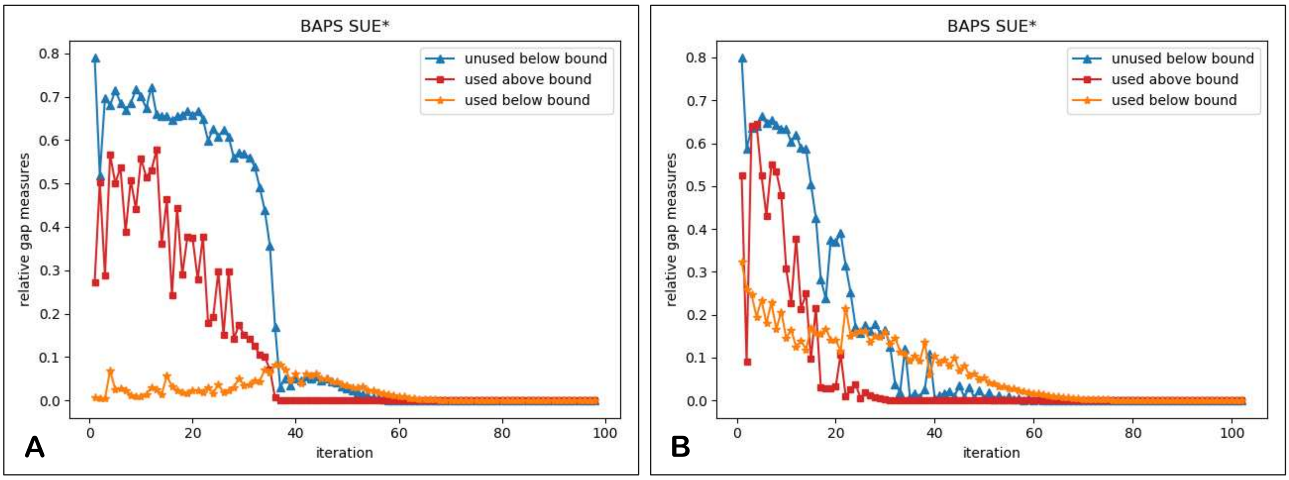

Fig. 13. Relative gap measures for BAPS SUE* at each iteration of the BPS SUE algorithm. **A:** Sioux Falls. **B:** Winnipeg.

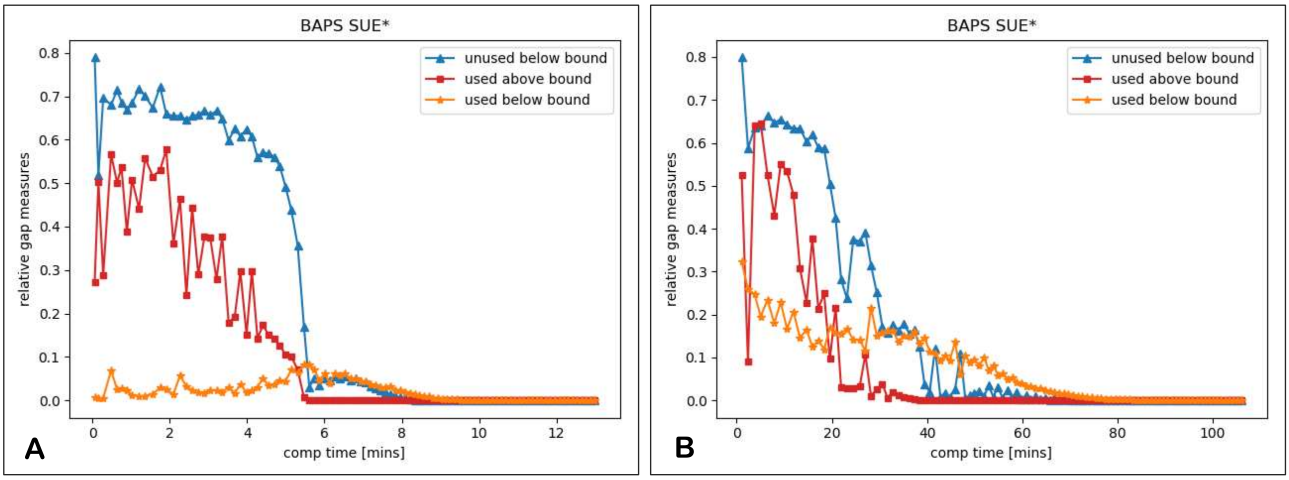

Fig. 14. Relative gap measures for BAPS SUE* in computation time [mins] of the BPS SUE algorithm. **A:** Sioux Falls. **B:** Winnipeg.

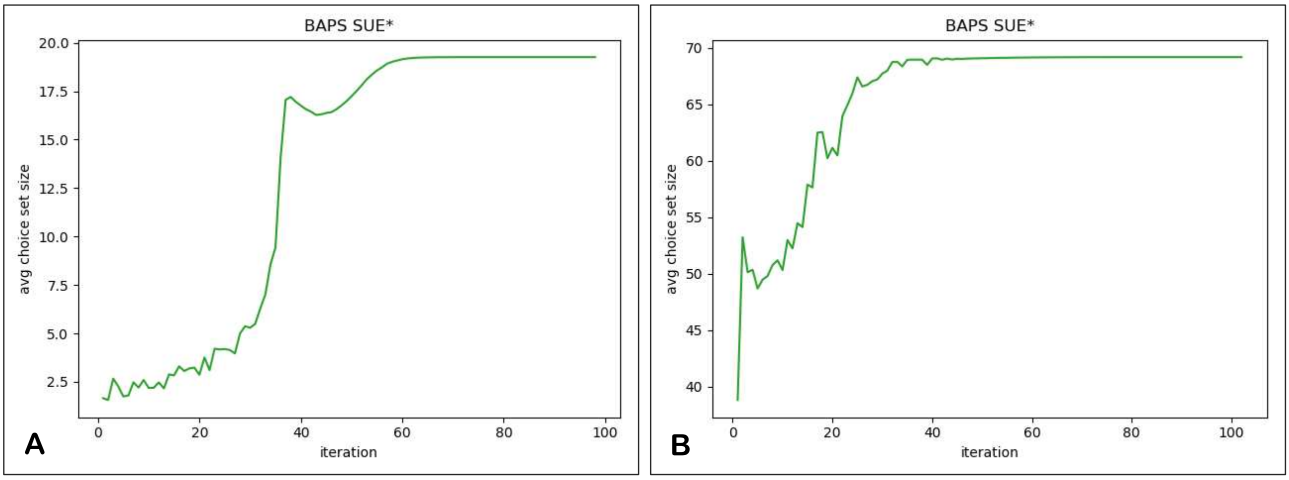

Fig. 15. Average used route choice set size for BAPS SUE* at each iteration of BPS SUE algorithm. **A:** Sioux Falls. **B:** Winnipeg.

Other factors that affect the computational performance of BAPS SUE, in terms of solving the BAPS probability fixed-point problems, include the values of β and φ. As shown in Duncan et al (2021), larger values of β and φ result in greater numbers of FPIM iterations being required for BAPS probability convergence (increasing computation times).

Fig. 16A-B display for the Sioux Falls and Winnipeg networks, respectively, how the computation time for BAPS SUE* as well as for solving BAPS SUE with follow-on and fixed initial FPIM conditions, varies as the β parameter is increased. Fig. 17A-B display how the average number of FPIM iterations per OD movement per BPS SUE algorithm iteration and how the total number of BPS SUE algorithm iterations vary as β is increased. As shown, for BAPS SUE follow-on & fixed, while the number of BPS SUE algorithm iterations do not vary considerably, the average number of FPIM iterations increases exponentially with β and hence so do computation times. For BAPS SUE*, the number of SUE iterations increases as β increases, while the average number of FPIM iterations remains low (decreasing slightly due to more SUE iterations), resulting in the technique significantly improving in effectiveness as β increases.

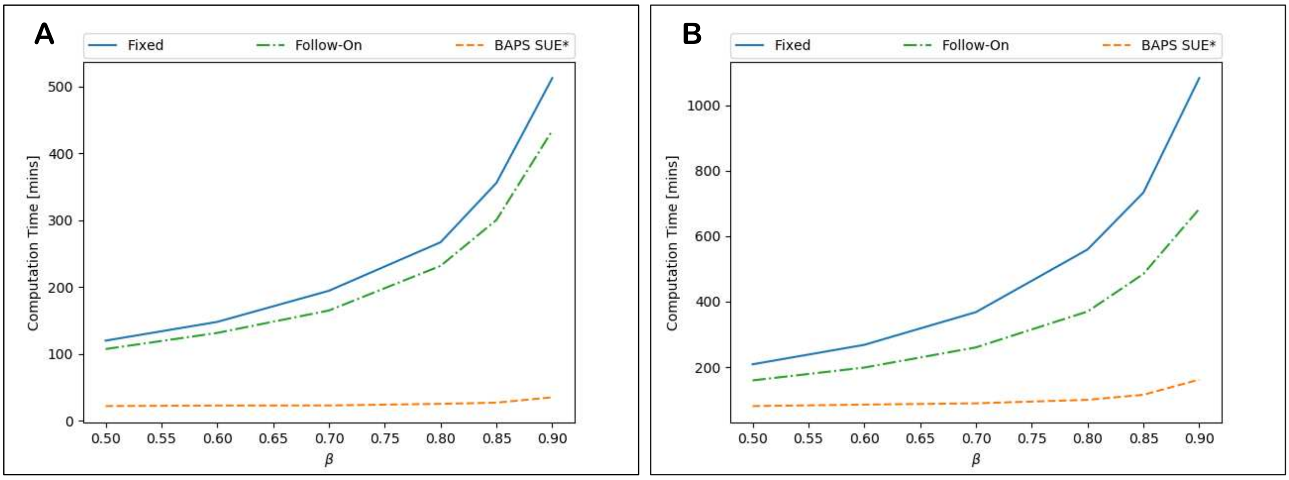

Fig. 16. Computation time for BAPS SUE* and solving BAPS SUE with follow-on and fixed initial FPIM conditions as β is increased. **A:** Sioux Falls. **B:** Winnipeg.

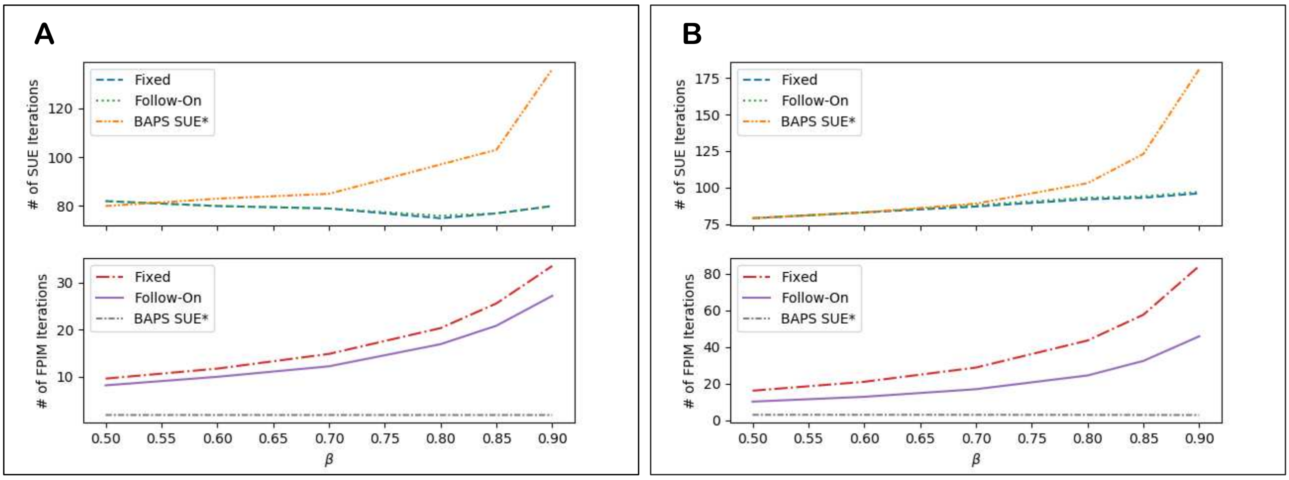

Fig. 17. Number of BPS SUE algorithm iterations, and average number of FPIM iterations for BAPS SUE*, and solving BAPS SUE with follow-on and fixed initial FPIM conditions as β is increased. **A:** Sioux Falls. **B:** Winnipeg.

Fig. 18A-B display for the Sioux Falls and Winnipeg networks, respectively, how the computation time for BAPS SUE* as well as for solving BAPS SUE with follow-on and fixed initial FPIM conditions, varies as the φ parameter is increased. Fig. 19A-B display how the average number of FPIM iterations per OD movement per BPS SUE algorithm iteration and how the total number of BPS SUE algorithm iterations vary as φ is increased. As shown for Sioux Falls, for this range of φ, there are no clear trends for the SUE convergence rates as φ is varied, though the average number of FPIM iterations increases with φ, as expected. For Winnipeg, however, there is a clear trend that the number of iterations required for SUE convergence decreases as φ increases. This is due to a greater number of iterations being required to equilibrate the choice sets, which are more restrictive for smaller φ. Total computation times for the bounded SUE models thus decrease with φ in this range, despite greater numbers of FPIM iterations being required for BAPS probability convergence.

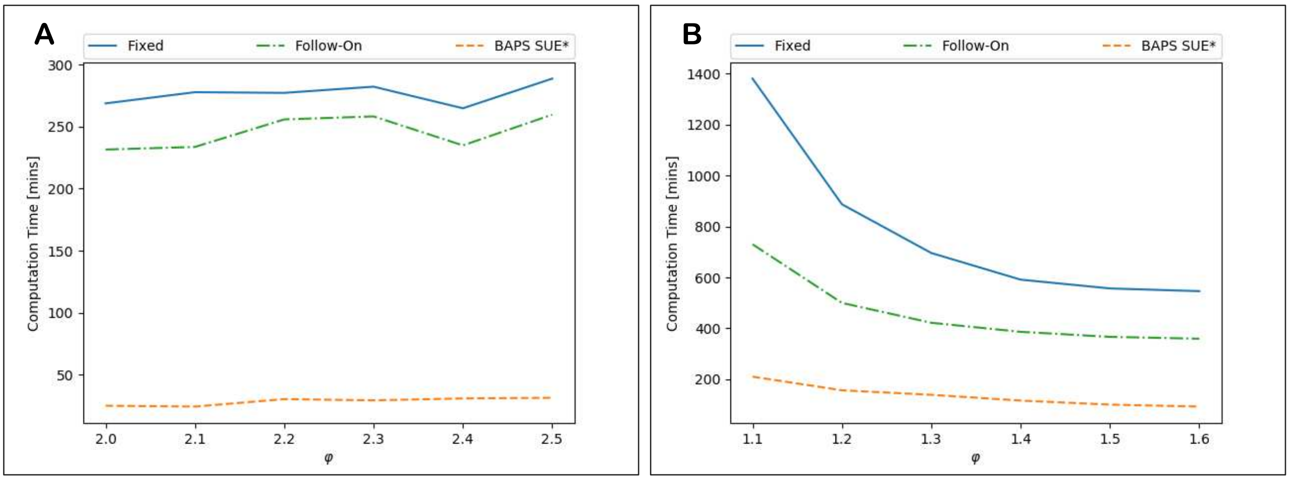

Fig. 18. Computation time for BAPS SUE* and solving BAPS SUE with follow-on and fixed initial FPIM conditions as φ is increased. **A:** Sioux Falls. **B:** Winnipeg.

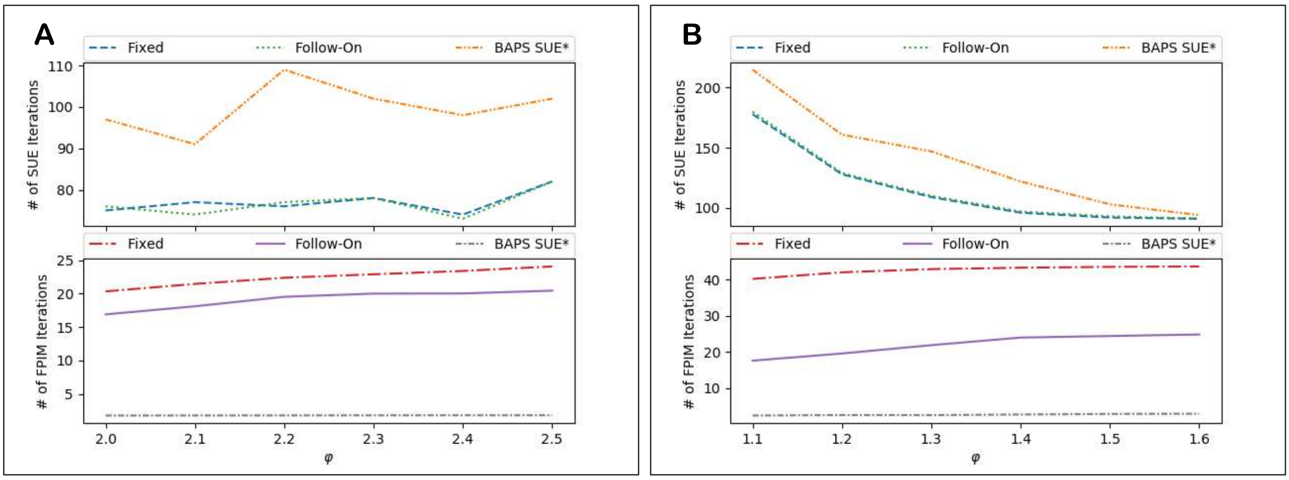

Fig. 19. Number of BPS SUE algorithm iterations, and average number of FPIM iterations for BAPS SUE* and solving BAPS SUE with follow-on and fixed initial FPIM conditions and φ is increased. **A:** Sioux Falls. **B:** Winnipeg.

5.2.3 Sensitivity Analysis

Next, we investigate for the bounded SUE models, how total computation times, number of BPS SUE algorithm iterations, and average used route choice set sizes vary according to levels of travel demand and the model parameters.

Fig. 20A-B display for the Sioux Falls and Winnipeg networks, respectively, how the number of iterations required for SUE convergence varies for the bounded SUE models as the level of travel demand is varied, where the demand is scaled according to the parameter ω so that the demand for OD movement m is $\omega \cdot q_m$, $m = 1, \dots, M$. Fig. 21A-B display results in terms of computation time, and Fig. 22A-B display how the average used route choice set size varies. As shown, and as expected, the number of iterations required for convergence generally increases for the bounded SUE models as the level of demand increases, resulting in longer computation times.

A surprising result is that (at least towards larger demand on Winnipeg) the average used route choice set sizes decrease as the demand level increases. If one considers what one might expect under Deterministic User Equilibrium (Wardrop, 1952), for low demand only the best costing routes are used, and increasing demand results in the used route choice sets expanding. For Winnipeg, the choice set sizes do expand initially as the demand level is increased, but then they decrease in size more significantly. For Sioux Falls, the more heavily congested network, the choice sets decrease in size quite significantly for ω in this range. The suspected reason for this is that for high levels of congestion the costs on all links are inflated, and routes that are used for one OD movement are likely inflating the costs so that routes in other OD movements are then too costly to be used. Sioux Falls is also potentially more susceptible to this due to the way the network is structured, i.e. heavily overlapping OD movements.

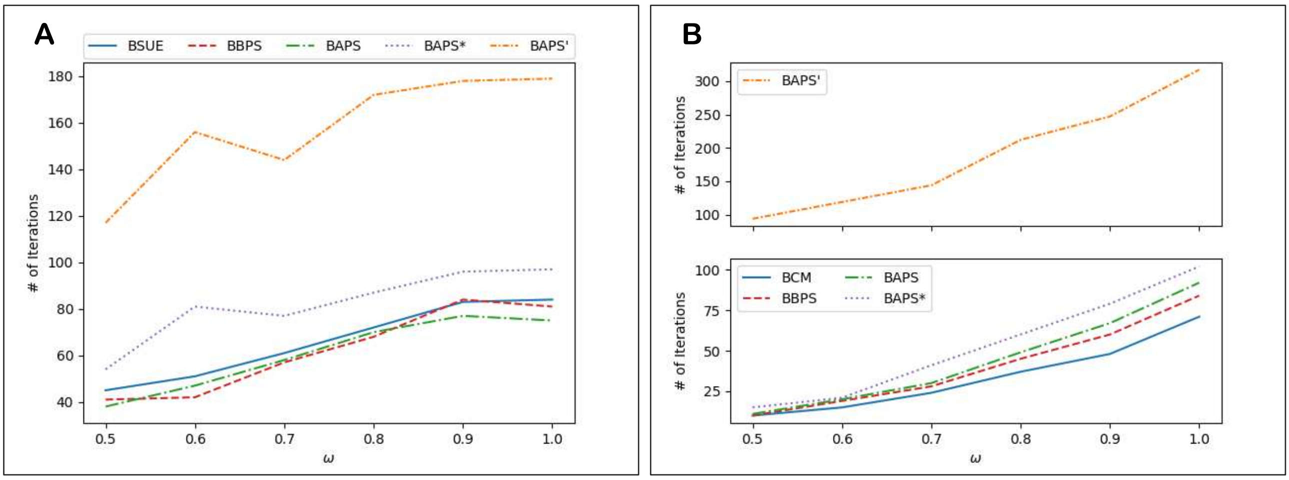

Fig. 20. Number of iterations required for SUE convergence for varying levels of travel demand, scaled by ω. **A:** Sioux Falls. **B:** Winnipeg.

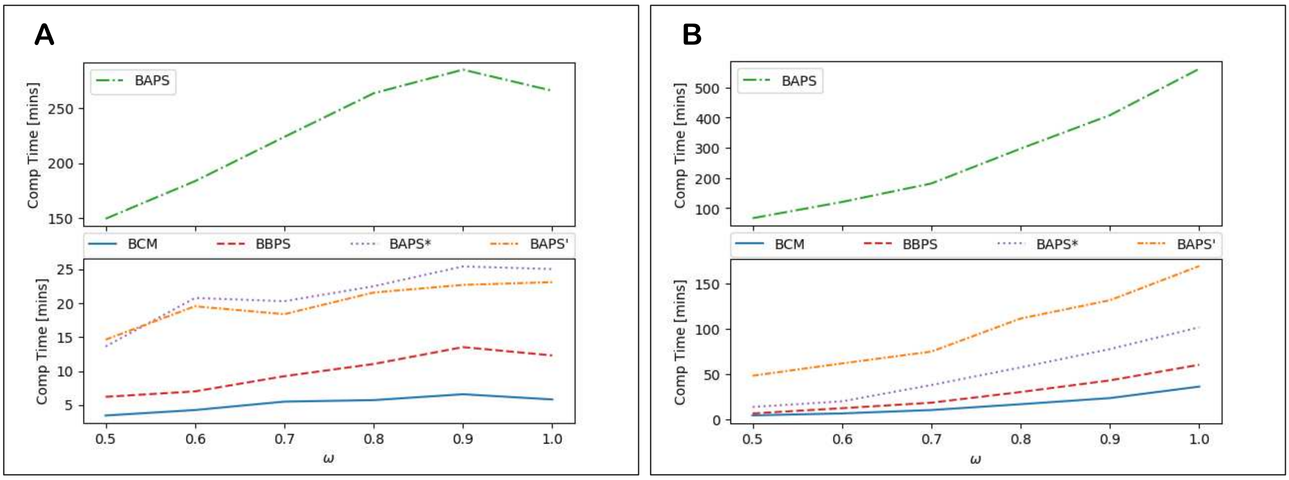

Fig. 21. Computation time [mins] required for SUE convergence for varying levels of travel demand, scaled by ω. **A:** Sioux Falls. **B:** Winnipeg.

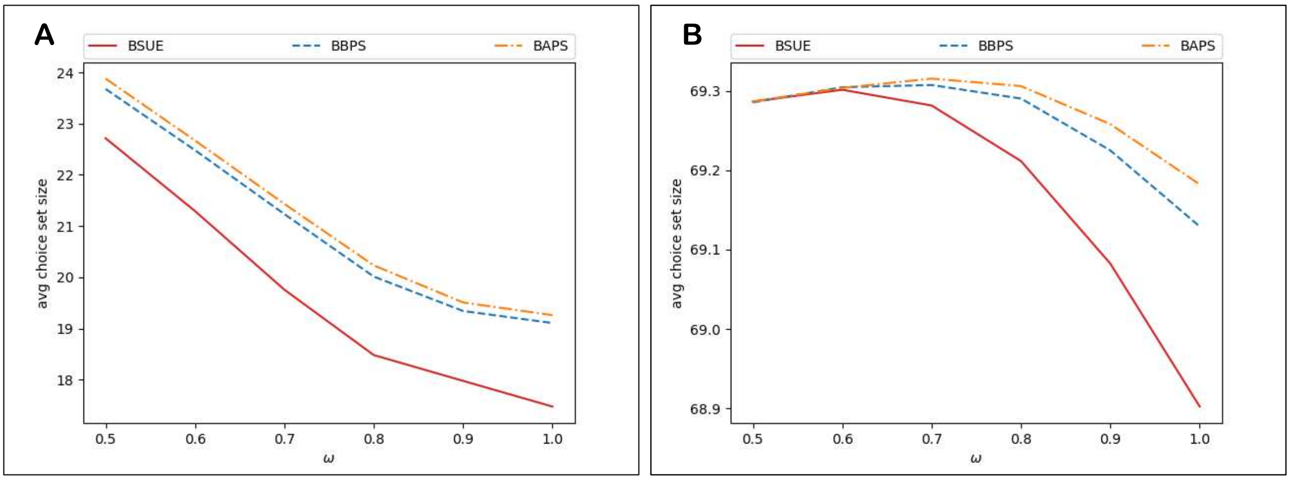

Fig. 22. Average used route choice set size for the bounded SUE models with different levels of travel demand, scaled by ω. **A:** Sioux Falls. **B:** Winnipeg.

Fig. 23A-B display for the Sioux Falls and Winnipeg networks, respectively, how the number of iterations required for SUE convergence varies for the BPS SUE models as the β parameter is varied. Fig. 24A-B display results in terms of computation time, and Fig. 25A-B display how the average used route choice set size varies. As shown, for BBPS SUE and BAPS SUE, only a small increase in the number of iterations required for convergence occurs as β is increased, though for BAPS SUE – as also shown in Fig. 16/Fig. 17 – total computation times increase exponentially with β due to the fixed-point probability computation. For BAPS′ SUE and BAPS SUE*, the number of BPS SUE algorithm iterations increases exponentially with β, and for $\beta = 0.9$ on Winnipeg, BAPS′ SUE actually takes longer than BAPS SUE. Albeit marginally, the average used route choice sizes increase for the BBPS/BAPS SUE models as β increases. As shown in Fig. 22 & Fig. 28, BSUE tends to equilibrate smaller used route choice sets than the BPS SUE models. Decreasing β tends the BPS SUE models towards BSUE and thus it makes sense that decreasing β results in smaller choice sets. The reason that BSUE is equilibrating smaller used route choice sets than the BPS SUE models, must be due to the path size correction factors in the probability relations pushing flow to the low costing route(s), thus expanding the bound and including more used routes.

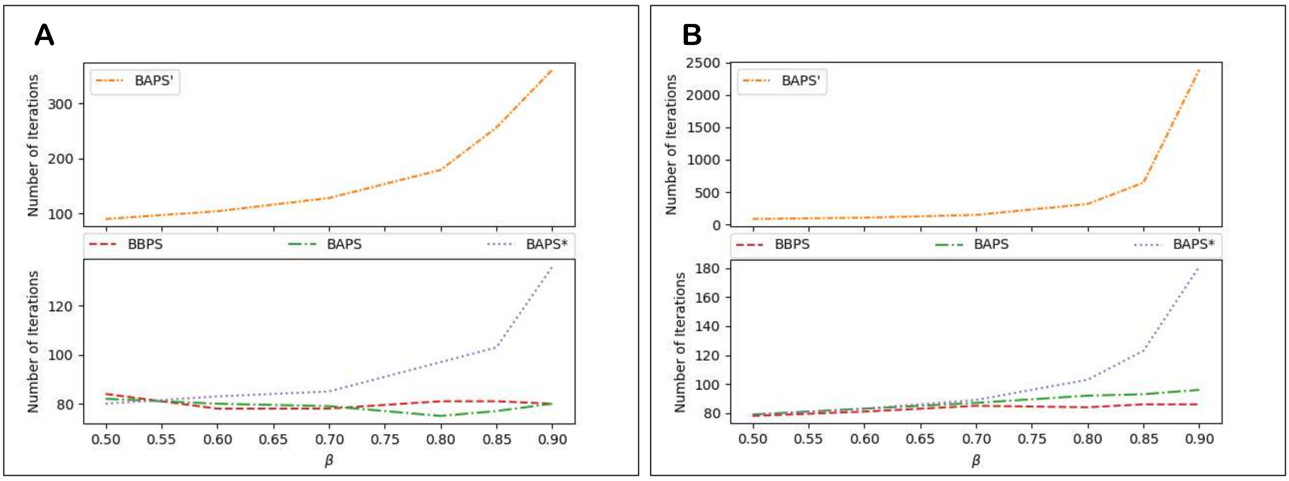

Fig. 23. Number of iterations required for SUE convergence as the β parameter is varied. **A:** Sioux Falls. **B:** Winnipeg.

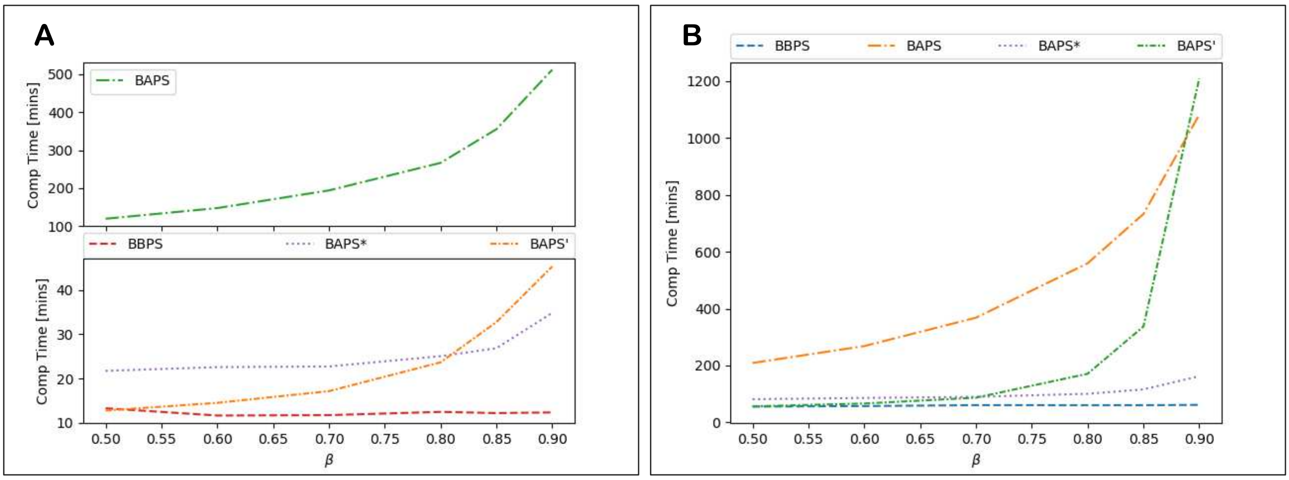

Fig. 24. Computation time [mins] required for SUE convergence as the β parameter is varied. **A:** Sioux Falls. **B:** Winnipeg.

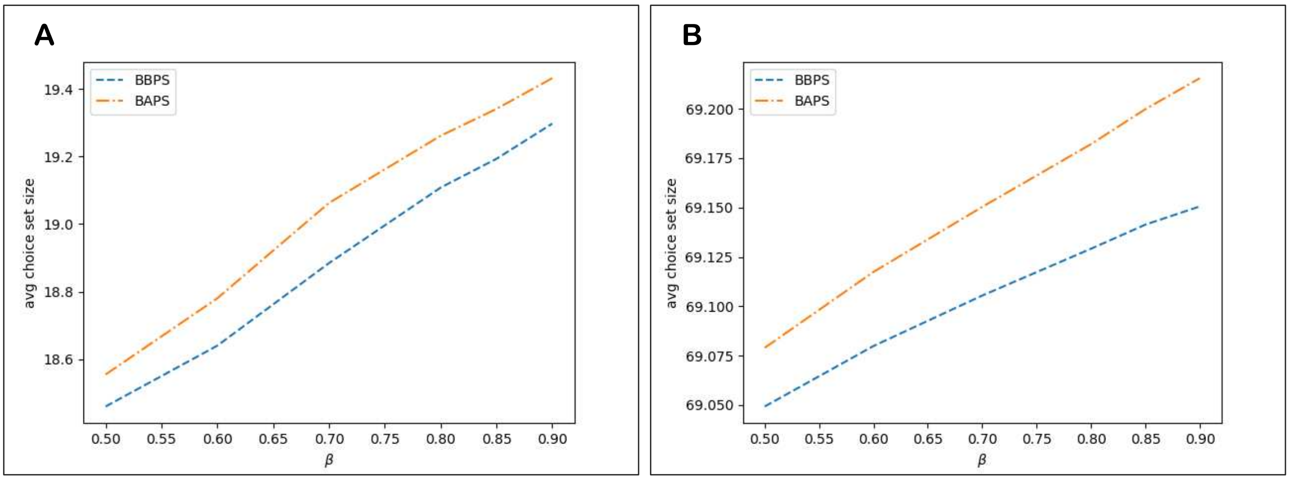

Fig. 25. Average choice set size for the BPS SUE models as the β parameter is varied. **A:** Sioux Falls. **B:** Winnipeg.

Fig. 26A-B display for the Sioux Falls and Winnipeg networks, respectively, how the number of iterations required for SUE convergence varies for the BPS SUE models as the φ parameter is varied. Fig. 27A-B display results in terms of computation time, and Fig. 28A-B display how the average used route choice set size varies. As expected, the used route choice set sizes expand as the bound parameter φ increases. As shown for Sioux Falls, there appears to be no clear trend for the SUE convergence rates in this range of φ, though computation times generally increase due to the greater number of active routes. For Winnipeg, the SUE convergence rates improve as φ increases in this range, improving computation times.

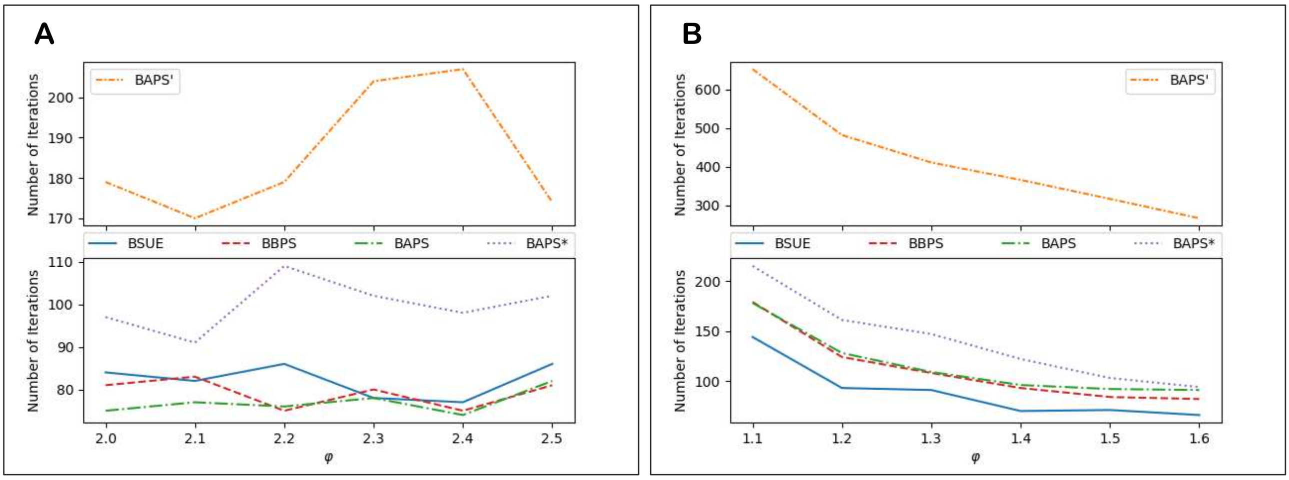

Fig. 26. Number of iterations required for SUE convergence as the φ parameter is varied. **A:** Sioux Falls. **B:** Winnipeg.

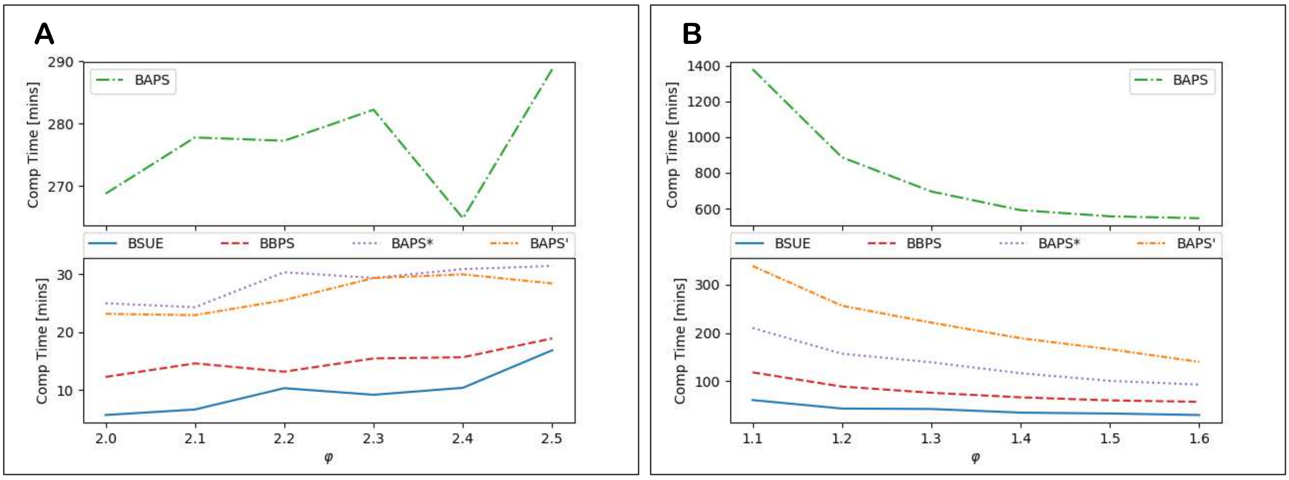

Fig. 27. Computation time [mins] required for SUE convergence as the φ parameter is varied. **A:** Sioux Falls. **B:** Winnipeg.

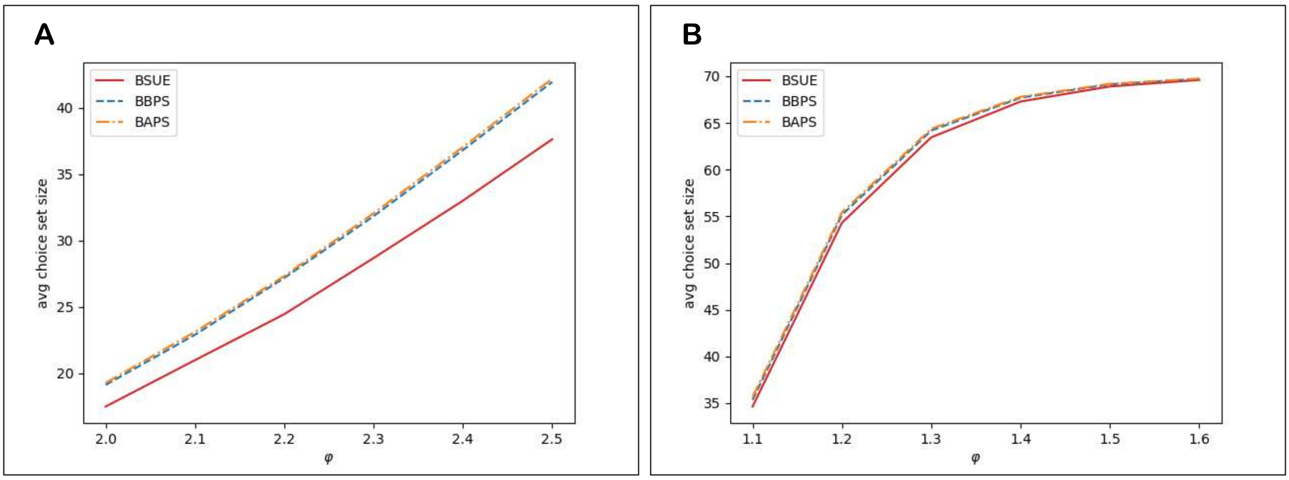

Fig. 28. Average choice set size for the bounded SUE models as the φ parameter is varied. **A:** Sioux Falls. **B:** Winnipeg.

The figures are omitted from the paper, but in similar experiments, for Sioux Falls and Winnipeg the SUE convergence rate worsened for the bounded SUE models as the θ parameter was increased, resulting in longer computation times. This is because the route cost differences are accentuated more with large θ resulting in greater flow fluctuations.

5.3 Flow Results

In this subsection we compare the flow results from the different SUE models. To compare the flow results $\boldsymbol{f}^{*R1}$ and $\boldsymbol{f}^{*R2}$ for Result 1 and Result 2, respectively, we measure the Root Mean Squared Error (RMSE):

$$RMSE = \sqrt{\sum_{m=1}^{M} \sum_{i \in R_m} \left(f_{m,i}^{*R1} - f_{m,i}^{*R2}\right)^2 / N},$$

where N is the total number of routes.

We begin by demonstrating the relationships between the bounded and non-bounded SUE models. The bounded models all approach limit models as the bound $\varphi \to \infty$ and all routes become used. MNL is the limit model of the BCM, GPSL$'$ is the limit model of the BBPS model, and APSL is the limit model of the BAPS model. Fig. 29 thus displays the differences between MNL SUE & BSUE, GPSL$'$ SUE & BBPS SUE, and APSL SUE & BAPS SUE respectively, as φ is increased, A: Sioux Falls, B: Winnipeg. As expected, similarity to the limit models increases as φ increases.

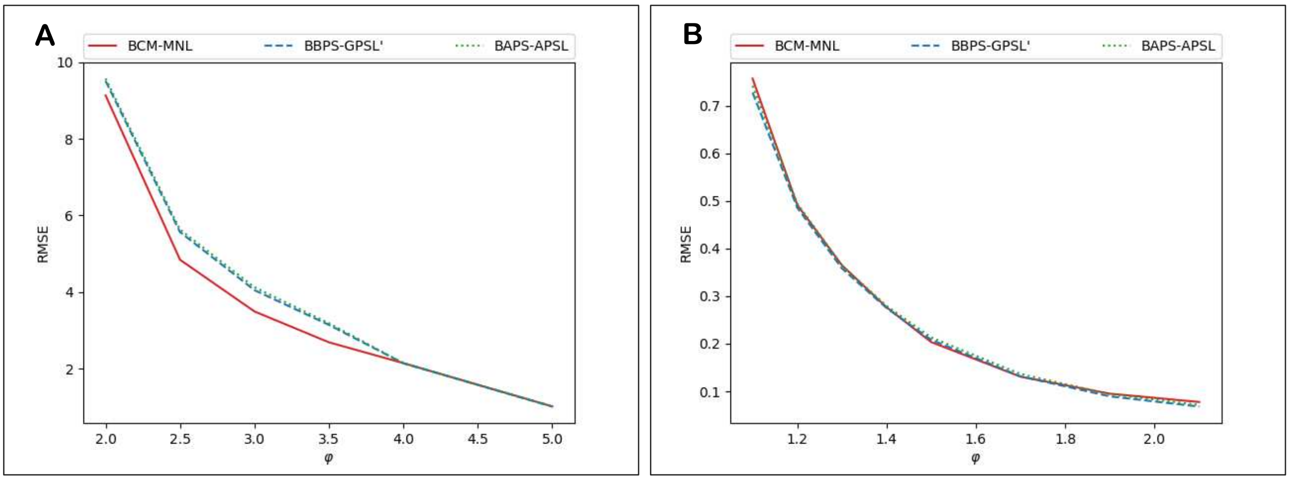

Fig. 29. Difference between MNL SUE & BSUE, GPSL$'$ SUE & BBPS SUE, and APSL SUE & BAPS SUE as the bound φ is increased. **A:** Sioux Falls. **B:** Winnipeg.

We next consider the differences in flow results between the bounded SUE models. Fig. 30A-B display for Sioux Falls and Winnipeg, respectively, the impact the φ parameter has on the differences in SUE flow between the models. As shown, BBPS & BAPS SUE as expected are the most similar, while BAPS SUE is the most different to BSUE. The similarity between BSUE and BBPS/BAPS SUE decreases as φ increases. This is likely because there are more routes to capture the correlation between as φ increases, and thus the path size terms have a greater impact upon the probability relations.

Fig. 31A-B display the impact of the θ parameter. As shown, the similarity between BBPS & BAPS SUE increases initially as θ increases: increasing θ increases the prominence of the travel cost components in the BAPS path size contribution factors, for low θ the distinctiveness components are more prominent increasing the difference to the BBPS factors.

Fig. 32A-B display the impact of the β parameter. The β parameter captures sensitivity to route distinctiveness, where increasing β moves the BBPS/BAPS probabilities away from the BCM probabilities. Therefore, as shown, the flow differences between the BPS SUE models and BSUE all increase as β increases. The flow differences between BBPS & BAPS SUE also increases as β increases as the difference between the model are the different path size correction terms scaled by β. For BAPS SUE, the impact is more significant for larger β, where the contribution influence of distinctiveness is more significant within the BAPS path size terms. Note that if routes are more overlapping, the sensitivity to the β parameter is expected to be greater since the path size correction factors will be greater (path size terms will be smaller).

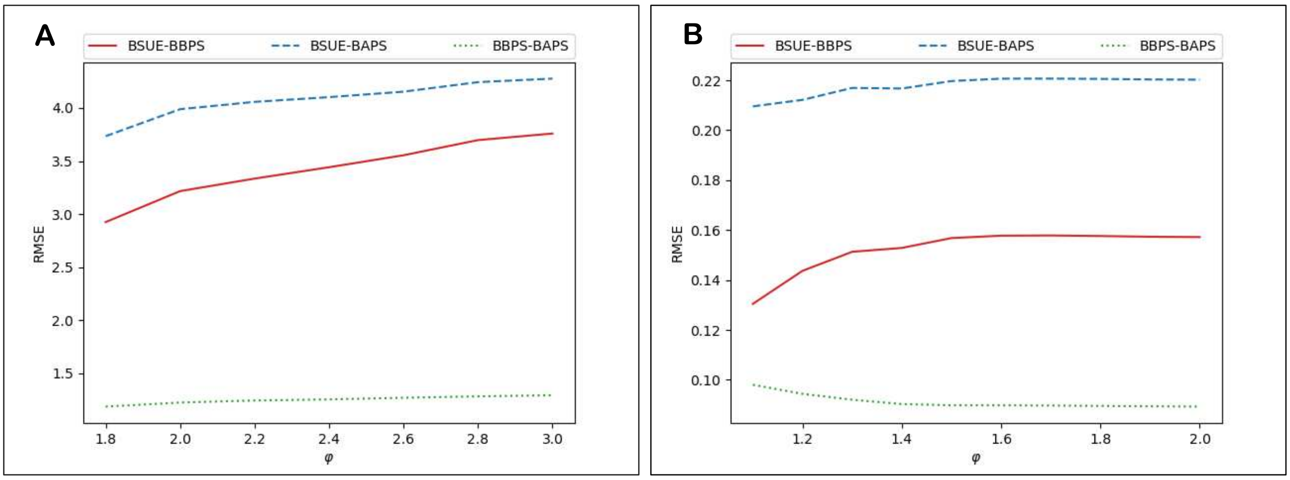

Fig. 30. Impact of the φ parameter on the difference in SUE flow between the bounded SUE models. **A:** Sioux Falls. **B:** Winnipeg.

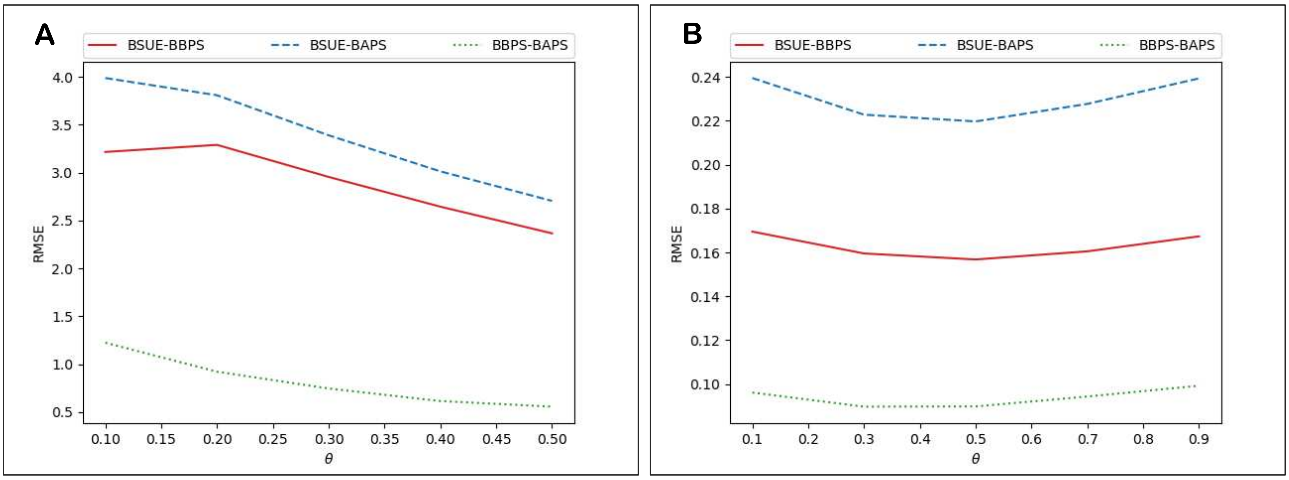

Fig. 31. Impact of the θ parameter on the difference in SUE flow between the bounded SUE models. **A:** Sioux Falls. **B:** Winnipeg.

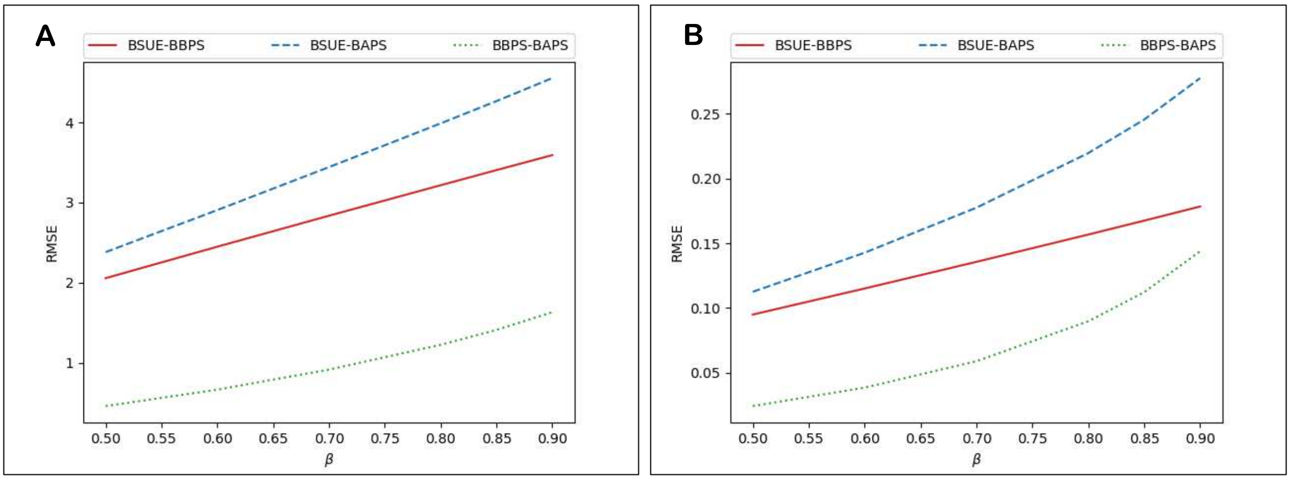

Fig. 32. Impact of the β parameter on the difference in SUE flow between the bounded SUE models. **A:** Sioux Falls. **B:** Winnipeg.

Next, we assess choice set robustness for the bounded SUE models (robustness to the approximated universal choice sets). In Duncan et al (2022) we assessed choice set robustness for internally consistent SUE formulations of numerous correlation-based route choice models, namely: PSL, GPSL, APSL, C-Logit (CL), Cross-Nested Logit (CNL), and Generalised Nested Logit (GNL). It was shown that GPSL & APSL SUE generally performed the best due to having explicit mechanisms for dealing with unrealistic routes in the correlation components. All routes receive non-zero flows however, and the mechanisms only reduce the effects of unrealistic routes. The BPS SUE models have significantly greater potential to be more effective in dealing with unrealistic routes, and we anticipate that choice set robustness should be significantly improved.

Adopting a similar experiment to that in Duncan et al (2022), Fig. 33A-B display for the Sioux Falls and Winnipeg networks, respectively, the impact that varying the bound parameter φ has on choice set robustness for the bounded SUE models. To assess choice set robustness, flow results are compared between two different approximated universal choice sets, where the second set of choice sets expands the first, thus mimicking choice set mis-generation and the inclusion of unrealistic routes. The two choice sets are obtained by generating all routes (from the full pre-generated choice sets) with a free-flow travel time less than ψ times as much as the free-flow travel time on the quickest route for each OD movement. For Sioux Falls, the base-level choice sets are those obtained with $\psi = 2.3$, and the expanded choice sets are those obtained with $\psi = 2.5$ (i.e. in this case the full pre-generated choice sets). For Winnipeg, the equivalent values are $\psi = 1.4$ and $\psi = 2.5$, respectively. Fig. 34A-B display for the Sioux Falls and Winnipeg networks, respectively, the average used route choice set sizes vary for the bounded SUE models as φ is varied, for the base-level and expanded approximated universal choice sets. Note that for Sioux Falls the $\psi = 2.3$ and $\psi = 2.5$ universal choice sets have average sizes 54.8 and 81.9, respectively. For Winnipeg, the $\psi = 1.4$ and $\psi = 2.5$ choice sets have average sizes 67.9 and 70.2, respectively.

As Fig. 33A-B show, the bounded SUE models do indeed have significant potential to improve choice set robustness. As $\varphi \to \infty$, BSUE tends towards MNL SUE, BBPS SUE tends towards GPSL′ SUE, and BAPS SUE tends towards APSL SUE. As can be seen, decreasing the bound parameter φ from large φ (where $\varphi \to \infty$ is approximated), improves choice set robustness for the bounded SUE models. For large bound values, the additional routes in the expanded choice sets have equilibrated costs within the bound and thus receive non-zero flows. This means that for the expanded choice sets solutions, the flows on the non-additional routes (those in the base-level choice sets) are adjusted from the base SUE solution. Lower bound values assign additional routes zero flows which reduces the impact they have on the non-additional route flows, thereby improving choice set robustness. As Fig. 34A-B show, decreasing φ reduces the difference between the equilibrated used routes from the base-level and the expanded approximated universal choice sets.

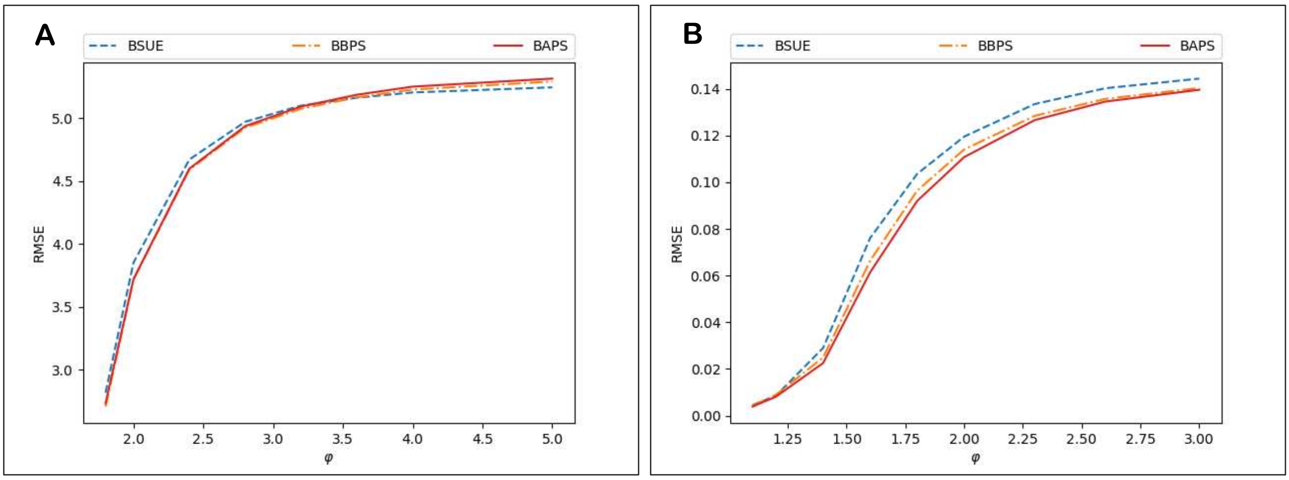

Fig. 33. Impact of the φ parameter on choice set robustness for the bounded SUE models. **A:** Sioux Falls. **B:** Winnipeg.

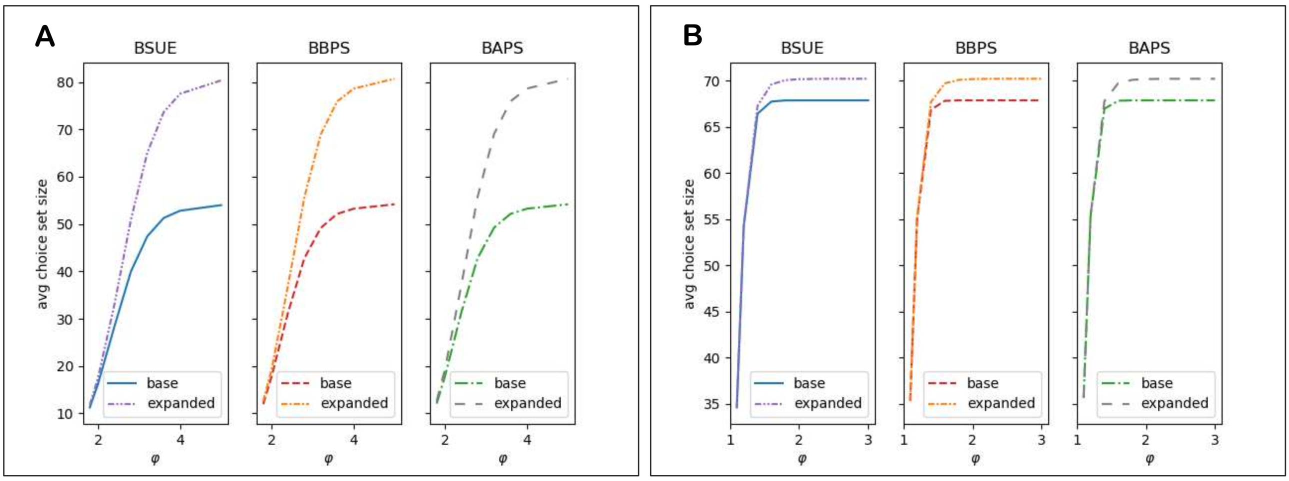

Fig. 34. How the average equilibrated used route choice set sizes vary for the bounded SUE models as the bound parameter φ is varied, for the base-level and expanded approximated universal choice sets. **A:** Sioux Falls. **B:** Winnipeg.

Lastly, we explore how the stringency of the SUE convergence criteria (i.e. values of ζ, see Section 5.1) impacts the differences between BAPS′ route flow proportion ratios and BAPS choice probability ratios at BAPS′ SUE / BAPS SUE. Fig. 35A displays for two overlapping routes (from the same OD movement) on the Sioux Falls network, how the ratio of the route flows at BAPS′ SUE and the ratio of the choice probabilities at BAPS SUE vary as the SUE convergence parameter ζ is increased (made more stringent). As shown, the difference between the BAPS′ SUE flow ratio (i.e. $\frac{f_{m,i}}{f_{m,k}}$) and BAPS SUE probability ratio (i.e. $\frac{P_{m,i}}{P_{m,k}}$) decreases as the convergence criteria increases in stringency, where for low stringency the difference can be quite big. This illustrates the importance of setting feasibly stringent convergent criteria. However, to be sure the BAPS′ SUE path size contribution factors are suitably similar to the BAPS SUE factors at convergence, one could at the last iteration solve the BAPS probabilities given the converged link costs, then output the corresponding auxiliary flow vector.

Fig. 35B displays how the RMSE difference between the BAPS′ SUE and BAPS SUE solutions varies. As shown, the difference between the BAPS′ SUE and BAPS SUE solutions naturally decreases with the increasing stringency. This is not different however than solving any other model with e.g. different initial SUE conditions – less stringent convergence criteria will of course mean greater differences between solutions. Note that in the experiments in this paper we set the convergence parameter to $\zeta = 4$, which provides a suitable level of convergence.

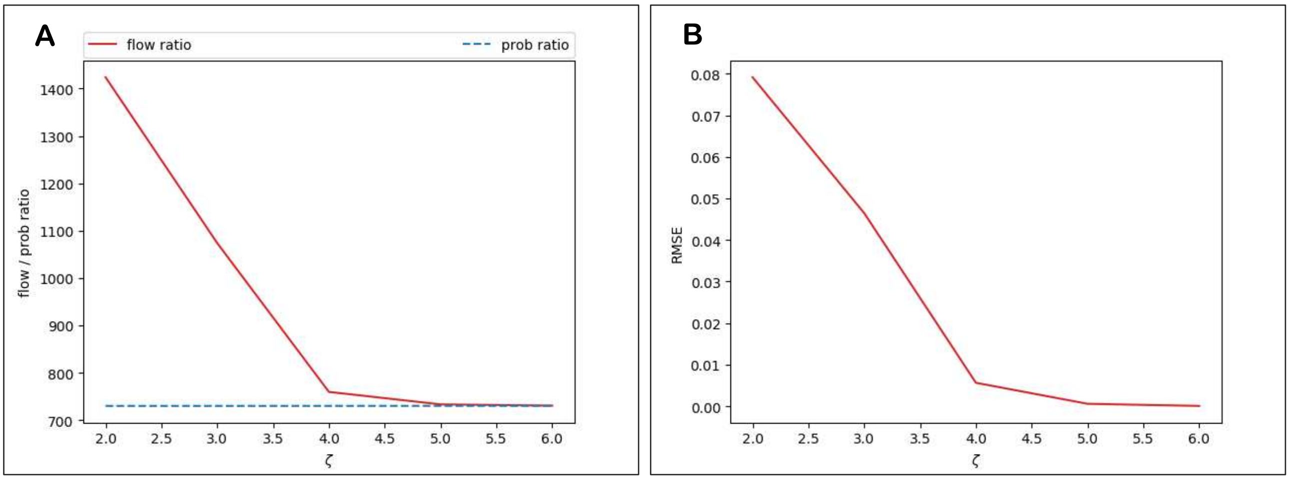

Fig. 35. Sioux Falls. **A:** How the ratio of route flow proportion at BAPS′ SUE and ratio of choice probability at BAPS SUE between two overlapping routes vary as the SUE convergence parameter ζ is increased (made more stringent). **B:** RMSE difference between the BAPS′ SUE and BAPS SUE solution as the SUE convergence parameter ζ is increased.

5.4 Uniqueness of BAPS SUE Solutions

As discussed in Section 3.3, it is not possible to prove that BBPS SUE or BAPS SUE solutions can be unique according to standard approaches. In Duncan et al (2022), the uniqueness of APSL SUE solutions was investigated numerically, where the results suggested uniqueness conditions exist. Due to the similarities between the APSL SUE and BAPS SUE models, we conduct similar experiments to investigate the uniqueness of BAPS SUE solutions numerically.

As demonstrated in Duncan et al (2021), for a given setting of the link costs $\boldsymbol{t}$ and θ and φ values, a β value exists, $\beta_{max,m}(\boldsymbol{t},\theta,\varphi) > 0$, for OD movement m such that BAPS model choice probability solutions are unique for all β in the range $0 \le \beta \le \beta_{max,m}(\boldsymbol{t},\theta,\varphi)$. This means that a β value exists, $\beta_{max}(\boldsymbol{t},\theta,\varphi) > 0$, such that solutions are unique for all OD movements for all β in the range $0 \le \beta \le \beta_{max}(\boldsymbol{t},\theta,\varphi)$, i.e. $\beta_{max}(\boldsymbol{t},\theta,\varphi) = \min\left(\beta_{max,m}(\boldsymbol{t},\theta,\varphi)\right)$. And, assuming the link costs are bounded, i.e. they have a maximum and minimum value (for example due the fixed demands), for a given θ value, a β value exists, $\bar{\beta}_{max}(\theta,\varphi) > 0$, such that BAPS model solutions are unique for all OD movements and for all feasible flow vectors (and thus costs) for all β in the range $0 \le \beta \le \bar{\beta}_{max}(\theta,\varphi)$. Obviously, $\bar{\beta}_{max}(\theta,\varphi) \le \beta_{max}(\boldsymbol{t},\theta,\varphi) \le \beta_{max,m}(\boldsymbol{t},\theta,\varphi)$.

In Duncan et al (2022) it was found that APSL SUE solutions appeared to be unique when APSL probabilities were universally unique. Thus, while it is not guaranteed that in all cases BAPS SUE solutions will be unique when BAPS models probabilities are universally unique, i.e. for β in the range $0 \le \beta \le \bar{\beta}_{max}(\theta,\varphi)$, as we show below, it appears from numerical experiments that this is also often the case.

Fig. 36A-B plot, for two runs, the small example network route flows at each iteration of the BPS SUE algorithm solving BAPS SUE, when the initial conditions for the FPIM computing the BAPS model probabilities are randomly generated, for $\beta = 0.9$ and $\beta = 1.1$, respectively, $\theta = 1$, $\varphi = 1$, $\xi = 10$. The MSWA step-size scheme is adopted with $d = 10$, and the algorithm is stopped after 20 iterations if convergence is not reached. As shown, for $\beta = 0.9$, because the BAPS model probabilities are unique for the route costs (from the flows) at each iteration, the route flows on both runs converge in the same way to the same BAPS SUE solution. For $\beta = 1.1$, however, as demonstrated clearly at iteration 12, there are multiple BAPS model probabilities for the route costs at each iteration, and hence due to the step-size the flows fluctuate randomly and do not converge. This suggests that BAPS model probability solutions are universally unique for $\beta = 0.9$, but not for $\beta = 1.1$, and hence that $0.9 \leq \bar{\beta}_{max}(1) < 1.1$.

Fig. 37A-B plot for $\beta = 0.9$ and $\beta = 1.1$, respectively, and for multiple runs, the flows at each iteration of the BPS SUE algorithm solving BAPS SUE utilising follow-on initial conditions for the FPIM computing the BAPS model probabilities, where the SUE initial conditions are randomly generated, $\theta = 1$, $\varphi = 1$, $\xi = 10$. The initial SUE conditions for the BPS SUE algorithm in Algorithm 1 are All-Or-Nothing assignments. To instead randomly generate initial SUE conditions here, we first suppose all routes are used and randomly generate flows for these routes (maintaining demand-feasibility). A bound condition phase is then conducted to remove routes with consequent costs above the bound and redistribute the flows accordingly. As shown, for $\beta = 0.9$, all initial SUE conditions lead to the same solution, whereas for $\beta = 1.1$, two solutions are found with different initial conditions. Fig. 38A-B plot the flows at each iteration of the BPS SUE algorithm solving BAPS′ SUE. As shown, for $\beta = 0.9$, all initial conditions again lead to the same solution, whereas for $\beta = 1.1$, two solutions are found.

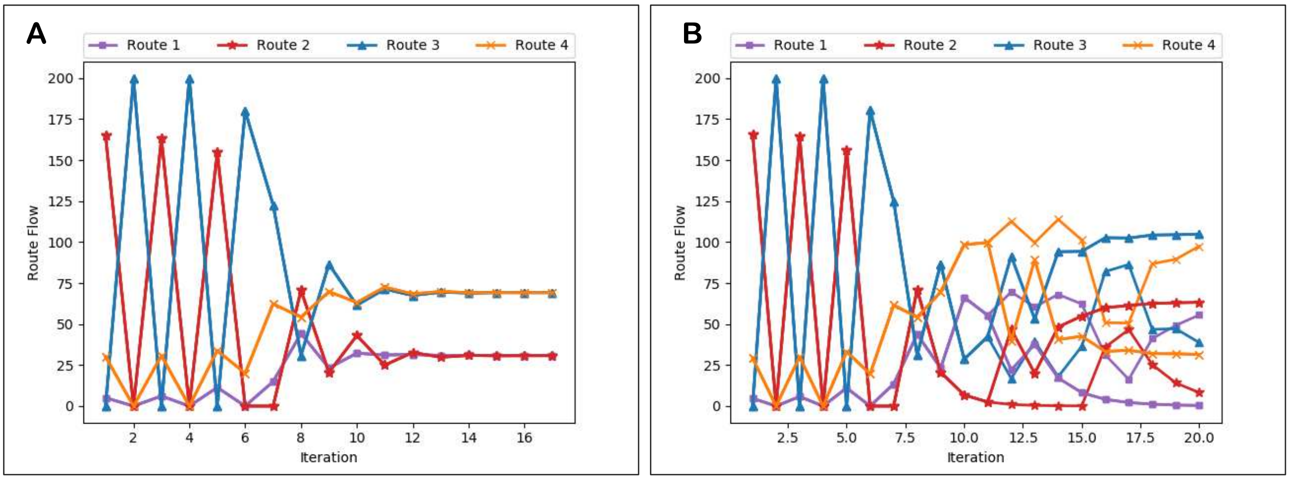

Fig. 36. Small example network: BAPS SUE route flows at each iteration of the BPS SUE algorithm with randomly generated initial FPIM conditions, two runs ($\theta = 1$, $\varphi = 2$, $\xi = 10$). **A:** $\beta = 0.9$. **B:** $\beta = 1.1$.

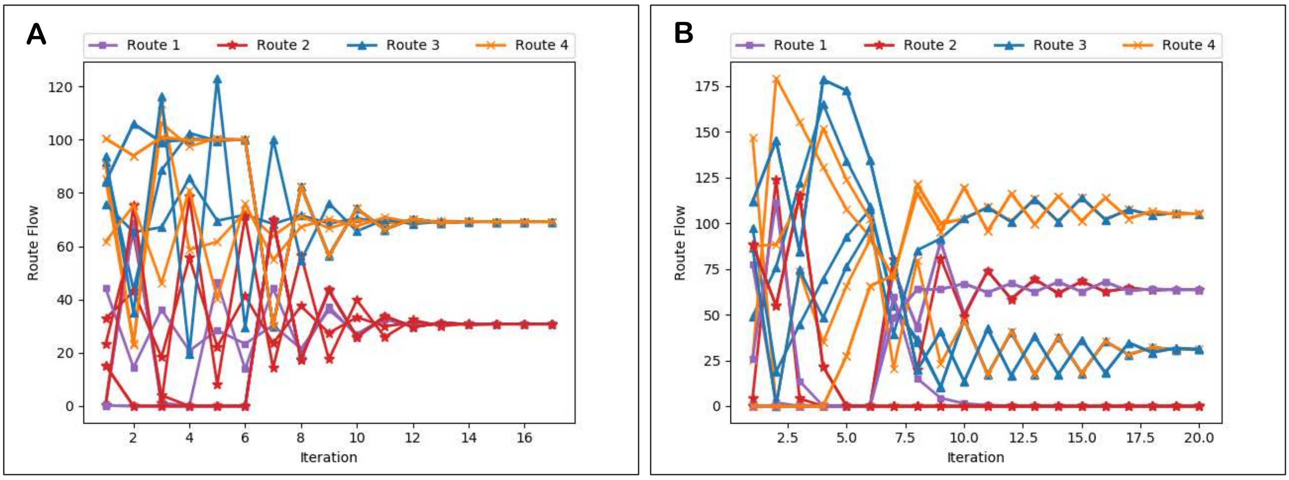

Fig. 37. Small example network: BAPS SUE route flows at each iteration of the BPS SUE algorithm with follow-on initial FPIM conditions and randomly generated initial SUE conditions, multiple runs ($\theta = 1$, $\varphi = 2$, $\xi = 10$). **A:** $\beta = 0.9$. **B:** $\beta = 1.1$.

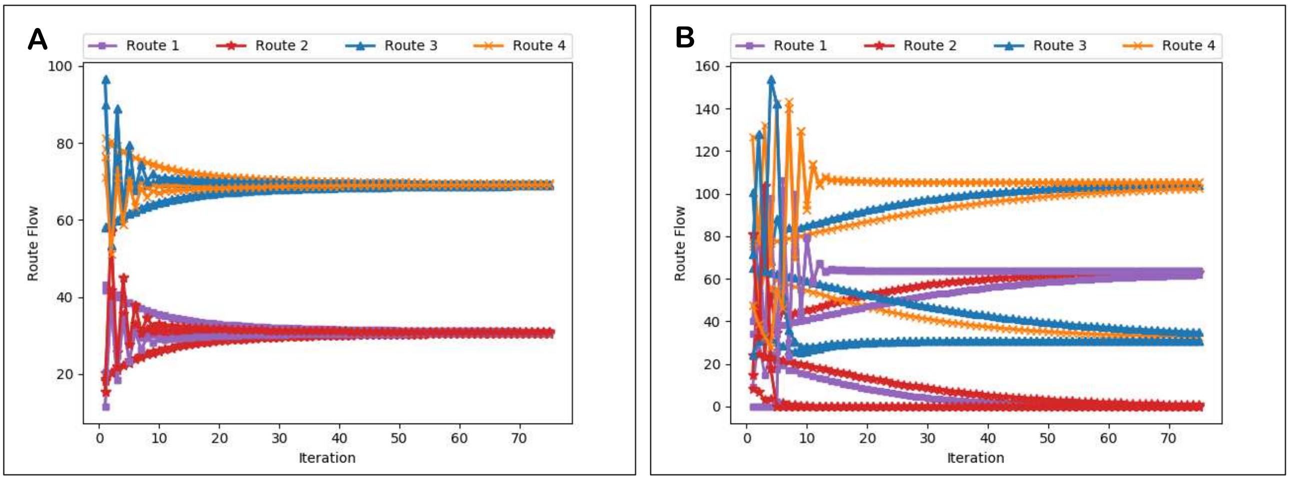

Fig. 38. Small example network: BAPS′ SUE route flows at each iteration of the BPS SUE algorithm with randomly generated initial SUE conditions, multiple runs ($\theta = 1$, $\varphi = 2$). **A:** $\beta = 0.9$. **B:** $\beta = 1.1$.

Fig. 37 & Fig. 38 suggest that the BAPS SUE solution is unique for $\beta = 0.9$, and solutions are non-unique for $\beta = 1.1$, and Fig. 36 suggests that this due to the BAPS choice probability solutions being universally unique for $\beta = 0.9$, but not for $\beta = 1.1$. One can imply from this that $0.9 \leq \bar{\beta}_{max}(1,2) < 1.1$, and potentially that BAPS SUE solutions are unique for β in the range $0 \leq \beta \leq 0.9 \leq \bar{\beta}_{max}(1,2)$.

Duncan et al (2022) describe a method for identifying the uniqueness conditions for APSL SUE solutions. Here, we utilise a similar method, to attempt to identify $\bar{\beta}_{max,m}(\theta,\varphi)$ values and thus $\bar{\beta}_{max}(\theta,\varphi) = \min(\bar{\beta}_{max,m}(\theta,\varphi): m = 1, \dots, M)$ for the BAPS SUE model. $\bar{\beta}_{max,m}(\theta,\varphi)$ is estimated by plotting trajectories of BAPS SUE solutions for OD movement m for varying β, and identifying where a unique trajectory of solutions ends and multiple trajectories begin. A simple method for obtaining trajectories of BAPS SUE solutions is as follows:

Step 1. Identify a suitably large value for β (where it is predicted that solutions will be non-unique).

Step 2. Solve BAPS SUE for this large β with a randomly generated initial SUE condition.

Step 3. Decrement β and obtain the next BAPS SUE solution with the initial SUE condition set as the solution for the previous β.

Step 4. Continue until a suitably low value of β (where it is predicted that solutions will be unique).

The randomly generated initial SUE conditions for the BPS SUE algorithm are obtained by the same method as described above: by randomly generating a non-zero flow for all routes (maintaining demand-feasibility), and performing a bound condition phase to remove routes with consequent costs above the bound, redistributing the flows accordingly. Since the φ parameter is fixed, a bound condition phase is not required for Step 3 when using the solution to the previous β.

By plotting the route flows for OD movement m at each decremented β, and repeating this method several times, one can determine where non-unique solution trajectories end and hence estimate $\bar{\beta}_{max,m}(\theta,\varphi)$. If after several repetitions (with different randomly generated initial conditions) only a single trajectory of solutions is shown, then the initial large β value is increased. Similarly, if only multiple trajectories are shown, the stopping low β value is decreased. However, one can test beforehand whether the initial and stopping β values are suitable by solving for each a few times with random initial conditions and observing whether there are different solutions for the initial β value and the same solution for the stopping β. In the experience of the authors, the $\bar{\beta}_{max,m}(\theta,\varphi)$ values typically range between 0.9 and 1.1 (usually around 1).

If in large-scale networks it is computationally burdensome to solve BAPS SUE once at a time for each decremented value of β, then one can instead (by possibly harnessing parallel processing) solve for different β values simultaneously, each with randomly generated initial conditions. This should also identify where solutions are and are not unique. Moreover, one can plot flow trajectories for all OD movements simultaneously, so the method does not need to be repeated for each OD movement. We illustrate the approach graphically here, but there is no need to draw graphs for general networks. One can instead observe the route flow values, where a finer grained decrement of β will provide a more accurate estimation of $\bar{\beta}_{max,m}(\theta,\varphi)$.

In the case of the small example network where there is a single OD movement, we estimate $\bar{\beta}_{max}(1,2)$ using the above method. Fig. 39 displays trajectories of BAPS SUE route flow solutions as the β parameter is varied for $\theta = 1$, $\varphi = 2$, $\xi = 10$. β was decremented by 0.005 and the initial large β value was 1.2. The solution trajectory plotting was repeated until multiple trajectories were shown. As shown, there is a unique trajectory of route flow solutions up until $\beta = \bar{\beta}_{max}(1,2)$ where there then becomes multiple trajectories. The estimated $\bar{\beta}_{max}(1,2)$ value is 0.995.

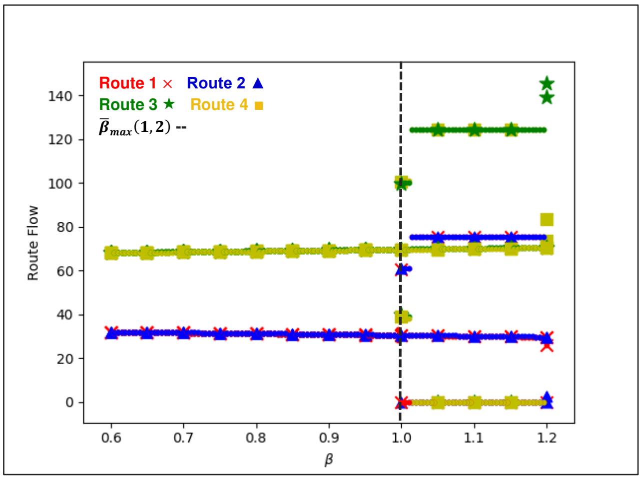

Fig. 39. Small example network: Trajectories of BAPS SUE solutions as β is varied ($\theta = 1$, $\varphi = 2$, $\xi = 8$).

We use the same technique of plotting flow trajectories to estimate the BAPS SUE uniqueness conditions for the Sioux Falls network. Fig. 40 displays for Sioux Falls the maximum route flow from two trajectories of BAPS SUE solutions as the β parameter is varied for two different randomly chosen OD movements. β was decremented by 0.01, and the initial large β and stopping small β values were $\beta = 1.1$ and $\beta = 0.9$, respectively. As shown, the $\bar{\beta}_{max,m}(0.1,2)$ values for these OD movements appear to be greater than 0.9.

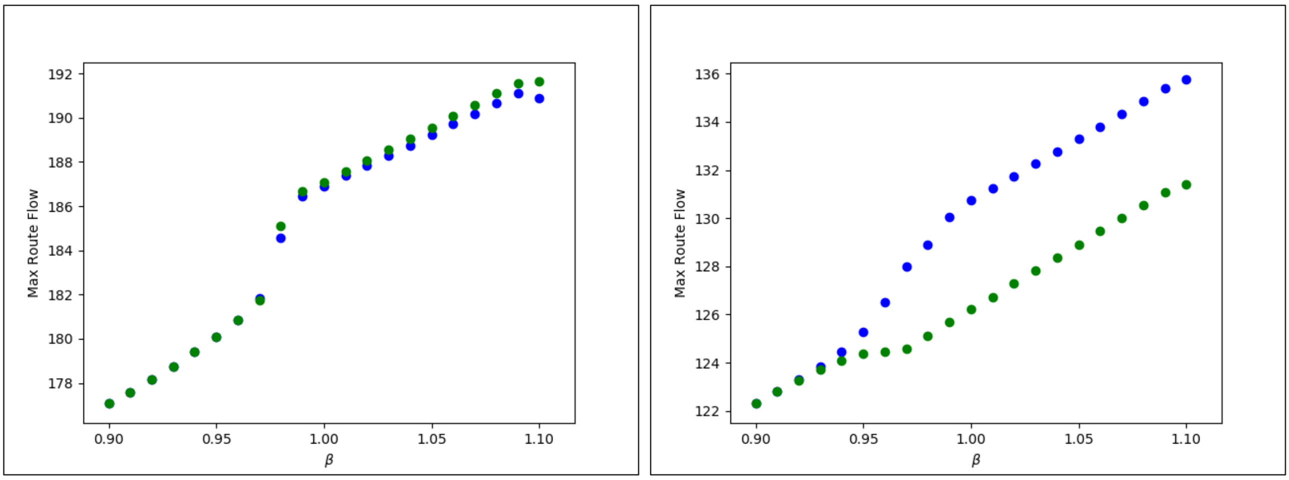

Fig. 40. Sioux Falls: Maximum route flow for two different OD movements from two trajectories of BAPS SUE solutions as β is varied.

5.5 Findings of the Numerical Experiments

To summarise, the key findings of the numerical experiments were that:

a) Flow results from the bounded SUE models converged towards their non-bounded limit models as the bound parameter was increased towards infinity.

b) Bounded SUE models have the potential to be significantly more robust than non-bounded SUE models to the inclusion of unrealistic routes to the adopted choice sets.

c) The BPS SUE models tended to equilibrate marginally larger used route choice set sizes than BSUE.

d) BBPS SUE converged in a similar number of BPS SUE algorithm iterations to BSUE, but total computation times were longer due to the more complex probability expression.

e) The features of solving APSL/APSL′ SUE explored in Duncan et al (2022) could be transferred to solving the analogous BAPS/BAPS′ SUE:

f) Convergence rates for solving BAPS SUE were similar to that for BSUE & BBPS SUE, however the computational burden involved in computing the fixed-point BAPS model choice probabilities for each BPS SUE algorithm iteration resulted in much longer total computation times.

g) On-the-other-hand, the computational burden involved in computing the BAPS′ model choice probabilities was similar to that for the BBPS model (similarly closed-form), but the BAPS′ SUE convergence rate was comparatively slow, and thus total computation times were also longer.

h) In general, the FPIM convergence parameter ξ (and thus the accuracy of the BAPS model choice probabilities) must be at a certain level for convergence of the BPS SUE algorithm to the BAPS SUE solution.

i) However, by utilising 'follow-on' initial FPIM conditions – where the initial conditions for solving the BAPS probabilities at iteration n of the BPS SUE algorithm are set as the route flow proportions from iteration $n-1$ – the BPS SUE algorithm will converge to the BAPS SUE solution for all ξ.

j) There was a computational trade-off between solving BAPS & BAPS′ SUE: solving BAPS SUE with low ξ and follow-on initial conditions simulated solving BAPS′ SUE where the convergence rate was slow, while larger values of ξ resulted in comparatively quick convergence rates but lengthy computation times for the iterations.

k) One can thereby, with ξ, trade-off SUE convergence rates with computation times for each of the BPS SUE algorithm iterations, to improve total computation times for solving BAPS SUE.

l) Also to improve BAPS SUE total computation times, one can stipulate a set number of FPIM iterations to perform at each BPS SUE algorithm iteration, or utilise a combination of a maximum number of FPIM iterations to perform and a maximum level of BAPS probability convergence (controlled with ξ).

m) However, since in earlier iterations the choice sets of used routes are being equilibrated and therefore changing between iterations, the BAPS SUE solution techniques utilising follow-on initial FPIM conditions are less efficient than for solving APSL SUE in Duncan et al (2022).

n) BAPS SUE can though be solved in feasible computation times, though typically longer than BSUE & BBPS SUE.

o) Uniqueness conditions appeared to exist for BAPS SUE: for β in the range $0 \leq \beta \leq \bar{\beta}_{max}(\theta)$, where BAPS probability solutions are unique.

p) $\bar{\beta}_{max,m}(\theta)$ values (uniqueness for OD movement m) in experiments were all close to one.

The 'optimal' values for the methods in j)-l) for solving BAPS SUE are particular to the network, model, and algorithm specifications, e.g. model parameters, adopted step-size scheme, choice set sizes. However, by fixing the optimised values for a given specification, and then varying the specifications, it was shown that the method was robust in its effectiveness compared to solving BAPS SUE in a standard way (i.e. where the BAPS fixed-point probabilities are accurately solved with non-follow-on initial conditions.

6 Conclusion

This paper investigates the integration of Bounded Path Size (BPS) route choice models within a Stochastic User Equilibrium (SUE) model. The BPS model form offers a theoretically consistent and practical approach for dealing with both route overlap and unrealistic routes on large-scale networks. It captures correlations between overlapping routes by including correction terms within the probability relations, and has a consistent criterion for assigning zero choice probabilities to unrealistic routes while eliminating their path size contributions. Two BPS models are proposed: one that is closed-form (the BBPS model), and another expressed as a fixed-point problem (the BAPS model). For the BAPS model, solving the choice probabilities requires a fixed-point algorithm to compute the solution. This has the potential to be computationally burdensome in large-scale networks even when the travel costs are fixed. As explored in the paper, however, the requirement of solving fixed-point problems to compute the BAPS model choice probabilities can be circumvented in SUE application, since at equilibrium the route flow proportions and choice probabilities equate.

The paper proves the existence of BBPS SUE solutions. BAPS SUE solution existence cannot be guaranteed by the standard proofs since the BAPS choice probability function is not technically continuous, though this is not an issue in practice and thus in practice BAPS SUE solution existence is not an issue. Uniqueness for BBPS SUE or BAPS SUE cannot be guaranteed. Instead, the paper investigates the uniqueness of BAPS SUE model solutions numerically, where experiments on the Sioux Falls network suggests that uniqueness conditions exist. These conditions are analogous to those for the uniqueness of BAPS model probability solutions, and BAPS SUE solutions appear to be unique when BAPS model solutions are unique.

The paper proposes a generic algorithm for solving BPS SUE models. The algorithm is an adaptation of the generic algorithm proposed by Watling et al (2018) for the Bounded SUE (BSUE) model. To equilibrate the choice sets of realistic routes, the BSUE algorithm generates realistic routes from the network as the algorithm progresses. With the current techniques available for generating these routes, there are questions over the suitability of the approach for large-scale networks. For the proposed BPS SUE algorithm, we thus take a more heuristic approach, by pre-generating approximated universal choice sets. From these routes, the restricted choice sets of realistic routes are equilibrated. With this approach, it does mean that the choice set generation method can impact on the solution quality, however it should be significantly less than for non-bounded SUE models (as shown in the paper). Future research could test though the impacts of different choice set generation methods on the solution quality. Otherwise, the algorithm can be easily adapted so that routes are generated as the algorithm progresses, just like the BSUE algorithm.

Adopting the Method of Successive Weighted Averages (MSWA) step-size scheme, the computational performance of the BPS SUE algorithm for solving BBPS & BAPS SUE is assessed in numerical experiments on the Sioux Falls and Winnipeg networks. The paper demonstrates how for BAPS SUE one can trade-off the accuracy of BAPS model probabilities (and thus computation times of each iteration) with rate of SUE convergence, and as such, it is shown that BAPS SUE can be solved in feasible computation times. Computational performance and flow results are also compared with BSUE and standard Path Size Logit (PSL) SUE models (solved with a flow-averaging algorithm and MSWA). The key findings of the numerical experiments were that:

a) Flow results from the bounded SUE models converged towards their associated non-bounded limit SUE model as the bound parameter was increased towards infinity.

b) The bounded SUE models have the potential to be significantly more choice set robust that non-bounded SUE models, i.e. less sensitive to the inclusion of unrealistic routes to the adopted choice sets.

c) BBPS SUE could be solved quicker than BAPS SUE, due to the closed-form BBPS probability expression, but BAPS SUE was more internally consistent (greater behavioural realism).

d) BPS SUE models can be solved in feasible computation times, though typically longer than non-bounded models.

The paper explored different solution techniques to improve computation times solving BAPS SUE with the BPS SUE algorithm. These included tuning the BAPS probability convergence parameter ξ and the maximum number of Fixed-Point Iteration Method (FPIM) iterations solving the BAPS model probabilities, to compromise the convergence rate if the BPS SUE algorithm with the computation time of each iteration. Future research could extend this further, for example by exploring an intelligent, adaptive process whereby the optimal values of ξ and the maximum number of FPIM iterations are learnt / worked out as the BPS SUE algorithm progresses.

7 References

Bekhor S & Prashker J, (2001). Stochastic user equilibrium formulation for the generalized nested logit model. Transportation Research Record 1752, p.84–90.

Bekhor S, Ben-Akiva M, & Ramming M, (2006). Evaluation of choice set generation algorithms for route choice models. Ann Oper Res 144, p.235–247.

Bekhor S, Toledo T, & Prashker J, (2008). Effects of choice set size and route choice models on path-based traffic assignment. Transportmetrica, 4(2), p.117-133.

Ben-Akiva M, & Bierlaire M, (1999). Discrete choice methods and their applications to short term travel decisions. In: Halled, R.W. (Ed.), Handbook of Transportation Science. Kluwer Publishers.

Bliemer M & Bovy P, (2008). Impact of Route Choice Set on Route Choice Probabilities. Transportation Research Record: Journal of the Transportation Research Board, 2076, p.10–19.

Bovy P, Bekhor S, & Prato C, (2008). The Factor of Revisited Path Size: Alternative Derivation. Transportation Research Record: Journal of the Transportation Research Board, 2076, Transportation Research Board of the National Academies, Washington, D.C., p.132–140.

Chen A, Pravinvongvuth S, Xu X, Ryu S, & Chootinan P, (2012a). Examining the scaling effect and overlapping problem in logit-based stochastic user equilibrium models. Transportation Research Part A, 46, p.1343-1358.

Chen A, Zhou Z, & Xu X, (2012b). A self-adaptive gradient projection algorithm for the non-additive traffic equilibrium problem. Computers and Operations Research, 39(2), p.127–138.

Chen A, Xu X, Ryu S, & Zhou Z, (2013). A self-adaptive Armijo stepsize strategy with application to traffic assignment models and algorithms. Transportmetrica A: Transport Science, 9(8), p.695–712.

Chen A, S Ryu, Xu X, & Choi K, (2014). Computation and Application of the Paired Combinatorial Logit Stochastic User Equilibrium Problem. Computers and Operations Research, 43, p.68–77.

Daganzo C & Sheffi Y, (1977). On stochastic models of traffic assignment. Transportation Science, 11, p.253–274.

Duncan L, Watling D, Connors R, Rasmussen T, & Nielsen O, (2020). Path Size Logit Route Choice Models: Issues with Current Models, a New Internally Consistent Approach, and Parameter Estimation on a Large-Scale Network with GPS Data. Transportation Research Part B, 135, p.1-40.

Duncan L, Watling D, Connors R, Rasmussen T, & Nielsen O, (2021). A bounded path size route choice model excluding unrealistic routes: formulation and estimation from a large-scale GPS study, Transportmetrica A: Transport Science, 18(3), p.435-493.

Duncan L, Watling D, Connors R, Rasmussen T, & Nielsen O, (2022). Choice set robustness and internal consistency in correlation-based logit stochastic user equilibrium models, Transportmetrica A: Transport Science.

Grange L, Raveau A, & González F, (2012). A Fixed Point Route Choice Model for Transit Networks that Addresses Route Correlation. Procedia - Social and Behavioral Sciences, 54, p.1197-1204.

Hoogendoorn-Lanser S, van Nes R, & Bovy P, (2005). Path Size Modeling in Multimodal Route Choice Analysis. Transportation Research Record: Journal of the Transportation Research Board, 1921, p.27–34.

Hoogendoorn-Lanser S, van Nes R, & Bovy P, (2006). A constrained enumeration approach to multi-modal choice set generation. In: Proceedings, 11th International Conference on Travel Behaviour Research (CD-ROM), Kyoto, Japan.

Isaacson E, & Keller H, (1966). Analysis of Numerical Methods. John Wiley & Sons, Inc., New York, USA.

Kitthamkesorn S, Chen A, & Xu X, (2015) Elastic demand with weibit stochastic user equilibrium flows and application in a motorised and non-motorised network. Transportmetrica A: Transport Science, 11:2, 158-185

Liu H, He X, & He B, (2009). Method of successive weighted averages (MSWA) and self regulated averaging schemes for solving stochastic user equilibrium problem. Networks and Spatial Economics, 9(4), p.485–503.

Liu Z, Meng Q, & Wang S, (2014) Variational inequality model for cordon-based congestion pricing under side constrained stochastic user equilibrium conditions, Transportmetrica A: Transport Science, 10:8, 693-704

Meng Q, Liu Z, & Wang S, (2014). Asymmetric stochastic user equilibrium problem with elastic demand and link capacity constraints. Transportmetrica A: Transport Science, 10:4, 304-326

Piet H. Bovy P, & Stella Fiorenzo-Catalano, (2007). STOCHASTIC ROUTE CHOICE SET GENERATION: BEHAVIORAL AND PROBABILISTIC FOUNDATIONS, Transportmetrica, 3:3, 173-189.

Prato C & Bekhor S, (2006). Applying branch & bound technique to route choice set generation. Transport. Res. Rec. 1985, p.19–28.

Prato C, (2009). Route choice modeling: past, present and future research directions. Journal of Choice Modelling, 2(1), p.65-100.

Ramming S, (2002). Network knowledge and route choice. Ph.D. Thesis, Massachusetts Institute of Technology, Cambridge, USA.

Rasmussen T, Nielsen O, Watling D, & Prato C, (2015). Stochastic user equilibrium with equilibrated choice sets: Part II – Solving the restricted SUE for the logit family. Transportation Research Part B, 77, p.146–165.

Rieser-Schüssler N, Balmer M, & Axhausen K, (2013). Route choice sets for very high-resolution data, Transportmetrica A: Transport Science, 9:9, 825-845

Sheffi Y & Powell W, (1982). An algorithm for the equilibrium assignment problem with random link times. Network: An International Journal, 12(2), p.191-207.

Tahlyan D & Pinjari A, (2020). Performance evaluation of choice set generation algorithms for analyzing truck route choice: insights from spatial aggregation for the breadth first search link elimination (BFS-LE) algorithm, Transportmetrica A: Transport Science, 16:3, 1030-1061

Wardrop J, (1952). Some theoretical aspects of road traffic research. Proc. Institute of Civil Engineers, Part II, 1, p.325-378.

Watling D, Rasmussen T, Prato C, & Nielsen O, (2015). Stochastic user equilibrium with equilibrated choice sets: Part I – Model formulations under alternative distributions and restrictions. Transportation Research Part B (77), p.166-181.

Watling D, Rasmussen T, Prato C, & Nielsen O, (2018). Stochastic user equilibrium with a bounded choice model. Transportation Research Part B, 114, p.254-280.

Xu X, Chen A, Zhou Z, & Behkor S, (2012). Path-based algorithms for solving C-logit stochastic user equilibrium assignment problem. Transportation Research Record, 2279, p.21–30.

Yao J, Cheng Z, Dai J, Chen A & An S, (2019). Traffic assignment paradox incorporating congestion and stochastic perceived error simultaneously. Transportmetrica A: Transport Science, 15:2, 307-325

Yan D & Guo J, (2021). A stochastic user equilibrium model solving overlapping path and perfectly rational issues. J. Cent. South Univ. 28, 1584–1600.

Zhou Z, Chen A, & Bekhor S, (2012). C-logit stochastic user equilibrium model: formulations and solution algorithm. Transportmetrica, 8(1), p.17–41.

Zill J, Camargo P, Daisy N, & Veitch T, (2019). Toll Choice and Stochastic User Equilibrium: Ticking All the Boxes. Transportation Research Record, 2673(4), 930–940.

8 Appendix

8.1 Appendix A – Model Definitions

8.1.1 Path Size Logit SUE Models

Here, we briefly detail definitions of SUE for Path Size Logit models with flow-dependent path size terms. We direct the reader to Duncan et al (2022) for more details and solution methods.

Path Size Logit models were developed to address the well-known deficiency of the Multinomial Logit (MNL) model in its inability to capture the correlation between routes. To do this, they include correction terms to penalise routes that share links with other routes, so that the deterministic utility of route $i \in R_m$ is $V_{m,i} = -\theta c_{m,i}(\boldsymbol{t}) + \kappa_{m,i}$, where $\theta > 0$ is the Logit scaling parameter and $\kappa_{m,i} \leq 0$ is the correction term for route $i \in R_m$. The choice probability for route $i \in R_m$ is:

$$P_{m,i}(\boldsymbol{c}_m(\boldsymbol{t}), \boldsymbol{\kappa}_m) = \frac{e^{-\theta c_{m,i}(\boldsymbol{t}) + \kappa_{m,i}}}{\sum_{j \in R_m} e^{-\theta c_{m,j}(\boldsymbol{t}) + \kappa_{m,j}}}.$$

Path Size Logit correction terms adopt the form $\kappa_{m,i} = \beta \ln(\gamma_{m,i})$, where $\beta \geq 0$ is the path size scaling parameter, and $\gamma_{m,i} \in (0,1]$ is the path size term for route $i \in R_m$. A distinct route with no shared links has a path size term equal to 1, resulting in no penalisation. Less distinct routes have smaller path size terms and incur greater penalisation. The path size terms are often based upon link lengths and thus $\gamma_{m,i}$ (in those cases) is not dependent upon the link/route generalised travel costs. However, this leads to internal inconsistency (see Duncan et al (2022)), and in this study we base the path size terms upon on generalised link travel costs (i.e. $\gamma_{m,i} = \gamma_{m,i}(\boldsymbol{t})$), which in SUE application are congested, flow-dependent costs. The choice probability for route $i \in R_m$ is thus:

$$P_{m,i}\left(\boldsymbol{c}_m(\boldsymbol{t}),\boldsymbol{\gamma}_m(\boldsymbol{t})\right)=\frac{e^{-\theta c_{m,i}(\boldsymbol{t})+\beta\ln\left(\gamma_{m,i}(\boldsymbol{t})\right)}}{\sum_{j\in R_m}e^{-\theta c_{m,j}(\boldsymbol{t})+\beta\ln\left(\gamma_{m,j}(\boldsymbol{t})\right)}}=\frac{\left(\gamma_{m,i}(\boldsymbol{t})\right)^{\beta}e^{-\theta c_{m,i}(\boldsymbol{t})}}{\sum_{j\in R_m}\left(\gamma_{m,j}(\boldsymbol{t})\right)^{\beta}e^{-\theta c_{m,j}(\boldsymbol{t})}}. \tag{21}$$

The general form for the path size term is as follows:

$$\gamma_{m,i}(\boldsymbol{t})=\sum\nolimits_{a\in A_{m,i}}\frac{t_a}{c_{m,i}(\boldsymbol{t})}\frac{1}{\sum_{k\in R_m}\left(\frac{W_{m,k}}{W_{m,i}}\right)\delta_{a,m,k}}, \tag{22}$$

where $W_{m,k}>0$ is the path size contribution weighting of route $k\in R_m$ to path size terms (different for each model), so that the contribution of route $k\in R_m$ to the path size term of route $i\in R_m$ (the path size contribution factor) is $\frac{W_{m,k}}{W_{m,i}}$. To dissect the path size term: each link a in route $i\in R_m$ is penalised (in terms of decreasing the path size term and hence the utility of the route) according to the number of routes in the choice set that also use that link $\left(\sum_{k\in R_m}\delta_{a,m,k}\right)$, where each contribution is weighted (i.e. $\sum_{k\in R_m}\left(\frac{W_{m,k}}{W_{m,i}}\right)\delta_{a,m,k}$), and the significance of the penalisation is also weighted according to how prominent link a is in route $i\in R_m$, i.e. the cost of route a in relation to the total cost of route $i\in R_m$ $\left(\frac{t_a}{c_{m,i}(t)}\right)$.

The Path Size Logit (PSL) model (Ben-Akiva & Bierlaire, 1999) proposes that $W_{m,k}=1$, $\forall k\in R_m$, $m=1,\dots,M$, so that all routes contribute equally to path size terms. This is problematic, however, as the correction terms and thus the choice probabilities of realistic routes are affected by link sharing with unrealistic routes.

To combat this, Ramming (2002) proposed the Generalised Path Size Logit (GPSL) model where $W_{m,k}=\left(c_{m,k}(\boldsymbol{t})\right)^{-\lambda}$, $\forall k\in R_m$, $m=1,\dots,M$, and routes contribute according to travel cost ratios, so that routes with excessively large travel costs have a diminished impact upon the correction terms of routes with small travel costs, and consequently the choice probabilities of those routes. $\lambda\geq 0$ is the path size contribution scaling parameter that accentuates the travel cost ratios to further reduce the contributions of costly routes.

Duncan et al (2020) reformulate the GPSL model (proposing the alternative GPSL model (GPSL$'$)) so that the contribution weighting resembles the probability relation, i.e. $W_{m,k}=e^{-\lambda c_{m,k}(\boldsymbol{t})}$, $\forall k\in R_m$, $m=1,\dots,M$. As they discuss, however, GPSL and GPSL$'$ are not internally consistent in how they define routes as being unrealistic: the path size terms consider only travel cost, whereas the route choice probability relation considers disutility *including* the correction term.

To address this, the Adaptive Path Size Logit (APSL) model is proposed where $W_{m,k}=P_{m,k}$, $\forall k\in R_m$, $m=1,\dots,M$, and routes contribute according to ratios of route choice probability. This ensures internal consistency, where routes defined as unrealistic by the path size terms – and consequently given reduced path size contributions – are exactly those with very low choice probabilities. Since the APSL path size contribution factors depend upon the route choice probabilities, the probability relation is an implicit function, naturally expressed as a fixed-point problem. The APSL model is thus not closed-form and solving the choice probabilities requires a fixed-point algorithm to compute the solution. Furthermore, in order to prove existence and uniqueness of solutions the APSL probability relation is modified from that in (21). See Duncan et al (2020) for more details on the derivation and theoretical properties of the APSL model, as well as definitions and details of the other Path Size Logit models.

SUE for a Path Size Logit model with flow-dependent path size terms can be formulated as follows:

Path Size Logit model SUE: A universal route flow vector $\boldsymbol{f}^*\in\Omega$ is an SUE solution for a Path Size Logit model iff the route flow vector for OD movement m, $\boldsymbol{f}^*_m$, is a solution to the fixed-point problem

$$\boldsymbol{f}_m=\boldsymbol{Q}_m\boldsymbol{P}_m\left(\boldsymbol{c}_m\left(\boldsymbol{t}(\boldsymbol{\Delta f})\right),\boldsymbol{\gamma}_m\left(\boldsymbol{t}(\boldsymbol{\Delta f})\right)\right),\qquad m=1,\dots,M, \tag{23}$$

where $P_{m,i}$ and $\gamma_{m,i}$ are as in (21) and (22) for route $i\in R_m$, respectively, given the universal route flow vector $\boldsymbol{f}$.

For APSL SUE, the probabilities in (23) are fixed-point probabilities. As shown in Duncan et al (2022), since the route choice probabilities and route flow proportions equate at SUE, the APSL path size contribution factors can be instead expressed in terms of route flow proportions, i.e. where $W_{m,k}=\frac{f_{m,k}}{q_m}$. This underlying route choice model is denoted APSL$'$ and is closed-form. This alternative definition of APSL SUE is hence denoted APSL$'$ SUE, and APSL SUE and APSL$'$ SUE are equivalent for route flow vectors at SUE only. Since the APSL probabilities are fixed-point, and the APSL$'$ probabilities are closed-form, APSL SUE and APSL$'$ SUE have different computational performances. The increased computational burden involved in computing each iteration solving APSL SUE means that total computation times are long, while convergence is very slow for APSL′ SUE also resulting in long total computation times. As explored in Duncan et al (2022), one can trade-off the accuracy of APSL choice probabilities with rate of SUE convergence, and several techniques are developed that significantly improve total computation times. This manipulation of the APSL SUE model as well as the developed solution techniques are highly relevant for the SUE application of the fixed-point BPS model as detailed in Section 3.2.

8.1.2 Bounded SUE

Bounded SUE (BSUE) is derived with the Bounded Choice Model (BCM) as the underlying route choice model. In this subsection we briefly formulate the BCM, see Watling et al (2018) and Duncan et al (2021) for more details on the derivation and theoretical properties of the model. The BCM proposes that a bound is applied to the difference in random utility between each given alternative and an imaginary reference alternative, so that an alternative only receives a non-zero choice probability if the difference between its random utility and the random utility of the reference alternative is within the bound. Furthermore, the probability each alternative is chosen relates to the odds associated with choosing each alternative versus the reference alternative. Watling et al (2018) consider a special case of the BCM where the reference alternative is the alternative with the maximum deterministic utility. While the application of the BCM can involve exerting an absolute bound upon the difference in utility from the maximum, (for example 25 units worse in deterministic utility), we consider in this paper exerting a relative bound upon the difference, i.e. where routes only receive a non-zero choice probability if they have a deterministic disutility less than φ times worse than the greatest route utility. If $V_{m,i} < 0$ is the deterministic disutility of alternative $i \in R_m$, then the probability alternative $i \in R_m$ is chosen under the BCM is:

$$P_{m,i}(\boldsymbol{V}_m) = \frac{\left(h_{m,i}(\boldsymbol{V}_m) - 1\right)_+}{\sum_{j \in R_m} \left(h_{m,j}(\boldsymbol{V}_m) - 1\right)_+}, \tag{24}$$

where $h_{m,i}(\boldsymbol{V}_m) = \exp\left(V_{m,i} - \varphi \max\left(V_{m,l}: l \in R_m\right)\right)$, $\varphi > 1$ is the relative bound parameter to be estimated, and $(\cdot)_+ = \max(0,\cdot)$. In a route choice context where the deterministic utility of route $i \in R_m$ is given by $V_{m,i} = -\theta c_{m,i}$, the probability of choosing route $i \in R_m$ is:

$$P_{m,i}\left(\boldsymbol{c}_m(\boldsymbol{t})\right) = \frac{\left(h_{m,i}\left(-\theta \boldsymbol{c}_m(\boldsymbol{t})\right) - 1\right)_+}{\sum_{j \in R_m} \left(h_{m,j}\left(-\theta \boldsymbol{c}_m(\boldsymbol{t})\right) - 1\right)_+}, \tag{25}$$

where $h_{m,i}\left(-\theta \boldsymbol{c}_m(\boldsymbol{t})\right) = \exp\left(-\theta c_{m,i}(\boldsymbol{t}) - \varphi \max\left(-\theta c_{m,l}(\boldsymbol{t}): l \in R_m\right)\right) = \exp\left(-\theta\left(c_{m,i}(\boldsymbol{t}) - \varphi \min\left(c_{m,l}(\boldsymbol{t}): l \in R_m\right)\right)\right)$. Thus, routes only receive a non-zero choice probability if they have a cost less than φ times the cost on the cheapest route, and the probability each route is chosen relates to the odds that that route has a cost within the bound.

BSUE can be formulated as follows:

BSUE: A universal route flow vector $\boldsymbol{f}^* \in \Omega$ is a BSUE solution iff the route flow vector for OD movement m, $\boldsymbol{f}^*_m$, is a solution to the fixed-point problem

$$\boldsymbol{f}_m = \boldsymbol{Q}_m \boldsymbol{P}_m\left(\boldsymbol{c}_m\left(\boldsymbol{t}(\boldsymbol{\Delta f})\right)\right), \qquad m = 1, \dots, M, \tag{26}$$

where $P_{m,i}$ is as in (25), respectively, for route $i \in R_m$, given the universal route flow vector $\boldsymbol{f}$.

8.1.3 Simplified Alternative Bounded Adaptive Path Size

The simplified alternative Bounded Adaptive Path Size (BAPS″) model, is formulated as follows. Given $\bar{R}_m(\boldsymbol{c}_m(\boldsymbol{t}); \varphi)$, the BAPS″ model choice probability relation for route $i \in R_m$ is:

$$P_{m,i}\left(\boldsymbol{c}_m(\boldsymbol{t}), \bar{\boldsymbol{\gamma}}_m^{BAPS''}(\boldsymbol{t}, \boldsymbol{f}_m)\right) = \begin{cases} \dfrac{\left(h_{m,i}\left(-\theta \boldsymbol{c}_m(\boldsymbol{t})\right) - 1\right) \cdot \left(\bar{\gamma}_{m,i}^{BAPS''}(\boldsymbol{t}, \boldsymbol{f}_m)\right)^{\beta}}{\sum_{j \in \bar{R}_m(\boldsymbol{c}_m(\boldsymbol{t}); \varphi)} \left(h_{m,j}\left(-\theta \boldsymbol{c}_m(\boldsymbol{t})\right) - 1\right) \cdot \left(\bar{\gamma}_{m,j}^{BAPS''}(\boldsymbol{t}, \boldsymbol{f}_m)\right)^{\beta}} & if\ i \in \bar{R}_m(\boldsymbol{c}_m(\boldsymbol{t}); \varphi) \\ 0 & if\ i \notin \bar{R}_m(\boldsymbol{c}_m(\boldsymbol{t}); \varphi) \end{cases}, \tag{27}$$

where $h_{m,i}\left(-\theta \boldsymbol{c}_m(\boldsymbol{t})\right) = \exp\left(-\theta\left(c_{m,i}(\boldsymbol{t}) - \varphi \min\left(c_{m,l}(\boldsymbol{t}): l \in R_m\right)\right)\right)$, and the path size term for route $i \in \bar{R}_m(\boldsymbol{c}_m(\boldsymbol{t}); \varphi)$ is:

$$\bar{\gamma}_{m,i}^{BAPS''}(\boldsymbol{t}, \boldsymbol{f}_m) = \sum_{a \in A_{m,i}} \frac{t_a}{c_{m,i}(\boldsymbol{t})} \frac{f_{m,i}}{\sum_{k \in \bar{R}_m(\boldsymbol{c}_m(\boldsymbol{t}); \varphi)} f_{m,k} \delta_{a,m,k}}, \qquad \forall \boldsymbol{f}_m \in \Omega_m^{\left(\bar{R}_m(\boldsymbol{c}_m(\boldsymbol{t}); \varphi)\right)}, \tag{28}$$

$$\Omega_m^{(\bar{R}_m(\boldsymbol{c}_m(\boldsymbol{t});\varphi))} = \left\{ \boldsymbol{f}_m \in \mathbb{R}_+^{N_m} : f_{m,i} > 0, \forall i \in \bar{R}_m(\boldsymbol{c}_m(\boldsymbol{t}); \varphi), and, f_{m,i} = 0, \forall i \notin \bar{R}_m(\boldsymbol{c}_m(\boldsymbol{t}); \varphi), \sum_{i \in R_m} f_{m,i} = q_m \right\}.$$

$\theta > 0, \beta \geq 0, \varphi > 1.$

BAPS$''$ SUE can thus be formulated as follows:

BAPS$''$ SUE: Let $\Omega'' \subseteq \Omega$ be the subset of demand-feasible universal route flow vectors $\boldsymbol{f}$ that satisfy the following conditions:

$$f_{m,i} > 0 \Leftrightarrow c_{m,i}(\boldsymbol{t}(\boldsymbol{\Delta f})) < \varphi \min(c_{m,l}(\boldsymbol{t}(\boldsymbol{\Delta f})) : l \in R_m), \qquad \forall i \in R_m, m = 1, \dots, M, \tag{29}$$

$$f_{m,i} = 0 \Leftrightarrow c_{m,i}(\boldsymbol{t}(\boldsymbol{\Delta f})) \geq \varphi \min(c_{m,l}(\boldsymbol{t}(\boldsymbol{\Delta f})) : l \in R_m), \qquad \forall i \in R_m, m = 1, \dots, M. \tag{30}$$

A universal route flow vector $\boldsymbol{f}^* \in \Omega''$ is a BAPS$''$ SUE solution iff the route flow vector for OD movement m, $\boldsymbol{f}_m^*$, is a solution to the fixed-point problem

$$\boldsymbol{f}_m = \boldsymbol{Q}_m \boldsymbol{P}_m \left(\boldsymbol{c}_m(\boldsymbol{t}(\boldsymbol{\Delta f})), \boldsymbol{\gamma}_m^{BAPS''}(\boldsymbol{t}(\boldsymbol{\Delta f}), \boldsymbol{f}_m) \right), \qquad m = 1, \dots, M, \tag{31}$$

where $P_{m,i}$ is as in (27) for route $i \in R_m$, and $\bar{\gamma}_{m,i}^{BAPS''}$ is as in (28) for route $i \in \bar{R}_m(\boldsymbol{c}_m(\boldsymbol{t}(\boldsymbol{\Delta f})); \varphi)$.